

Reply to Referee #1

We would like to thank the referee for thoughtful and useful comments. In the following, we describe our responses (in blue) point-by-point to each referee comment (*italic*).

In this study, the authors combine field measurements (DGPS), satellite image analysis (debris thickness estimation, surface velocity fields) and modelling (2D flow model, surface mass balance (SMB) simulated from an energy balance model) to assess how sensitive the thinning rate of two glaciers in Bhutan is to the presence or not of a proglacial lake. This question is important because many studies have already observed higher thinning rates for lacustrine terminating glaciers than for land terminating glaciers (a complete list of references addressing such observations is available line. But the reasons for this different behavior are still not entirely clear (accelerated flow and calving, flotation).

This study includes different steps:

- 1. Thinning rates estimation using DGPS measurements;*
- 2. Debris thickness estimation using thermal ASTER images*
- 3. SEB modelling*
- and 4. Flow modelling.*

Major comments:

My main concern comes from the fact that each step mentioned above has large uncertainties (see my comments below) that are not possible to quantify because there is almost no validation (except surface velocity fields derived from optical satellite images). As a consequence, the results are rather subjective and are, in my opinion, not supported. This is a pity, because the study is interesting and exhaustive, but in state, it looks like more a theoretical numerical exercise than a field case study. I have some suggestions below to try to evaluate (only qualitatively though) the reliability of some results, but without validation dataset, I doubt that the results can be fully supported. I found interesting the

experimental strategy (starting from the present state for experiment 1, and exploring the opposite situation removing or adding a proglacial lake for experiment 2), but according to me, given that the debris thickness spatial variability is likely to be badly reproduced, the SMB is highly uncertain, or the bedrock topography extremely simplified, such experimental exercise concerns more synthetic glaciers than true case studies. If there is no possibility to validate the results at each step, I recommend to stick with the theoretical approach (applying the flow model to a synthetic glacier with and without proglacial lake, prescribing a vertical mass balance gradient observed on Himalayan glaciers, including a debris cover part such as Chhota Shigri Glacier, India for instance – Azam et al, Annals Glaciol. 57, 328–338, 2016) than trying to relate this study to a true case study.

Because some in-situ data (e.g., SMB and bedrock topography) is unavailable for the studied glaciers, validation of the results at each step is difficult. We therefore performed (1) validation of spatial representativeness in thinning rate obtained from DGPS with that from satellite-derived DEM (see reply to the major comment #2). We also performed sensitivity analyses for (2) SMB modelling and (3) glacier flow modelling to estimate uncertainties. For the SMB modelling, we recalculated spatial distribution of debris thermal resistance with considering sensible heat flux (see reply to the major comment #3). Detailed bedrock topography is unavailable for all glaciers, but we alternatively evaluated sensitivity of modelled ice speed against changes in ice thickness and basal sliding coefficient. We also computed RMSE between modelled and observed ice speed as a measure of the uncertainty (see reply to the major comment #4).

Surface elevation changes have been obtained by interpolating points surveyed by DGPS in the field with obviously a limited number of points (approx. 5000 to 26000 surveyed points over glaciers TabS1). Given that those glaciers are rather large (approx. 13, 11 and 3 km², respectively for thorthormi, Luge and Luge II), the number of points is not very large (corresponding to a relative coverage <1% of the total glacier surface). These glaciers are also heavily debris covered (with

supra glacial lakes and likely cliffs, the latter not being mentioned in the text though), and in turn with a large variability of their thinning rates (e.g., Immerzeel et al., Remote Sensing Env., 150 (2014) 93–103). Consequently, using an interpolation technique to derive the glacier surface thinning rate is questionable. The expected accuracy is therefore probably very bad, and I doubt that the standard errors displayed in table 1 (a few cm) obtained from the surveyed points can be applied to the whole glacier surface. The authors should comment on this, and should explore how sensitive the results of their study are to these glacier surface thinning rates, which are likely to be very different from their point thinning rates (with a difference potentially as high as a few meters in some areas i.e. cliffs, ponds...). In my opinion, the authors should compare their DEM with DEM obtained from satellite images.

In order to evaluate spatial representativeness of glacier surface elevation change obtained from our DGPS measurements, we compared elevation changes obtained from DGPS-DEMs and from ASTER-DEMs acquired on 11 October 2004 and 6 April 2011, which cover similar period of our field campaign (2004–2011). ASTER-DEMs with 30 m resolution provided by the ASTER-VA (<https://gbank.gsj.jp/madas/map/index.html>) were used to compute the surface elevation change. Elevation of ASTER-DEMs was calibrated by the DGPS data on ice-free terrain in 2011. The 2004 and 2011 ASTER-DEMs showed positive biases (dZ) of 12.73 and 11.20 m, and standard deviations (σ) of 20.24 and 14.04 m, respectively (Fig. R1). Vertical coordinates of the ASTER-DEMs were then corrected for the corresponding bias. Elevation change over the glacier surface was computed as difference of the calibrated DEMs (Fig. R2). Given the error range of ASTER-DEM, the rate of elevation change derived from DGPS-DEMs is similar to that from ASTER-DEMs (Fig. R3). In order to evaluate spatial representativeness of the DGPS survey, we compared the rate of elevation change of 1-m-grid DGPS-DEMs with that of 30-m-grid ASTER-DEMs along elevation (Fig. R4). Mean rates of elevation change with its standard deviation from DGPS-DEMs are -1.40 ± 0.77 and -4.67 ± 1.36 m a⁻¹ for Thorthormi and Lugge Glaciers, respectively, while those from ASTER-DEMs over the elevation range

where the DGPS measurements exist are -0.70 ± 1.25 and -4.87 ± 1.29 m a^{-1} for Thorthormi and Lugge Glaciers, respectively. Figure R4 shows that the rates from DGPS-DEMs fall within those of ASTER-DEMs, and thus it supports applicability of our survey results to the entire ablation zone. In the revised manuscript, we will take into account spatial variability in the rate of elevation change from ASTER-DEMs to uncertainty of the mean rate over the entire ablation zone.

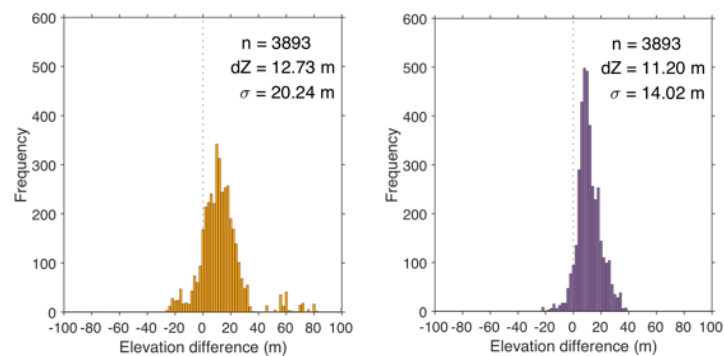


Figure R1: Elevation differences in the ice-free area (left) between 2004 ASTER-DEM and DGPS-DEM and (right) between 2011 ASTER-DEM and DGPS-DEM.

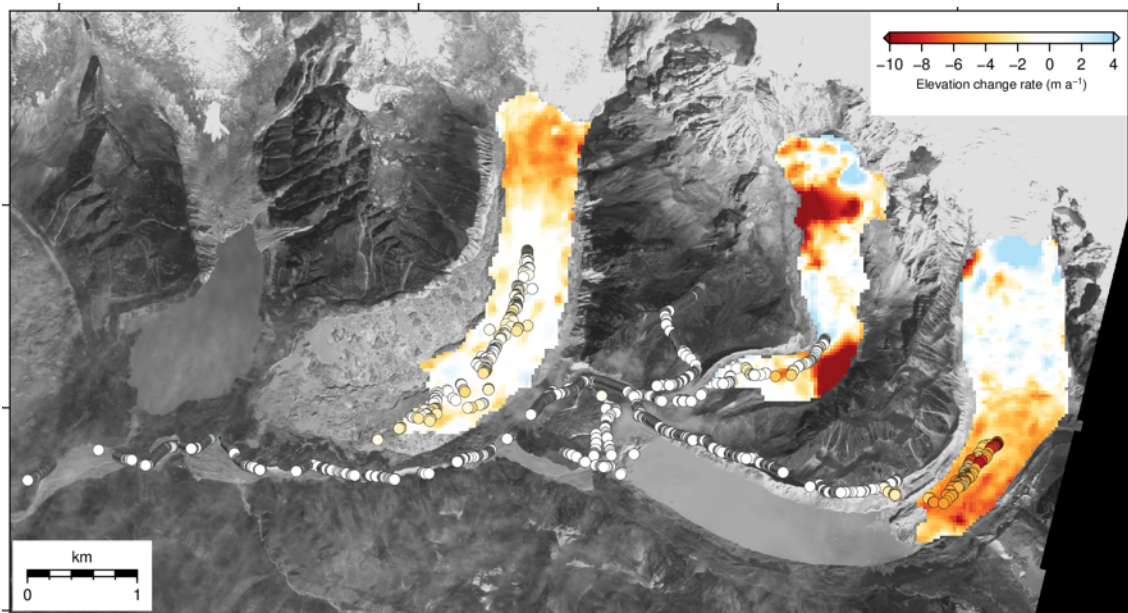


Figure R2: Rate of elevation change for the 2004–2011 period derived from ASTER-DEMs (background shadings) and DGPS-DEMs (circles filled with the same color scale). Glacier outlines are of December 2011.

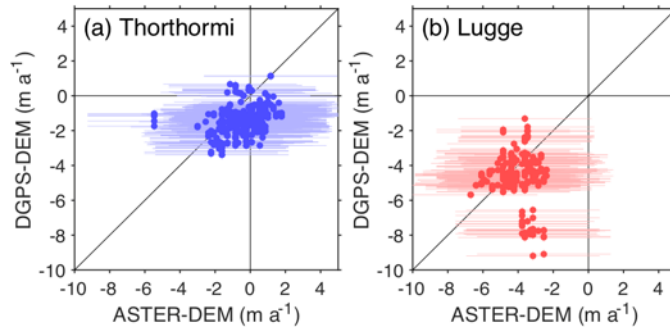


Figure R3: Scatter plot of the rate of surface elevation change between from ASTER-DEMs and DGPS-DEMs at (a) Thorthormi and (b) Lugge Glaciers. Error bars denote standard deviations of DEM differences over the ice-free terrain.

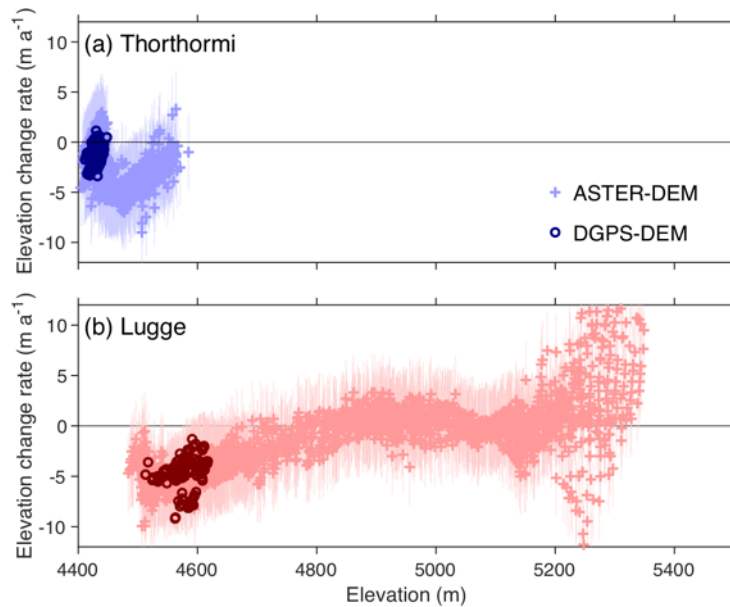


Figure R4: Rate of elevation change along elevation at (a) Thorthormi and (b) Lugge Glaciers. Dark-colored circles are from DGPS-DEMs and light-colored crosses are from ASTER-DEMs. Error bars denote standard deviations of DEM differences over the ice-free terrain.

SMB simulations depend on the debris thickness (obtained from ASTER thermal imagery known to be potentially inaccurate), as well as a surface energy balance model based on a large set of hypothesis and parameters (i.e. $T=0\text{ }^{\circ}\text{C}$ at the ice-debris interface, linear debris temperature profile within the debris (lines 162-63),

surface roughness, albedo of the debris, or bare ice to list only some sensitive parameters – see table 1 of Fujita and Sakai, 2014 for a complete list of parameters). Even though there is no information regarding the used parameter set, I presume that most of these parameters have been taken from a previous study conducted on Tso Rolpa catchment in Nepal (Fujita and Sakai, 2014) where the surface energy balance has been validated using hydrological and meteorological observations. We do not know if the parameters used in Fujita and Sakai (2014) are transferable to this present catchment in Bhutan. In short, there are a large amount of sources of uncertainties (not discussed in this present study), which prevent the results from being reliable if not validated. Looking at results of SMB (Fig 1c), point surface mass balance are very negative. The authors compute SMB of -7 m w.e./a over debris cover areas (section 4.4). To my knowledge, such very negative values of point SMB have never been observed in the Himalayas beneath debris. Plausibly, such values could correspond to very thin debris cover (a few mm or cm, before the maximum of the Ostrem curve) but given the location of these areas (in the lower part of the glaciers where the debris thickness is expected to be the largest), it is highly unlikely. Moreover, the studied glaciers are debris covered, with potentially cliffs and ponds at their surface (is it true? No information regarding cliffs in this study) so the SMB spatial variability is supposed to be very high (e.g., Immerzeel et al, Remote Sensing Env., 150 (2014) 93–103; Buri et al., Ann Glaciol. 57(71), 199–211, 2016, Miles et al, Ann glaciol., 57(71), 29–40,2016) although the SMB map displayed in Fig1c does not show large spatial heterogeneities. In order to evaluate the reliability of the SMB results, a map showing the debris thickness over the 3 glaciers would be necessary. It would be useful also to show the SMB gradient as a function of elevation. And a sensitivity test including all parameters is necessary to test the reliability of the results.

Although debris thickness was not measured during the field campaign, ice is exposed from place to place over Thorthormi and Lugge Glaciers (Figs R5a and R5b), suggesting that debris-cover is rather thin than that of Lugge II Glacier (Fig. R5c). In addition, few supraglacial ponds and ice cliff exist over Thorthormi and

Lugge Glaciers. So we emphasize that spatial variability of elevation change, thermal resistance and SMB are less than those the reviewers supposed. Anyhow, following the referees suggestion, we recalculated thermal resistance with considering sensible heat, for which pressure level temperature and geopotential height of NCEP2 are taken into account (Fig. R6). Scatter plot and spatial distribution of thermal resistances derived from the original method (net radiation only) and from recalculated one (net radiation + sensible heat) are shown in Figs R7 and R8. Spatial distribution of the difference between the two results is also shown in Fig. R8c. Thermal resistance significantly increased after the consideration of sensible heat (Fig. R7). However, large difference appeared only near the western margin (Fig. R8) probably because of relatively thick debris covering the area. We will recalculate the SMB distribution with the revised thermal resistance in the revised manuscript. We evaluated sensitivity of calculated meltwater against meteorological parameters (Fig. R9). We chose the meltwater instead of SMB to quantify the uncertainty in percentage. The tested parameters are surface albedo, air temperature, precipitation, relative humidity, solar radiation, thermal resistance and wind speed. Uncertainty of thermal resistance and albedo were assumed to be 100% and 40% based on Figs R6b and R6d. Uncertainties of each meteorological variable were assumed to be RMSEs of ERA-Interim reanalysis data against the observational data (see Fig. R13). Variations in meltwater within a possible parameter range are estimated by quadratic sum of results from each parameter shown in Fig. R9. Estimated uncertainty of meltwater is less than 50% at a large part of Thorthormi and Lugge Glaciers (Fig. R10). We will replace figures by the recalculated results and add Figs R9 and R10 to the revised supplement.

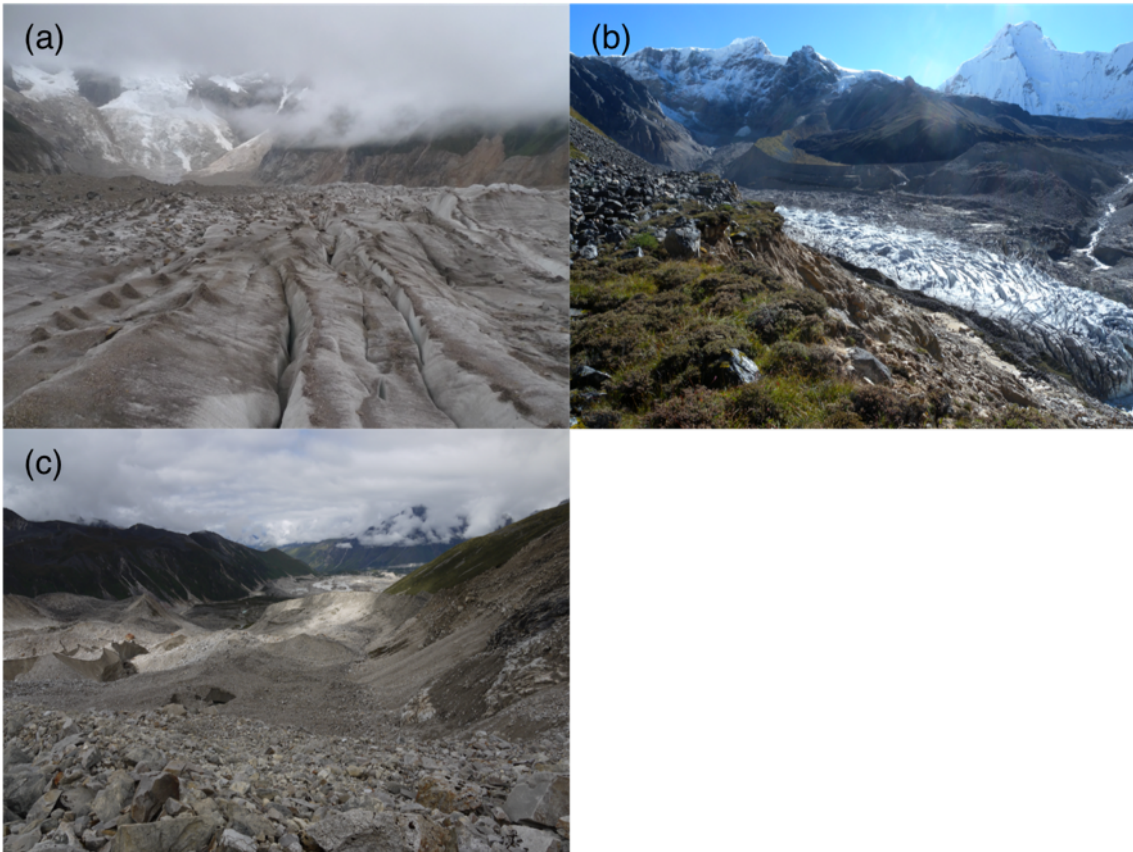


Figure R5: Photographs showing surface condition near the termini of (a) Thorthormi (18 September 2011), (b) Luge Glaciers (20 September 2011) and Luge II Glaciers (21 September 2011).

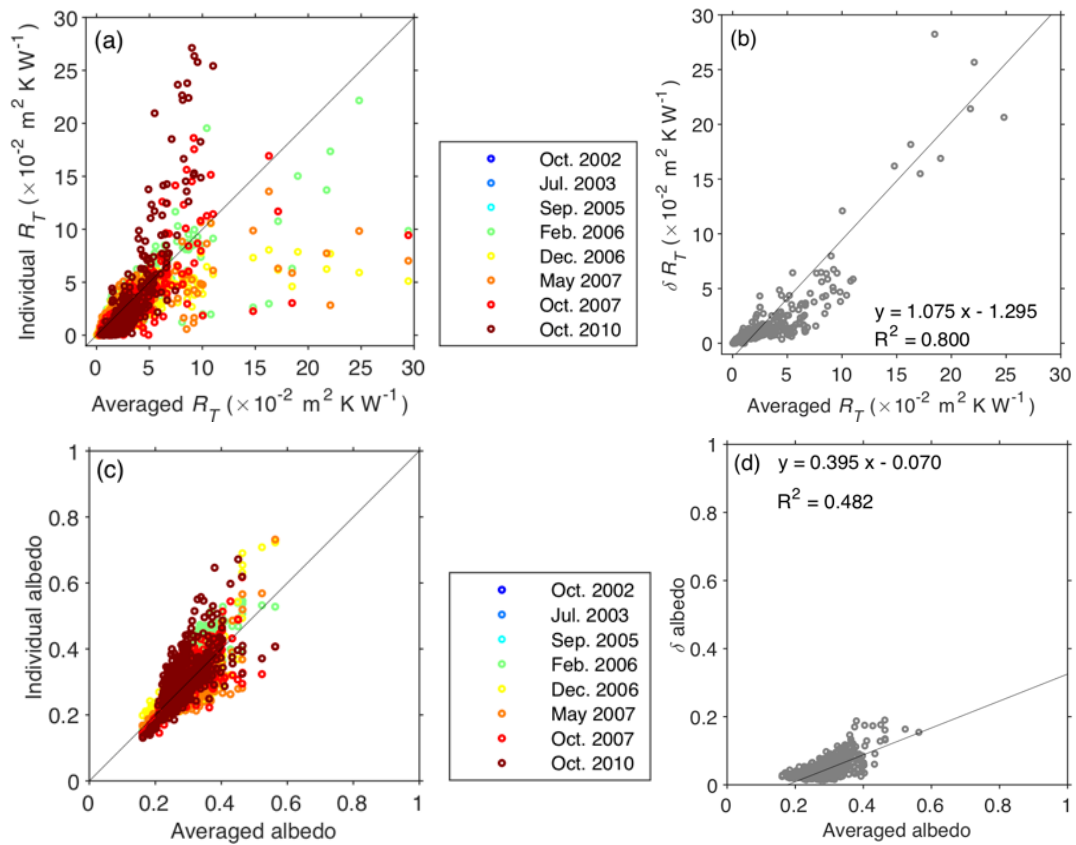


Figure R6: Scattergram of (a) thermal resistance (R_T) of the multitemporal ASTER data against their average derived from net radiation + sensible heat. The mean thermal resistance is used to calculate ice melting under the debris-covered surface of Thorthormi and Lugge Glaciers. (b) Standard deviations (δ) of thermal resistance. (c) Scattergram and (d) standard deviations of albedo.

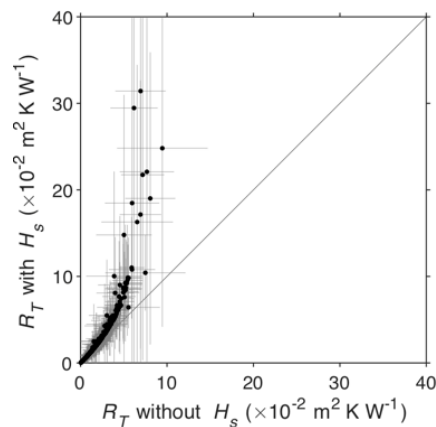


Figure R7: Scatter plot between thermal resistance calculated from only net radiation (without H_s) and from net radiation + sensible heat (with H_s).

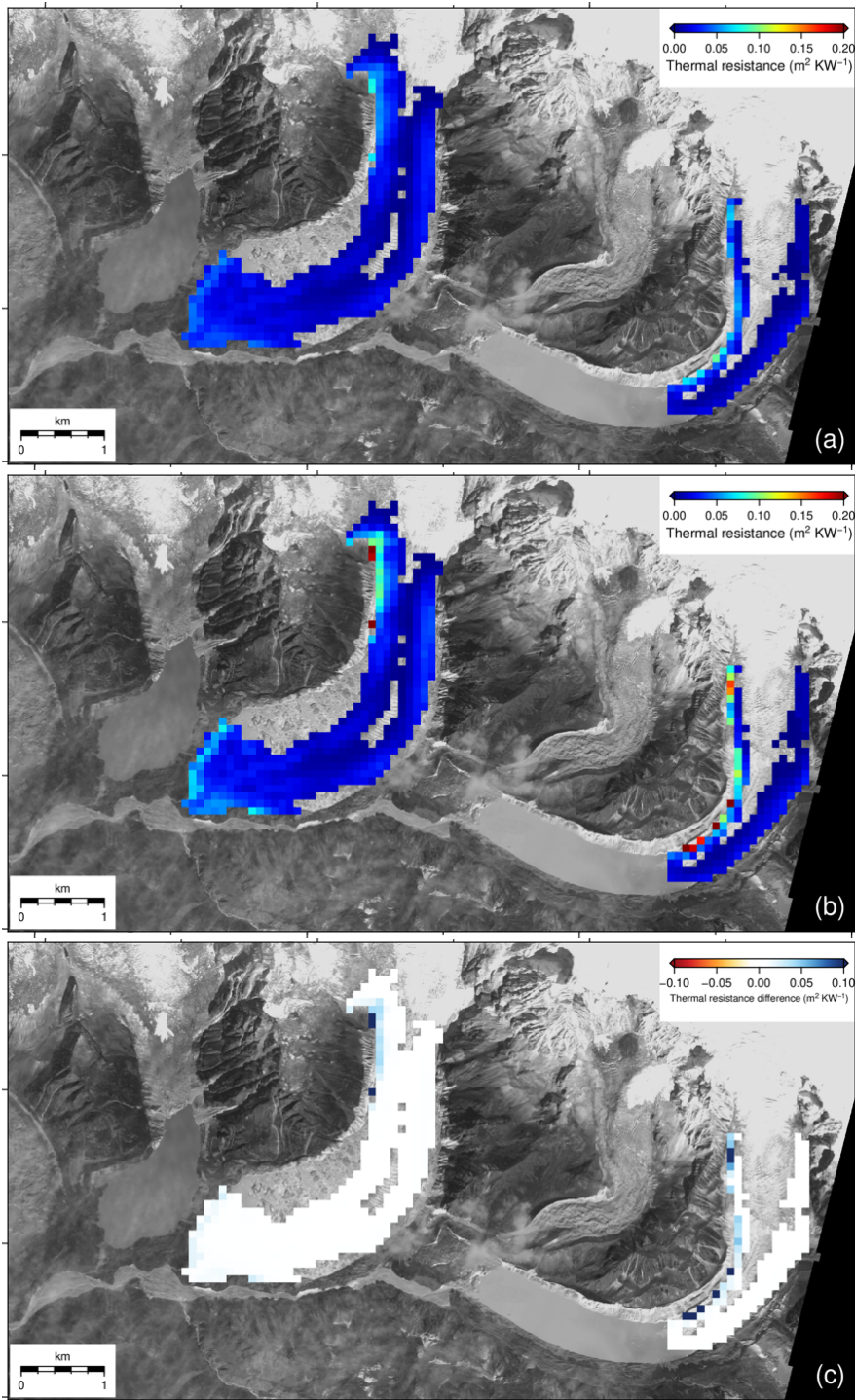


Figure R8: Spatial distribution of thermal resistance calculated (a) from only net radiation, (b) from net radiation + sensible heat and (c) difference of thermal resistance calculated by the two methods.

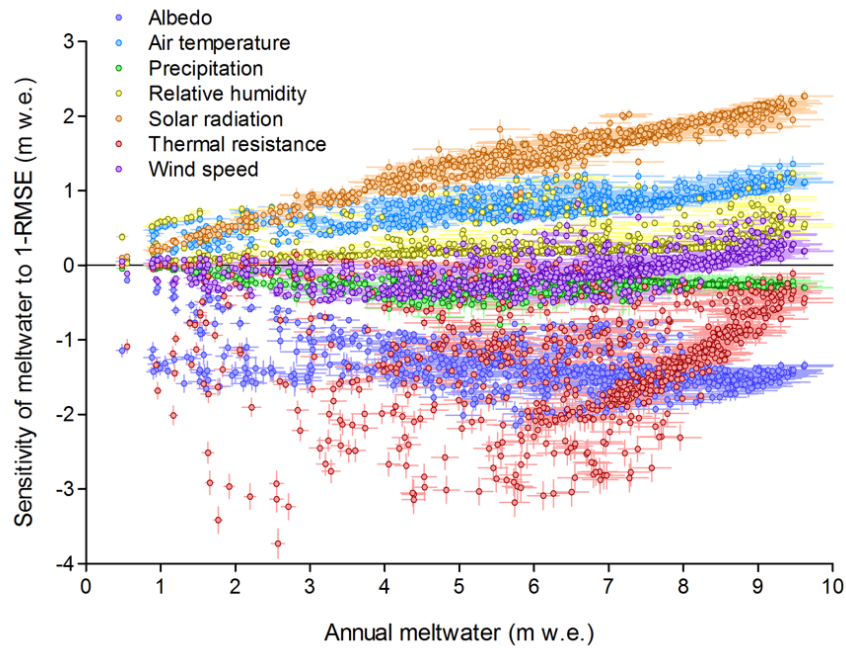


Figure R9: Sensitivity analysis of annual meltwater as a function of RMSE of each meteorological parameter at debris-covered area. Horizontal axis is variable annual meltwater calculated each grid in the SMB model. RMSEs except for albedo and thermal resistance are obtained from ERA-Interim and observed data for 2002–2004 (Fig. R13). Uncertainties of albedo and thermal resistance are derived from 8 satellite images (Fig. R6).

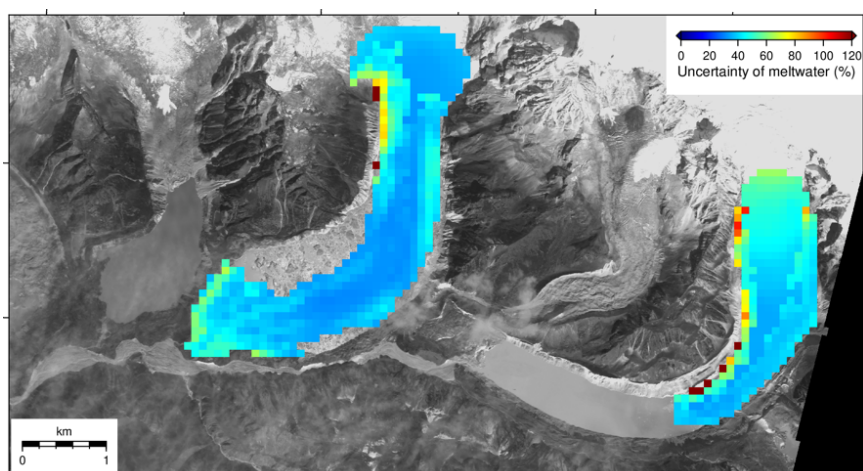


Figure R10: Spatial distribution of estimated uncertainty in the computed annual meltwater volume.

The application of the debris flow model in 2 opposite configurations (experiments 1 and 2) is interesting but the bedrock topography is potentially very different from reality. Either the authors stick with a theoretical case (using an idealized synthetic glacier with a prescribed bedrock topography) or they make a sensitivity analysis using different bedrock topographies, sliding coefficients. . . A sensitivity test has been performed (section 5.2) but I believe that the explored range of ice thickness (± 10 m) or sliding coefficient ($\pm 10\%$) should be much wider.

We performed sensitivity analysis using the broader range ($\pm 30\%$) of the sliding coefficient and ice thickness (Fig. R11). The RMSE between the modeled and measured flow velocities were computed as a measure of the model performance (Fig. R12). For Thorthormi Glacier, the model is similarly sensitive to sliding coefficient and ice thickness. For Luge Glacier, the model is more sensitive to ice thickness than sliding coefficient. Figs R11 and R12 will be added to the revised supplement.

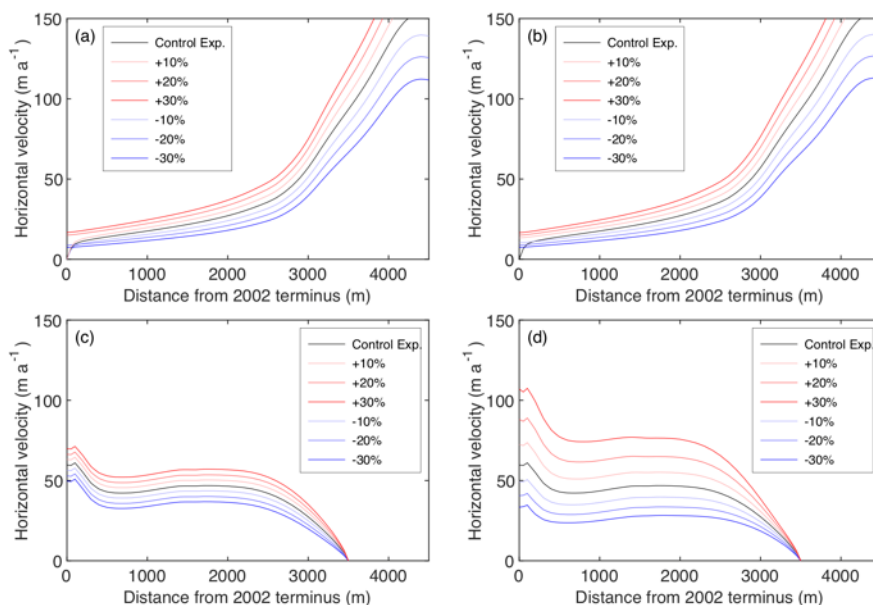


Figure R11: Surface velocity computed for (a and b) Thorthormi and (c and d) Luge Glaciers obtained by changing (a and c) the sliding coefficient (C) by $\pm 30\%$, and (b and d) ice thickness by $\pm 30\%$. The black line is the control experiment.

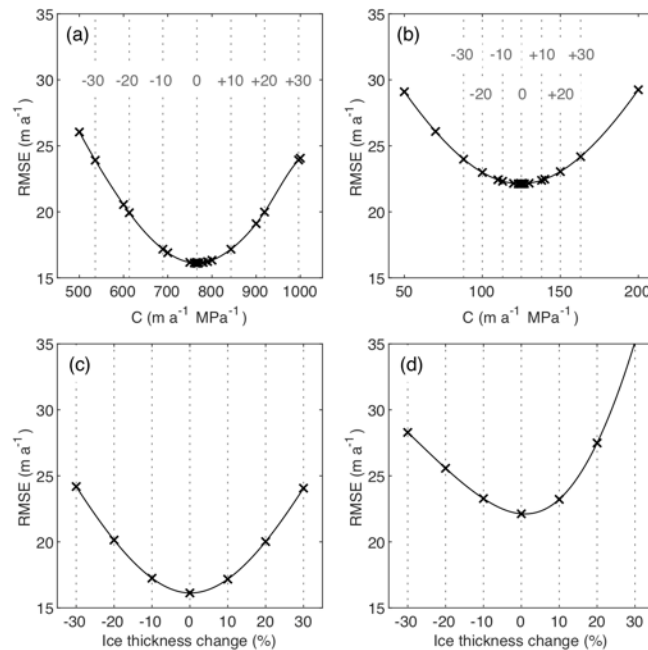


Figure R12: RMSEs between the modelled and measured surface velocities of (a and c) Thorthormi and (b and d) Luge Glaciers, modelled with various (a and b) sliding coefficient (C), and (c and d) various ice thickness.

Maybe I missed something but SMB is estimated over the period 2002-2004, elevation change over the period 2004-2011 and flow velocities are simulated over the period 2002-2010 (but it is not clear for the latter). The periods do not match although results of thinning rate, or SMB are compared each other. How are data/results extrapolated in time? This might bring another layer of uncertainty to the results.

We extended calculating period of SMB for 38 years (1979–2017), which covers the period of the surface elevation change survey (2004–2011). Meteorological variables such as air temperature, precipitation, solar radiation, relative humidity and wind speed in the ERA-Interim reanalysis data (2002–2004) was calibrated with observational data (Fig. R13). Wind speed of ERA-Interim was simply multiplied with 1.3 for obtaining the same average with the observational data. SMBs calculated with observed and calibrated ERA-Interim data for 2002–2004 were compared with those from ERA-Interim data for 1979–2017 (Fig. R14).

SMBs for 2002–2004 (both from observational and ERA-Interim data) showed no clear anomaly against the long-term mean SMB (1979–2017). We will add Figure R13 in the revised supplement. We will replace the SMB result by the 1979–2017 ERA-Interim version in the revised manuscript.

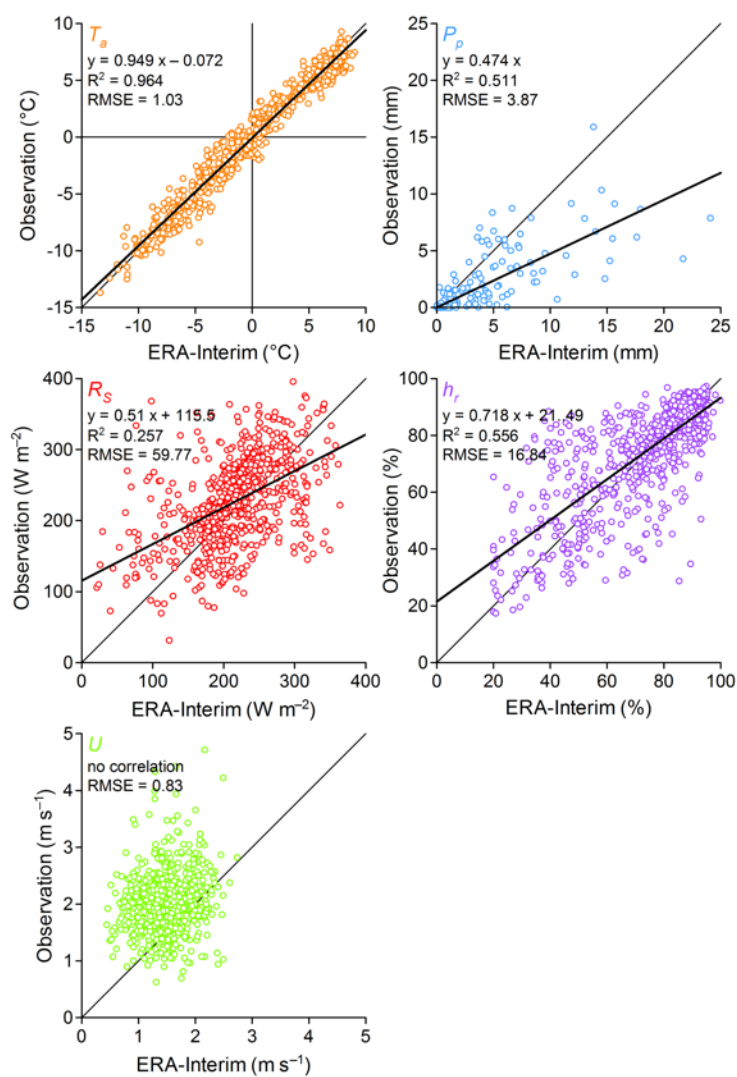


Figure R13: Scatter plot of air temperature, precipitation, solar radiation, relative humidity and wind speed between ERA-Interim reanalysis and observational data for 2002–2004.

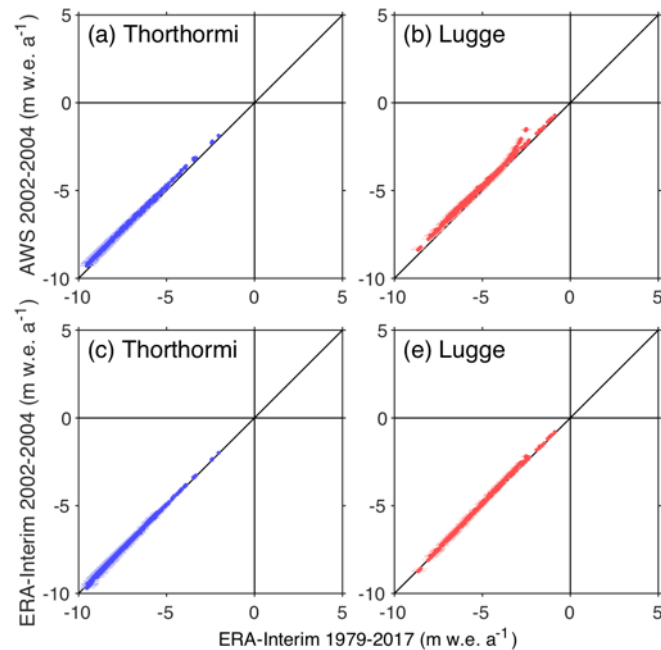


Figure R14: Scatter plot between SMBs of (a and c) Thorthormi and (b and d) Lugge Glaciers. SMBs calculated from ERA-Interim reanalysis data (1979–2017) against (a and b) observational meteorological data (2002–2004) and (c and d) ERA-Interim data (2002–2004). Error bars denote standard deviations derived from the long-term variability (1979–2017).

I found it confusing to have a study focusing on 2 glaciers (Thorthormi, Lugge) but including in fact 3 glaciers (the 2 previous glaciers and Lugge II). I know that finally most of the study is based on the comparison between Thorthormi and Lugge, because the flow model has not been applied on Lugge II, but finally why? Would the results have been different? With this partial study on Lugge II, I do not see any added value.

We excluded Lugge II Glacier from the detailed discussion because lack of the bed topography hampered the flow modelling. Spatial variability in surface elevation change derived from ASTER-DEMs is greater than those of Thorthormi and Lugge Glaciers (Fig. R2). Therefore, it is unsure whether the elevation change derived from DGPS-DEMs is representative. For these reasons we excluded Lugge II Glacier from the surface velocity measurements, SMB modelling and the

detailed discussion. We will remove descriptions and figures related to Lugge II Glacier from the revised manuscript but we will leave the rate of elevation change of the glacier as an observational fact.

Specific comments

Line 19: Mölg instead of Mörg, same in the reference list

We will change here and the reference list in the revised manuscript.

Line 21-22: images used by Bajracharya et al (2014) in 1980 to quantify the area reduction of Himalayan glaciers were full of snow, and in turn the area reduction from 1980 to 2010 is likely to be exaggerated. I recommend to report here the area reduction from 1990 to 2010, likely more accurate. This comment is valid for every places where this study is cited (section study area). It might be useful to compare the glacier area reduction obtained in this present study (section 3.3 – period 2000-2011) with the results of Bajracharya et al (2014) for the period 2000-2010.

We will change the area reduction from 1980–2010 to 1990–2010. Our analysis of glacier area reduction from 2000 to 2011 will be compared with the results from Bajracharya et al. (2014) in the revised manuscript.

L24: -0.22 +/- 0.12 m w.e./a (Gardelle et al, 2013) is not restricted to the ablation area but for the entire glaciers: this figure corresponds to the region-wide mass balance. Same comment for Maurer et al (2016), -0.17 m w.e./a is the glacier wide mass balance, not the ablation area

We will change “the ice thinning rate in the ablation are of” to “glacier-wide mass balance of” in the revised manuscript.

L30: may be worth updating the reference and citing Huss and Hock, 2018 here (Nature Climate Change, VOL 8 | FEBRUARY 2018 | 135–140 | www.nature.com/natureclimatechange)

We will change the citation to their latest study in the revised manuscript.

L54: I disagree with this statement, DEM differencing using satellite images do allow extracting signals of a few meters, especially with the new generation of satellite images i.e. Pléiades, World view. . . The best proof of this are the references just cited above.

Reviewer #2 and #3 also pointed out accuracy of DEMs derived from UAV and laser/radar altimetry, and we agree. We will remove the statement “However, the accuracy of the remotely sensed DEMs is still insufficient to measure several metres of glacier elevation change.” in the revised manuscript.

L56-58: in Nepal, Vincent et al (2016) show that the repeated DGPS profiles performed in the field were accurate enough to extract a thinning rate along the considered profile, but more importantly, they also said that this thinning rate along the profile is not representative of the whole glacier surface, or cannot be extrapolated in space given that the spatial variability of this thinning rate is extreme over debris covered tongues, due to the large variability of debris thickness and heterogeneity, presence of ponds or cliffs. Therefore, using remote sensing techniques (satellite, UAV) to obtain a thinning rate over the debris cover tongue is more accurate than performing sporadic repeated DGPS profiles.

The repeated DGPS survey accurately measured spatially homogeneous thinning rate over a debris-free glacier without supraglacial ponds and ice cliffs. As Vincent et al. (2016) argued, remote-sensing techniques (e.g., UAV) has advantage to study thinning of a debris-covered glacier. This is because significantly variable debris thickness and surface conditions (ponds and ice cliffs) are more covered by such techniques than DGPS survey. We will describe such an advantage of remote-sensing observations after “(e.g., Gardelle et al., 2013; Maurer et al., 2016; Brun et al., 2017)” and remove “Nepal (Vincent et al., 2016)” in the revised manuscript.

L67: it might be worth including the elevation range of each glacier, at least to have an idea of their maximum elevation, and the fact that they are potentially cold or polythermal. This issue is important for flow modelling

We will add minimum, medium and maximum elevations of each glacier in Table S1 in the revised supplement. We agree that ice temperature condition is important for flow modelling. Polythermal structure was reported at higher elevation (>5000 m) in Yala and Khumbu Glaciers in the Nepal Himalaya (Mae et al., 1975; Watanabe et al., 1984; Ozawa, 1991). However, ice temperature is not known for Bhutanese glaciers. Figs 6e and 6f in the discussion paper show that ice flow is mostly due to basal sliding in the ablation zone of both Thorthormi and Lugge Glaciers. Therefore, we assumed the glaciers as temperate in the flow model, the influence of this assumption to the modelling is small because our model showed active sliding at the bed of the glaciers. We will add this discussion in the revised manuscript.

L100: the benchmarks for DGPS measurements are indicated in fig 1 (4 green crosses) but there is no benchmark visible on Fig 1 2.5 km from Thorthormi snout. Did you relate benchmarks indicated in Fig 1 to the benchmark obtained with PPP processing?

We will extend a plot area of Fig. 1a further to the western side and add the benchmark at 12.5 km from the terminus of Thorthormi Glacier in the revised manuscript.

L174 details without e

We will change in the revised manuscript.

L200: are the glaciers of this study temperate?

No information is available for thermal condition of the studied glaciers. We assumed the glaciers are temperate because our model showed active sliding at the bed of the glaciers.

L203: what is the elevation at 5100 and 3500 m of the termini of Thorthormi and Lugge glaciers, respectively?

We will add elevations at the termini (Thorthormi: 4442 m, Lugge: 4530 m) and upper most boundary of the model domains (Thorthormi: 4813 m, Lugge: 5244 m) in the revised manuscript.

L207: strange to see the appearance of Fig 6 right after fig1

We agree to your suggestion. We will change citation from Fig. 6 to Fig. 1 in the revised manuscript.

L255-59: not very consistent to say earlier that the inter annual variability is somehow questionable (1129) and then to discuss here this interannual variability! Is it truly significant?

We will remove interannual variability in flow velocity in the revised manuscript.

Fig 4a: it is strange and not very consistent to see the annual glacier outlines crossing each other, as if from one year to the following, some areas of the glacier were expanding while some others were shrinking. This is likely not to be realistic.

Glacier outlines were judged from multiple Landsat images, and it was verified using ALOS PRISM images from the same period and Google Earth. Many floating icebergs were observed in the lake by in-situ measurements and satellite images. Presumably, these icebergs came from the bottom of the lake by acting subaqueous calving. We excluded floating icebergs in the lake from the glacial area. Although glacier outlines are not necessarily clear because of debris covering, the

obtained glacier terminus retreated or advanced depending on the location. According to analysis using Landsat images with 30 m resolution (Paul et al., 2013), a user-induced accuracy error was estimated to be 5% of delineated area of glaciers with more than 1 km². Following the previous study, we estimated user-induced accuracy error by 5% in the revised manuscript.

Line 268-69: on fig 4b, we observe the opposite, with the northern half retreating less rapidly than the southern half

In this sentence, we focus on the period of 2009–2011. During the period, the northern half retreated more rapidly than the southern half.

L281: given that the uncertainty on the SMB difference between both glaciers is expected to be very high (see general comment), the result “substantial influence of glacier dynamics on ice thickness change” is not supported as long as there is no sensitivity test on the SMB results, or any additional information to validate SMB simulations.

See reply to the major comment #3.

L292-94: I do not agree with the authors when they are mentioning that the agreement between observed and simulated surface velocities are good (fig 6e and f, lines red and blue, respectively). Looking at fig 7f, it is hard to believe that there is no more than 7% difference between observations and simulations: how is it obtained? More importantly, the velocity depends on the bedrock topography, obtained from Farinotti et al (2009). How reliable is it? how sensitive is the bedrock topography on velocity fields?

Difference between observed and calculated surface velocities (7%) in Fig. 6f was obtained by taking mean velocities (observation: 43.19 m a⁻¹, calculation: 40.22 m a⁻¹) over the calculation domain (0–3500 m). We performed sensitivity analysis of ice thickness. See reply to the major comment #4.

L327: “over recent decades” give the exact period to facilitate the comparison with the period 1974-2006.

We will change “in recent decades” to “during the period of 2004–2011” in the revised manuscript.

Table 1: I am confused about the periods: dh or dh/dt are obtained during 2004-2011, but SMB are obtained during 2002-04 and simulated dh/dt during 2002-2010. Not all periods match which makes also the comparison not very reliable. Another question regarding SMB in table 1, over which area of the glacier is it calculated?

SMB was recalculated for the period of 1979–2017 (see reply to the major comment #5). We used simulated dh/dt during 2002 to 2010 as for 2004–2011. We also estimated uncertainty of simulated dh/dt from the interannual variability in flow velocity over the observation period ($<5.6 \text{ m a}^{-1}$). The SMB in Table 1 covers only the area of GPS measurements. The mean emergence velocity in Table 1 was calculated only in the elevation range covered by the GPS survey. We will add the above explanation in Table 1 in the revised manuscript.

L332-33: Gardelle, Brun and Kaab studies cover more or less the same period i.e. 1999-2001; 2000-2016 and 2003-2008 respectively (with Kaab study being shorter though) and the results are not always significantly different (i.e. Brun and Kaab) so I agree that we can say that the mass loss is intensified since 2000, but only based on the comparison of these 3 studies with Maurer’s covering 1974-2006. I also totally agree that this acceleration is potentially not significant as stated lines 327-328

We agree to your suggestion that the mass loss has increased since 2000 based on the studies by Gardelle, Brun, Kaab and this study with Maurer’s result. We will change to “Regional mass balances in northern Bhutan have accelerated from the

period for 1974–2006 to after 1999. For example, the region-wide mass balance is -0.17 ± 0.05 m w.e. a^{-1} for 1974–2006 (Maurer et al., 2016), -0.22 ± 0.12 m w.e. a^{-1} for 1999–2011 (Gardelle et al., 2013), -0.42 ± 0.20 m w.e. a^{-1} for 2000–2016 (Brun et al., 2017) and -0.52 ± 0.16 m w.e. a^{-1} for 2003–2008 (Kääb et al., 2012).” in the revised manuscript.

L344-47: somehow senseless and not very relevant to compare SMB and thinning rates over disconnected periods (2002-04 and 2004-11, respectively) especially because SMB may have large inter-annual variability.

SMB was recalculated for the period of 1979–2017. Interannual variability of SMB was discussed by comparing long-term (1979–2017) and observed periods (2002–2004) (see reply to the major comment #5).

L355: the emergence velocity obtained from equation 11 is very sensitive to the choice of the surface slope alpha. How is it obtained? From a DEM, which resolution?

Surface elevation was extracted from the ASTER-DEM (15 m resolution) every 100 m along the central flowline of the glacier. This elevation data was filtered with a bandwidth of 1000 m and used for the upper boundary of the flow model. Surface slope α was obtained every 100 m from the surface topography of the model domain. We will add this explanation in the revised manuscript.

L358: negative emergence velocity is submergence velocity?

Yes, the negative emergence velocity indicates submergence velocity. But, we consolidate to use only emergence velocities to avoid misunderstanding.

L374-76: the mismatch between model and observation may have other origins than only the ice thickness or sliding coefficient: other sources of uncertainties may come from SEB computation affecting the model results or interpolation of

DGPS measurements impacting thinning rate observations. A systematic sensitivity analysis is needed. Farther in the text, the authors claim that the SEB uncertainty is 11% based on fig S1b which shows the standard deviation of the thermal resistance. Actually, there are much more sources of uncertainties and the SEB uncertainty is likely much higher. (see general comments)

We performed a sensitivity analysis of each meteorological parameter in the SMB model. See reply to the major comment #3. We discussed spatial representativeness of the rate of elevation change derived from DGPS-DEMs. See reply to the major comment #2.

References:

- Mae, S., H. Wushiki, Y. Ageta and K. Higuchi (1975): Thermal drilling and temperature measurements in Khumbu Glacier, Nepal Himalayas, Seppyo, 37(4), 161–169 (in Japanese with English abstract).
- Ozawa, H. (1991): Thermal regime of a glacier in relation to glacier ice formation. (PhD thesis, Hokkaido University)
- Watanabe, O., S. Takenaka, H. Iida, K. Kamiyama, K.B. Thapa and D.D. Mulmi (1984): First results from Himalayan glacier boring project in 1981–1982. Part I. Stratigraphic analyses of full-depth cores from Yala Glacier, Langtang Himal, Nepal, Bull. Glacier Res., 2, 7–23

Reply to Referee #2

We would like to thank the referee for thoughtful and useful comments. In the following, we describe our responses (in blue) point-by-point to each referee comment (*italic*).

This manuscript presents measurements of areal and surface elevation change, satellite-derived surface velocity data and modelled mass balance and ice dynamics data for three glaciers in the Bhutan Himalaya. One of these glaciers is land-terminating, another is transitioning between land-terminating and lake-terminating, and the third is lake-terminating. The ultimate goal is to be able to test whether proglacial lake development leads to increased glacier thinning rates. The conclusion is that it does, and that the glacier transitioning from land- to lake-terminating will accelerate and thin further as the proglacial lake develops. The manuscript is well-written, appropriately and clearly structured and the figures are good quality, but further work is required before it can be published in The Cryosphere.

Major comments:

1. My main concern relates to the lack of any real sensitivity testing to the many components that are assumed or estimated in the modelling – particularly relating to the surface mass balance. The stated uncertainty in the thermal resistance calculations are > 60 % alone. . . As a minimum it would be helpful to see the output from the debris thickness modelling to see if it is realistic. There are further assumptions relating to the linear temperature profile and albedo, for example, that need to be accounted for since the estimated mass balances are very negative compared with previous studies. How much impact are these terms having on the results? The ice flow modelling is simple, which is not a problem in itself, but certainly it would help to see some of the input datasets such as the ice thickness map to convince the reader it is somewhat realistic. And what impact does the chosen sliding coefficients have on the modelled results (beyond figure S3)?

Although debris thickness was not measured during the field campaign, ice is exposed from place to place over Thorthormi and Lugge Glaciers (Figs R1a and R1b), suggesting that debris-cover is rather thin than that of Lugge II Glacier (Fig. R1c). In addition, few supraglacial ponds and ice cliff exist over Thorthormi and Lugge Glaciers. So we emphasize that spatial variability of elevation change, thermal resistance and SMB are less than those the reviewers supposed. Anyhow, following the referees suggestion, we recalculated thermal resistance with considering sensible heat, for which pressure level temperature and geopotential height of NCEP2 are taken into account (Fig. R2). Scatter plot and spatial distribution of thermal resistances derived from the original method (net radiation only) and from recalculated one (net radiation + sensible heat) are shown in Figs R3 and R4. Spatial distribution of the difference between the two results is also shown in Fig. R4c. Thermal resistance significantly increased after the consideration of sensible heat (Fig. R3). However, large difference appeared only near the western margin (Fig. R4) probably because of relatively thick debris covering the area. We will recalculate the SMB distribution with the revised thermal resistance in the revised manuscript. We evaluated sensitivity of calculated meltwater against meteorological parameters (Fig. R5). We chose the meltwater instead of SMB to quantify the uncertainty in percentage. The tested parameters are surface albedo, air temperature, precipitation, relative humidity, solar radiation, thermal resistance and wind speed. Uncertainty of thermal resistance and albedo were assumed to be 100% and 40% based on Figs R2b and R2d. Uncertainties of each meteorological variable were assumed to be RMSEs of ERA-Interim reanalysis data against the observational data (Fig. R6). Variations in meltwater within a possible parameter range are estimated by quadratic sum of results from each parameter shown in Fig. R5. Estimated uncertainty of meltwater is less than 50% at a large part of Thorthormi and Lugge Glaciers (Fig. R7). We will replace figures by the recalculated results and add Figs R5, R6 and R7 to the revised supplement.

Detailed bedrock topography is unavailable for all the glaciers. Available bedrock topography data were shown in Figs 6a and 6b in the discussion paper. Because our model geometry is not based on data, we performed sensitivity

analysis using the broader range ($\pm 30\%$) of the sliding coefficient and ice thickness (Fig. R8). The RMSE between the modeled and measured flow velocities were computed as a measure of the model performance (Fig. R9). For Thorthormi Glacier, the model is similarly sensitive to sliding coefficient and ice thickness. For Lugge Glacier, the model is more sensitive to ice thickness than sliding coefficient. Figs R8 and R9 will be added to the revised supplement.

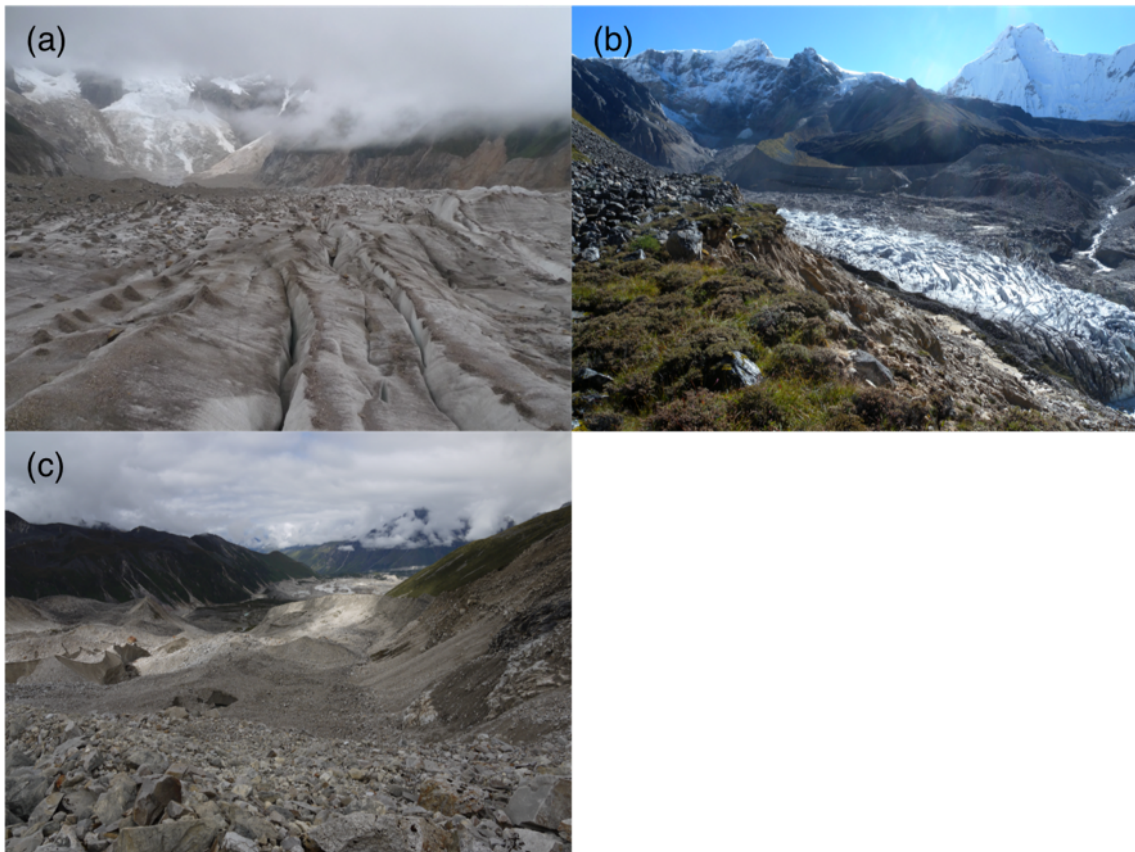


Figure R1: Photographs showing surface condition near the termini of (a) Thorthormi (18 September 2011), (b) Lugge (20 September 2011) and Lugge II Glaciers (21 September 2011).

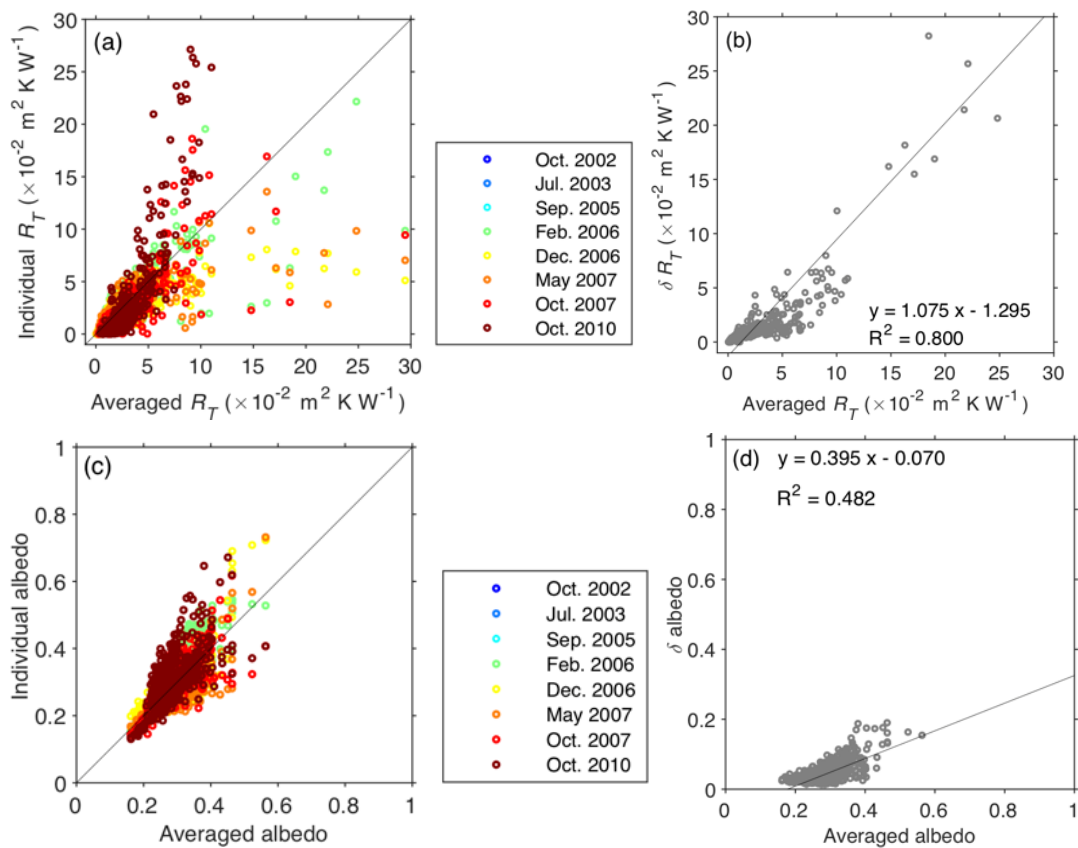


Figure R2: Scattergram of (a) thermal resistance (R_T) of the multitemporal ASTER data against their average derived from net radiation + sensible heat, which is used to calculate ice melting under the debris-covered surface of Thorthormi, Lugge and Lugge II Glaciers. (b) Standard deviations (δ) of thermal resistance. (c) Scattergram and (d) standard deviations of albedo.

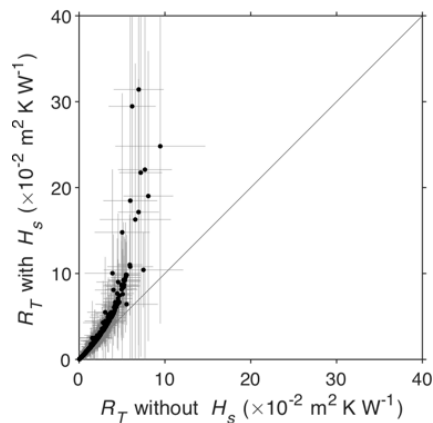


Figure R3: Scatter plot between thermal resistance calculated from only net radiation (without H_s) and from net radiation + sensible heat (with H_s).

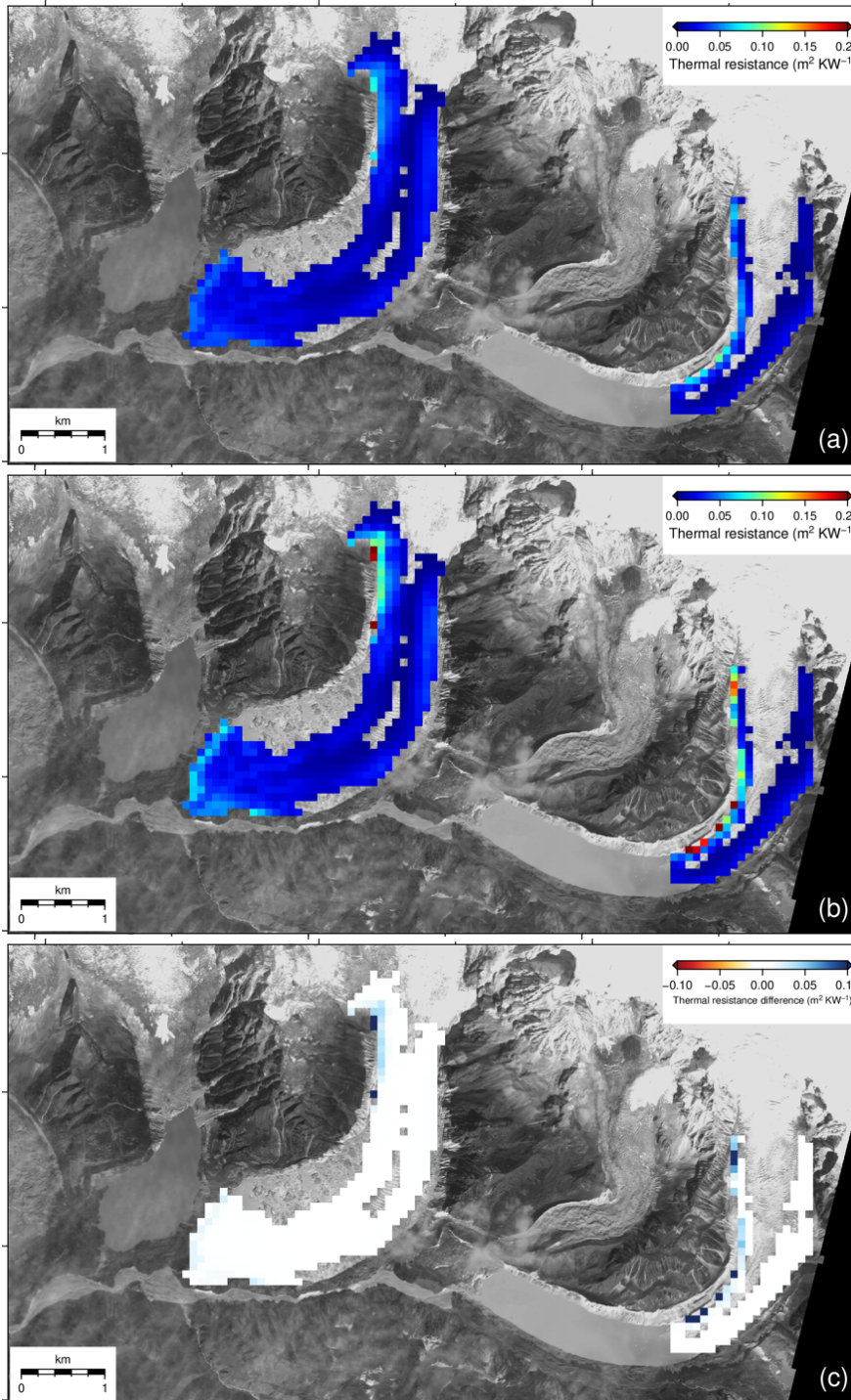


Figure R4: Spatial distribution of thermal resistance calculated (a) from only net radiation, (b) from net radiation + sensible heat and (c) difference of thermal resistance calculated by the two methods.

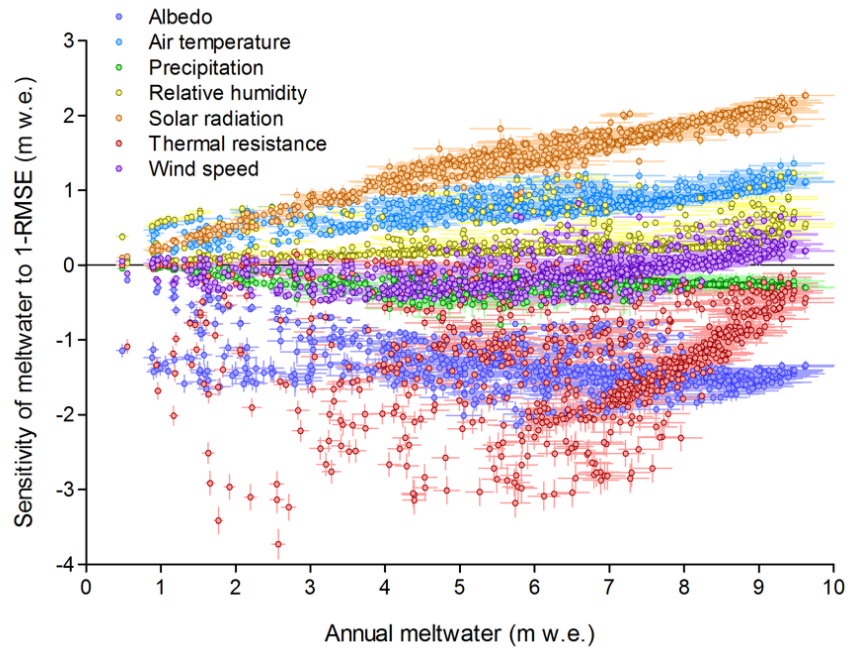


Figure R5: Sensitivity analysis of annual meltwater as a function of RMSE of each meteorological parameter at debris-covered area. Horizontal axis is variable annual meltwater calculated each grid in the SMB model. RMSEs except for albedo and thermal resistance are obtained from ERA-Interim and observed data for 2002–2004 (Fig. R6). Uncertainties of albedo and thermal resistance are derived from 8 satellite images (Fig. R2).

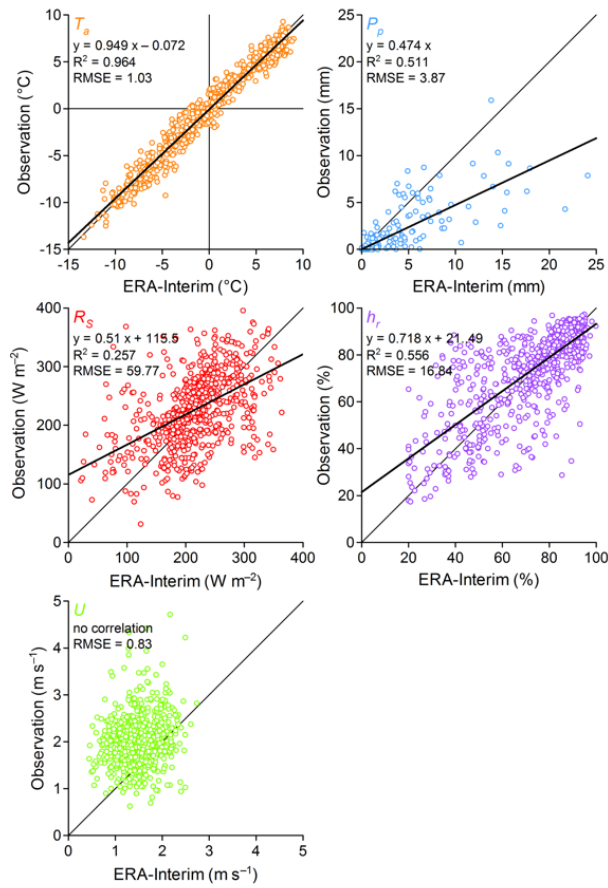


Figure R6: Scatter plot of air temperature, precipitation, solar radiation, relative humidity and wind speed between ERA-Interim reanalysis and observational data for 2002–2004.

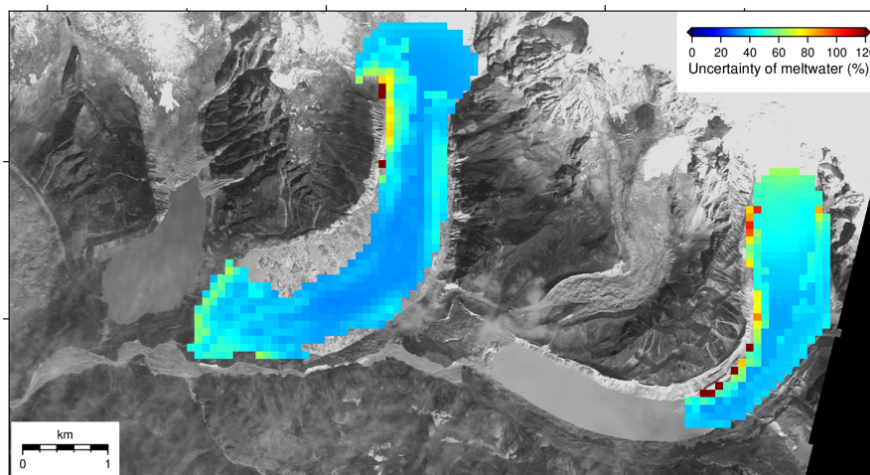


Figure R7: Spatial distribution of estimated uncertainty in the computed annual meltwater volume.

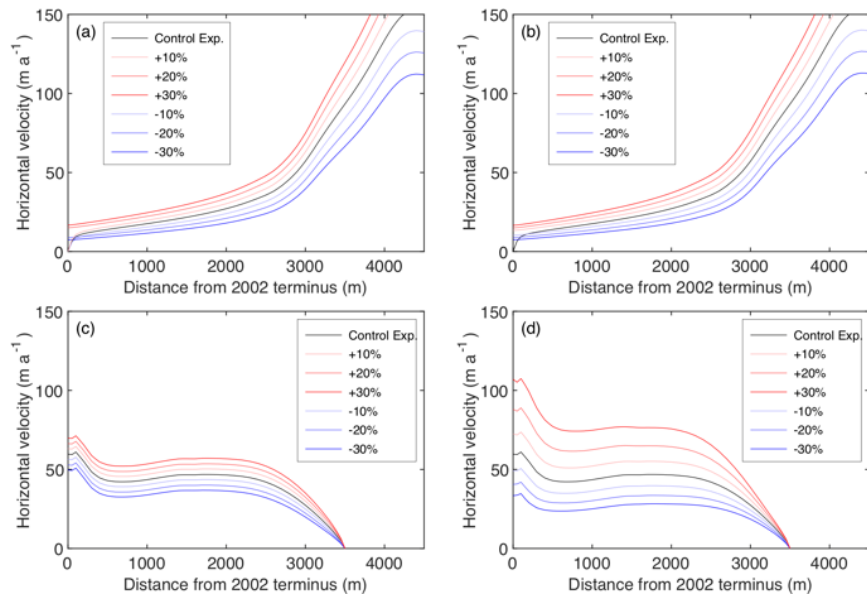


Figure R8: Surface velocity computed for (a and b) Thorthormi and (c and d) Luge Glaciers obtained by changing (a and c) the sliding coefficient (C) by $\pm 30\%$, and (b and d) ice thickness by $\pm 30\%$. The black line is the control experiment.

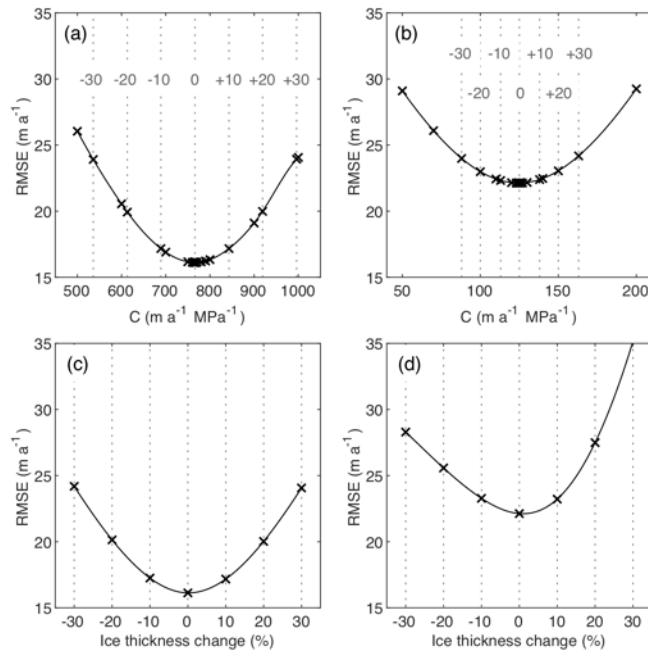


Figure R9: RMSEs between the modelled and measured surface velocities of (a and c) Thorthormi and (b and d) Luge Glaciers, modelled with various (a and b) sliding coefficient (C), and (c and d) various ice thickness.

2. The main conclusion of the manuscript is, as I understand it, that lake development does impact ice dynamics, and therefore thinning rates. I didn't get this from first reading, mainly because the two glaciers on which the manuscript focuses (Thorthormi and Luggé) are not easy to compare – they have very different geometries, different debris distributions, and different flow regimes (even before accounting for lake vs nolake). Given this, perhaps spending a bit more time looking at the lake- vs no-lake simulations for Luggé Glacier might help (the latter of which is given little attention at present). And/or looking further at what has happened at Thorthormi following lake development (see point 4 below). There are also several statements about the low impact of ice dynamics on the thinning rates of Luggé Glacier, yet a final forecast of rapid changes at Thorthormi Glacier once the lake develops – how can these two assertions be reconciled? Is it that emergence velocity at Luggé would be (more) positive in the absence of a lake? Overall, spending some further time sharpening the take-home message would be beneficial.

The main conclusion of this study is that the dynamically-induced ice thickness change is small, and thinning of Luggé Glacier is mainly caused by negative SMB. On the other hand, more negative SMB is counterbalanced by dynamically-induced ice thickening, resulting in a smaller thinning rate of Thorthormi Glacier. Based on this conclusion, we hypothesize that the emergence velocity will decrease at Thorthormi Glacier after the expansion of the supraglacial lake, resulting in an increase in ice thinning rate. To test this hypothesis, we will discuss the influence of lake expansion on the emergence velocity based on lake- (Experiment 1) and land-terminating (Experiment 2) simulations for Luggé Glacier in the revised manuscript. We do not conduct additional analysis on surface elevation change of recent Thorthormi Glacier using satellite data (see reply to the major comments #3 below).

3. Somewhere it needs to be explicitly acknowledged that this is a very (very) small sample. While the field data clearly cannot be replicated, an abundance of satellite remote sensing data are available to test some of these ideas across the broader

Lunana area. I acknowledge this would require significant further data processing, but augmenting the dataset would certainly give the study more substance.

Satellite-based observations of glacier elevation change across the Bhutan Himalaya were carried out by Gardelle et al. (2013) and Maurer et al. (2016). We acknowledge the studies covering a large area and a greater number of samples. Nevertheless, our study has advantages in accuracy, and we performed additional analysis as described below. We evaluated surface elevation change of the studied glaciers by ASTER-DEMs, which is however to examine spatial representativeness of DGPS-DEMs. According to the accuracy analysis, we found that ASTER-DEMs ($\sigma \sim 20$ m; Fig. R10) has 10 times larger uncertainty in vertical coordinates than DGPS-DEMs ($\sigma = 1.91$ m; see Fig. 2a in the discussion paper). The unique point of this study is to evaluate glacier surface elevation change by highly accurate DGPS data. We also investigate the contribution of ice dynamics to ice thinning that has not been quantified in the previous studies. We explain these points in the revised manuscript and take the suggested satellite analysis over a broader area as a future work.

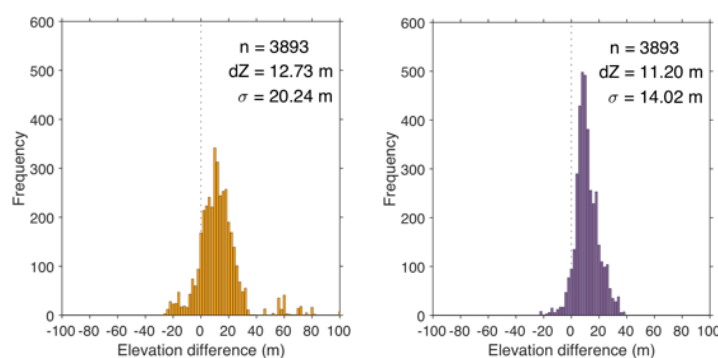


Figure R10: Elevation differences in the ice-free area (left) between 2004 ASTER-DEM and DGPS-DEM and (right) between 2011 ASTER-DEM and DGPS-DEM.

4. The forecast for an impact on ice dynamics at Thorthormi is interesting, but represents a missed opportunity I think. Why not test this prediction, using velocity (and perhaps also surface elevation) data derived from more recent satellite imagery (it has been 7 years since detachment from the terminus). If this

analysis does indeed show that the glacier has accelerated and thinned, it would add great weight to the existing conclusions.

We acknowledge the test our prediction using surface velocity data derived from satellite images acquired after 2011. Nevertheless, quantifying interannual variability in surface velocity is difficult because of insufficient accuracy of the observation. Surface velocity observations of Thorthormi Glacier after 2013 was carried out by multitemporal Landsat 8 OLI images (Fahnestock et al., 2015). However, it is also difficult to quantify velocity change because of coarser spatial resolution and lower accuracy than our velocity data. We will not carry out additional analysis of surface velocity and surface elevation change of the glaciers by satellite remote sensing data because of the reasons described above and as a reply to the major comment #3.

Minor comments (per line number)

1-5: these two sentences are almost identical. Suggest rewording one or the other.

We will change in the revised manuscript as follows. “Despite the importance of glacial lake development in ice dynamics and glacier thinning, in situ and satellite based measurements from lake-terminating glaciers are sparse in the Bhutan Himalaya, where a number of supraglacial lakes exist. We acquired in situ and satellite based observations across lake- and land-terminating debris-covered glaciers in the Lunana region, Bhutan Himalaya.”

5: spell out GPS in full

We will change as suggested in the revised manuscript.

6: move ‘for the 2004-2011 period’ to end of sentence

We will change as suggested in the revised manuscript.

12: does it really 'more than offset' glacier thinning? Surely this would result in thickening? Suggest 'compensates'...

We will change from “more than offsets” to “compensates” in the revised manuscript.

24: insert 'particularly' before 'sensitive' given that all glaciers are impacted by changes in temperature and precipitation

We will change as suggested in the revised manuscript.

28: remove 'therefore' given this sentence is not substantiated by preceding text

We will remove it in the revised manuscript.

29: what is meant by 'mechanisms' – this is rather vague. . .

“mechanisms” here means mechanisms of much greater mass loss of Bhutanese glaciers than other glaciers in eastern Himalayas. We will change from “their mechanisms” to “mechanisms of mass loss of Bhutanese glaciers”.

47: spell out GPS at first use in main text

We will change as suggested in the revised manuscript.

54: I'm not sure remote sensing methods can't measure several metres of change. How about lidar? Suggest change to 'small' changes in surface elevation.

Reviewer #2 and #3 also pointed out accuracy of DEMs derived from UAV and laser/radar altimetry, and we agree. We will remove the statement “However, the accuracy of the remotely sensed DEMs is still insufficient to measure several metres of glacier elevation change.” in the revised manuscript.

55: change 'sub-metre' to 'centimetric'?

We will change as suggested in the revised manuscript.

57: change 'performed' to 'acquired'

We will change as suggested in the revised manuscript.

59: remove 'rapid' since no results have been presented at this stage of the manuscript

We will remove it in the revised manuscript.

63-64: yes, but the glaciers are entirely different in geometry – some better justification for site selection is required here

We will change reasons of selecting the glaciers as follows. “Thorthormi and Lugge glaciers were selected for analysis because these glaciers are situated around the same elevation. Lugge Glacier terminates a proglacial lake of Lugge Glacial Lake, while the terminus of Thorthormi Glacier is grounded but developing a large supraglacial lake (Bajracharya et al., 2014). Thus, making them suitable for evaluating the contribution of ice dynamics to the observed ice thickness changes. The glaciers are also suitable for field measurements because of its relatively safe ice-surface conditions and proximity to trekking route.”

65: using 'dynamic thinning' here is pre-emptive – it could be thickening too. . . maybe change to 'dynamics'?

We will change to “dynamics” in the revised manuscript.

65-66: change 'the surveyed glacier thinning' to 'changes in glacier surface

elevation'

We will change as suggested in the revised manuscript.

72: is this thinning rate a mean value for the ablation area? Needs specifying.

We will change to “Ablation area of the glacier thinned...” in the revised manuscript.

75: is this what defines a land-terminating glacier? Does whether it is grounded or floating not represent a better criterion?

We will change to “In 2011, the glacier terminus was grounded, and thus Thorthormi Glacier was a land-terminating glacier” in the revised manuscript.

101 and elsewhere: I'm not sure what TCD protocol is for referencing web pages but this is awkward – can the full url not be put in the reference list?

As replied to a comment from Referee #3, this format was used in a paper recently published in *The Cryosphere* (e.g., Friedl et al., 2018). Therefore, our manuscript also follows this format.

112: very few points of elevation change are shown in Figure 1. . . where can I see these 431, 248 and 258 points?

The grid size of the rate of elevation change in Fig. 1a is enlarged to 50 m, which was averaged from 1-m resolution DEMs for better visibility.

114: 'off-glacier' should be hyphenated

We will change as suggested in the revised manuscript.

119: specify the sample number is 'n'

We will change “the sample number n ” in the revised manuscript.

125: comment on the quality of the co-registration?

The accuracy of the co-registration is estimated to be 0.05 pixel (ASTER Science Project, Japan Space Systems, 2012). We will add it in the revised manuscript.

131: how can a single window size of 16 x 16 pixels be multi-scale?

We will change to “with a correlation window size of 16 x 16 pixels” in the revised manuscript.

136: replace 'aerial' with 'areal'

We will change as suggested in the revised manuscript.

141-143: why exclude the ponds? Would these not have ice beneath or do you think they have melted down to bedrock? Does this explain the very odd digitising of glacier area presented in Figure 4a?

It is difficult to identify whether glacial ice exist beneath supraglacial lakes and ponds. However, many floating icebergs were observed in the lake by in-situ measurements and satellite images. Presumably, these icebergs came from the bottom of the lake by acting subaqueous calving. We excluded floating icebergs in the lake from the glacial area. The annual glacier outlines were judged based on previously proposed manual / automatic digitise methods (e.g., Bajracharya et al., 2014; Nuimura et al., 2015; Nagai et al., 2016). According to the previous studies, supraglacial lakes and ponds are excluded from glacial area.

152: change 'calculated' to 'estimated' given there are many uncertainties in the

modelling

We will change as suggested in the revised manuscript.

159: that's a large uncertainty. How does it propagate through for the rest of the modelling?

See a reply to the major comment #1.

230: make it clear here that you're simulating a lake-free Lugge Glacier – I read this that at present the lake is frozen! Suggest 'For Lugge Glacier, we simulate a lake-free situation, with ice flowing to the contemporary terminal moraine' or similar

We will change as suggested in the revised manuscript.

315-316: are these both '-3 to 0 m a-1' by coincidence or is there a typo?

These two thinning rates are coincidence.

341-342: but you go on to show that dynamics only play a minor role in thinning at Lugge. . . are you suggesting dynamics were more important following initial lake development?

We will change from “dynamic thinning was enhanced” to “dynamic thickening was weakened” in the revised manuscript.

344: specify this is 'simulated' SMB. . .

We will add “simulated” here in the revised manuscript.

427: does this statement that dynamic thinning is small at Lugge not undermine

the main take-home message of the manuscript?

Our conclusion is that the dynamically-induced ice thickness change is small, and significant ice thinning of current Lügge glacier is mainly caused by negative SMB. So that the statement here is consistent with our conclusion.

537: replace 'Mörg' with 'Mölg'...

We will change here and in the reference list in the revised manuscript.

Figure 1: can you indicate the ponds that ultimately coalesce into a lake on Thorthormi?

Because the location and size of the ponds are significantly varied from year to year, we could not indicate the ponds that coalesce into a large supraglacial lake. Coalescence of these ponds into a lake is confirmed by the Google Earth.

Figure 3: can you be sure these data towards the terminus of Lügge are not tracking the recession of the ice-front? How do you avoid matching the ice-front (i.e. the dominant feature) in these locations?

We excluded velocity measured near the glacier frontal margin to avoid such problems.

Figure 4: how were these outlines derived? They look very odd to me, with no obvious distinction in the debris-cover around any of the digitised outlines...

Glacier outlines were judged from multiple Landsat images, and it was verified using ALOS PRISM images from the same period and Google Earth. Many floating icebergs were observed in the lake by in-situ measurements and satellite images. Presumably, these icebergs came from the bottom of the lake by acting subaqueous calving. We excluded floating icebergs in the lake from the glacial area.

Although glacier outlines are not necessarily clear because of debris covering, the obtained glacier terminus retreated or advanced depending on the location. According to analysis using Landsat images with 30 m resolution (Paul et al., 2013), a user-induced accuracy error was estimated to be 5% of delineated area of glaciers with more than 1 km². Following the previous study, we estimated user-induced accuracy error by 5% in the revised manuscript.

References:

- Fahnestock, M., T. Scambos, T. Moon, A. Gardner, T. Haran, and M. Klinger: Rapid large-area mapping of ice flow using Landsat 8, *Remote Sensing of Environment*, 185, 84–94, <https://doi.org/10.1016/j.rse.2015.11.023>, 2015.
- Friedl, P., Seehaus, T. C., Wendt, A., Braun, M. H., and Höppner, K: Recent dynamic changes on Fleming Glacier after the disintegration of Wordie Ice Shelf, Antarctic Peninsula, *The Cryosphere*, 12, 1347–1365, <https://doi.org/10.5194/tc-12-1347-2018>, 2018.

Reply to Referee #3

We would like to thank the referee for thoughtful and useful comments. In the following, we describe our responses (in blue) point-by-point to each referee comment (*italic*).

The manuscript by Tsutaki et al. presents a comparison of three glaciers in the Bhutan Himalaya. Two of the three glaciers are studied to determine differences in glacier dynamics, retreat and mass wastage between land-terminating and lake-terminating glaciers, and whether the presence of a proglacial lake increases dynamics and ice wastage. To do this the authors: (a) present in situ measurements of surface elevation made using DGPS in 2004 and 2011 and compare them with remotely sensed elevation changes reported in literature; (b) derive glacier surface flow velocities using feature tracking on ASTER satellite imagery; (c) manually delineate retreat of the tongues using Landsat 7 imagery; (d) model surface mass balance of the debris covered glaciers, and (e) present a two-dimensional ice dynamics model and two model experiments. The results show that the lake-terminating glacier (Lugge) has considerable higher thinning rates than the land-terminating glacier (Thorthormi), but that this is mainly caused by differences in ice dynamics and not by differences in surface mass balance. A strong emergence is present for Thorthormi due to its longitudinally compressive flow regime that offsets its much more negative surface mass balance, and this is largely absent for Lugge. The manuscript is generally well-written besides some style issues, and the subject is of interest to the readers of the Cryosphere. There are, however, some technical issues and uncertainties with the modelling. At least moderate revisions are required before the manuscript can be published.

Major comments:

The authors present three glaciers in the manuscript: Thorthormi, Lugge and Lugge II. Lugge II was measured using the DGPS, was included in the spaceborne flow velocity measurements and was included in the SMB calculations, and its

results are presented in figures 1–3. However, it is not included in the ice dynamics model experiments, is barely discussed in the results and discussion, is not included in the abstract and therefore seems of little significance to the overall story. The authors argue in the introduction that Lugge II is at a different elevation and is therefore difficult to compare to the other two glaciers, but there are many more factors that control the dynamics and mass balance of the glaciers that can complicate the comparison, also between Thorthormi and Lugge, which should be acknowledged. In this light it is also odd that the authors state that the surface mass balance of Thorthormi is 37% more negative than Lugge because it is situated at lower elevation (L360). I would suggest that the authors decide to either remove Lugge II Glacier completely from the manuscript to focus more on a clear comparison of Thorthormi and Lugge, or to consistently include all glaciers in all analyses.

We excluded Lugge II Glacier from the detailed discussion because lack of the bed topography hampered the flow modelling. Spatial variability in surface elevation change derived from ASTER-DEMs is greater than those of Thorthormi and Lugge Glaciers (Fig. R1). Therefore, it is unsure whether the elevation change derived from DGPS-DEMs is representative. For these reasons we excluded Lugge II Glacier from the surface velocity measurements, SMB modelling and the detailed discussion. We will remove descriptions and figures related to Lugge II Glacier from the revised manuscript but we will leave the rate of elevation change of the glacier as an observational fact.

Comparison of Thorthormi and Lugge Glaciers are not easy. We hypothesize that the emergence velocity will decrease at Thorthormi Glacier after the expansion of the supraglacial lake, resulting in an increase in ice thinning rate as observed in Lugge Glacier. To test this hypothesis, we will discuss the influence of lake expansion on the emergence velocity based on lake- (Experiment 1) and land-terminating (Experiment 2) simulations for Lugge Glacier in the revised manuscript.

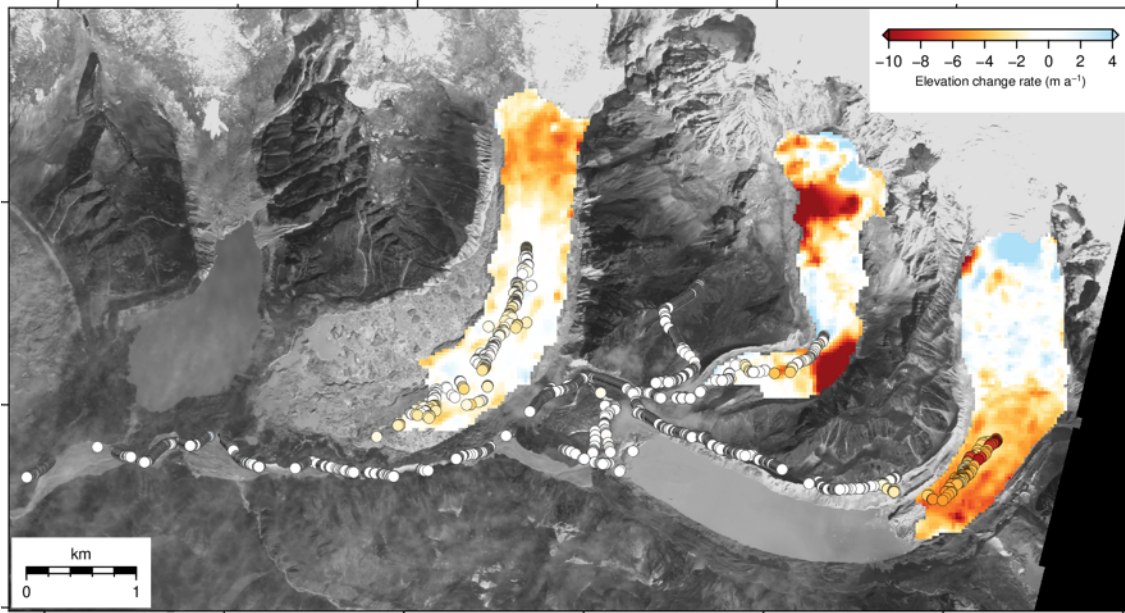


Figure R1: Rate of elevation change for the 2004–2011 period derived from ASTER-DEMs (background shadings) and DGPS-DEMs (circles filled with the same color scale). Glacier outlines are of December 2011.

I think more discussion on and comparison with other lake/land terminating glaciers reported in literature is required in the manuscript. This is touched on lightly in the manuscript but needs be more elaborate, especially because at present only two glaciers are used in draw conclusions and hypothesise on the dynamics of lake/land terminating glaciers. Can the differences in dynamics that are found for these glaciers transfer to others? Why, why not?

More rapid thinning of lake-terminating glacier than neighboring land-terminating glacier has been revealed by satellite remote sensing observations in Bhutan (Maurer et al., 2016), Nepal (Nuimura et al., 2012; King et al., 2017), Pamir-Karakoram-Himalaya (Gardelle et al., 2013) and Alaska (Trüssel et al., 2013). However, the previous studies have not quantified contributions of ice dynamics and SMB to those contrasted glacier thinning. This point is a unique approach of this study. In the revised manuscript, we will discuss the differences in ice dynamics affecting ice thinning by comparing a ratio of thinning rates between land- and lake-terminating glaciers reported by the previous studies.

Most of the methods deployed by the authors have considerable ranges of uncertainty and those should be addressed and discussed better. Especially the SMB modelling that is largely based on the rather uncertain thermal resistance obtained from ASTER data and a few (risky) assumptions seems to prone to uncertainty. The relatively very large negative SMB of Thorthormi is therefore questionable in my opinion. It has been shown in a number of articles in the last few years that using spaceborne thermal infrared imagery over debris-covered glaciers (e.g. Rounce & McKinney, Foster et al., Mihalcea et al, Gibson et al.) provides opportunities but also numerous difficulties and these should be acknowledged.

Although debris thickness was not measured during the field campaign, ice is exposed from place to place over Thorthormi and Lugge Glaciers (Figs R2a and R2b), suggesting that debris-cover is rather thin than that of Lugge II Glacier (Fig. R2c). In addition, few supraglacial ponds and ice cliff exist over Thorthormi and Lugge Glaciers. So we emphasize that spatial variability of elevation change, thermal resistance and SMB are less than those the reviewers supposed. Anyhow, following the referees suggestion, we recalculated thermal resistance with considering sensible heat, for which pressure level temperature and geopotential height of NCEP2 are taken into account (Fig. R3). Scatter plot and spatial distribution of thermal resistances derived from the original method (net radiation only) and from recalculated one (net radiation + sensible heat) are shown in Figs R4 and R5. Spatial distribution of the difference between the two results is also shown in Fig. R5c. Thermal resistance significantly increased after the consideration of sensible heat (Fig. R4). However, large difference appeared only near the western margin (Fig. R5) probably because of relatively thick debris covering the area. We will recalculate the SMB distribution with revised thermal resistance in the revised manuscript. We evaluated sensitivity of calculated meltwater against meteorological parameters (Fig. R6). We chose the meltwater instead of SMB to quantify the uncertainty in percentage. The tested parameters are surface albedo, air temperature, precipitation, relative humidity, solar

radiation, thermal resistance and wind speed. Uncertainty of thermal resistance and albedo were assumed to be 100% and 40% based on Figs R3b and R3d. Uncertainties of each meteorological variable were assumed to be RMSEs of ERA-Interim reanalysis data against the observational data (Fig. R7). Variations in meltwater within a possible parameter range are estimated by quadratic sum of results from each parameter shown in Fig. R6. Estimated uncertainty of meltwater is less than 50% at a large part of Thorthormi and Lugge Glaciers (Fig. R8). We will replace figures by the recalculated results and add Figs R6, R7 and R8 to the revised supplement.

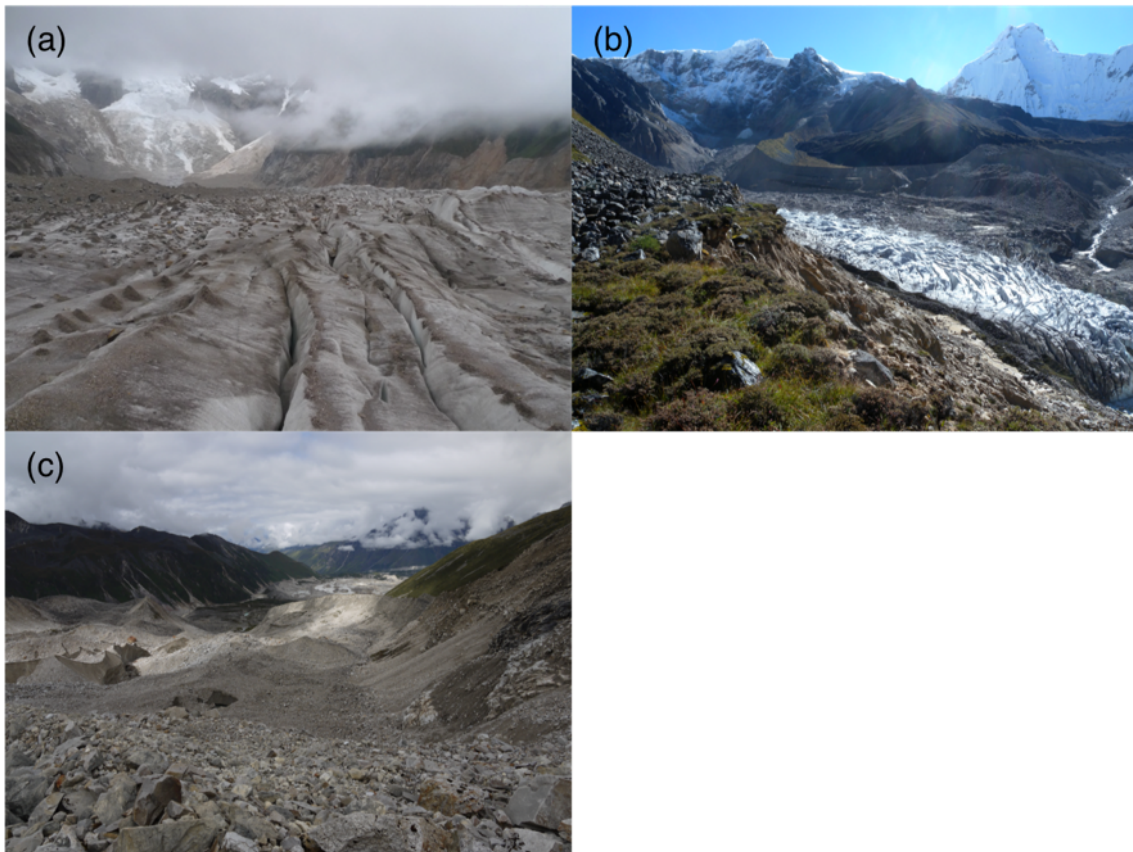


Figure R2: Photographs showing surface condition near the termini of (a) Thorthormi (18 September 2011), (b) Lugge (20 September 2011) and Lugge II Glaciers (21 September 2011).

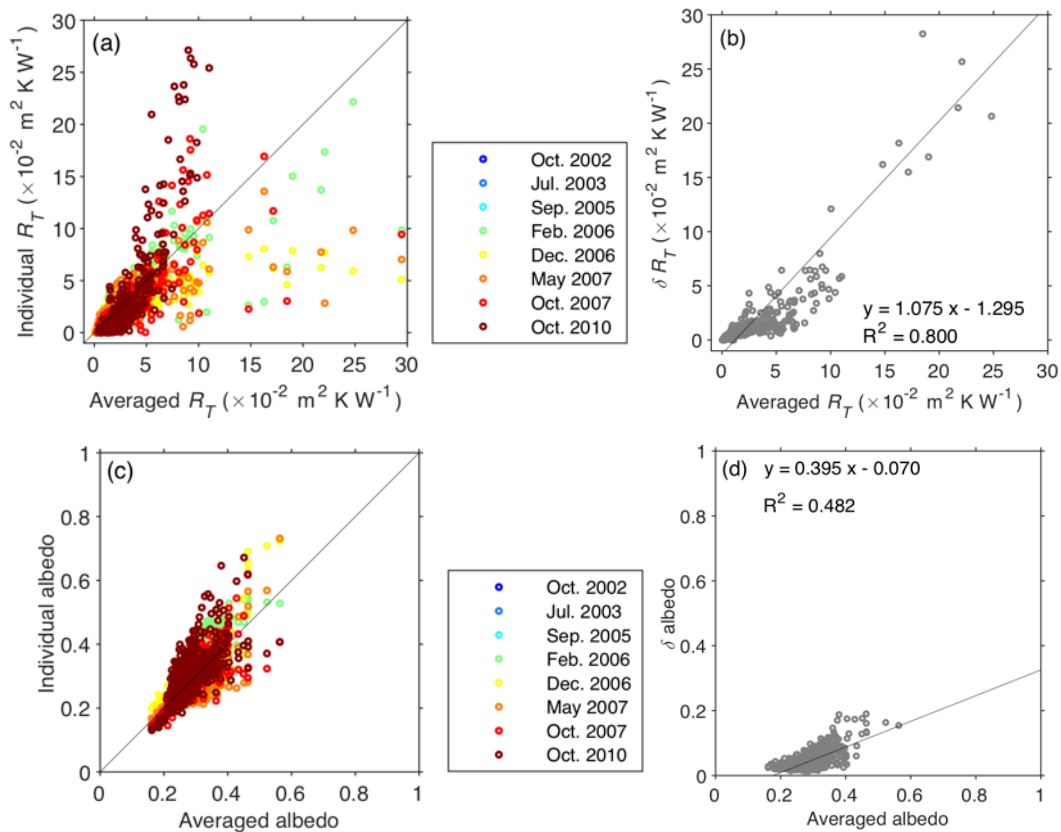


Figure R3: Scattergram of (a) thermal resistance (R_T) of the multitemporal ASTER data against their average derived from net radiation + sensible heat, which is used to calculate ice melting under the debris-covered surface of Thorthormi, Lugge and Lugge II Glaciers. (b) Standard deviations (δ) of thermal resistance. (c) Scattergram and (d) standard deviations of albedo.

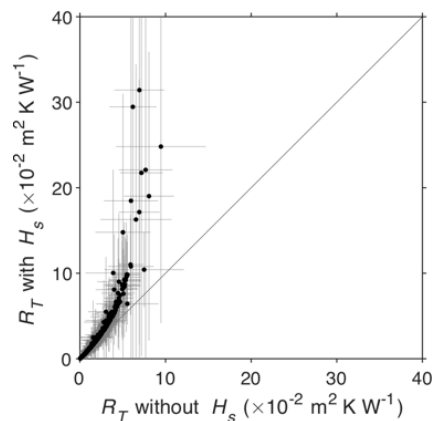


Figure R4: Scatter plot between thermal resistance calculated from only net radiation (without H_s) and from net radiation + sensible heat (with H_s).

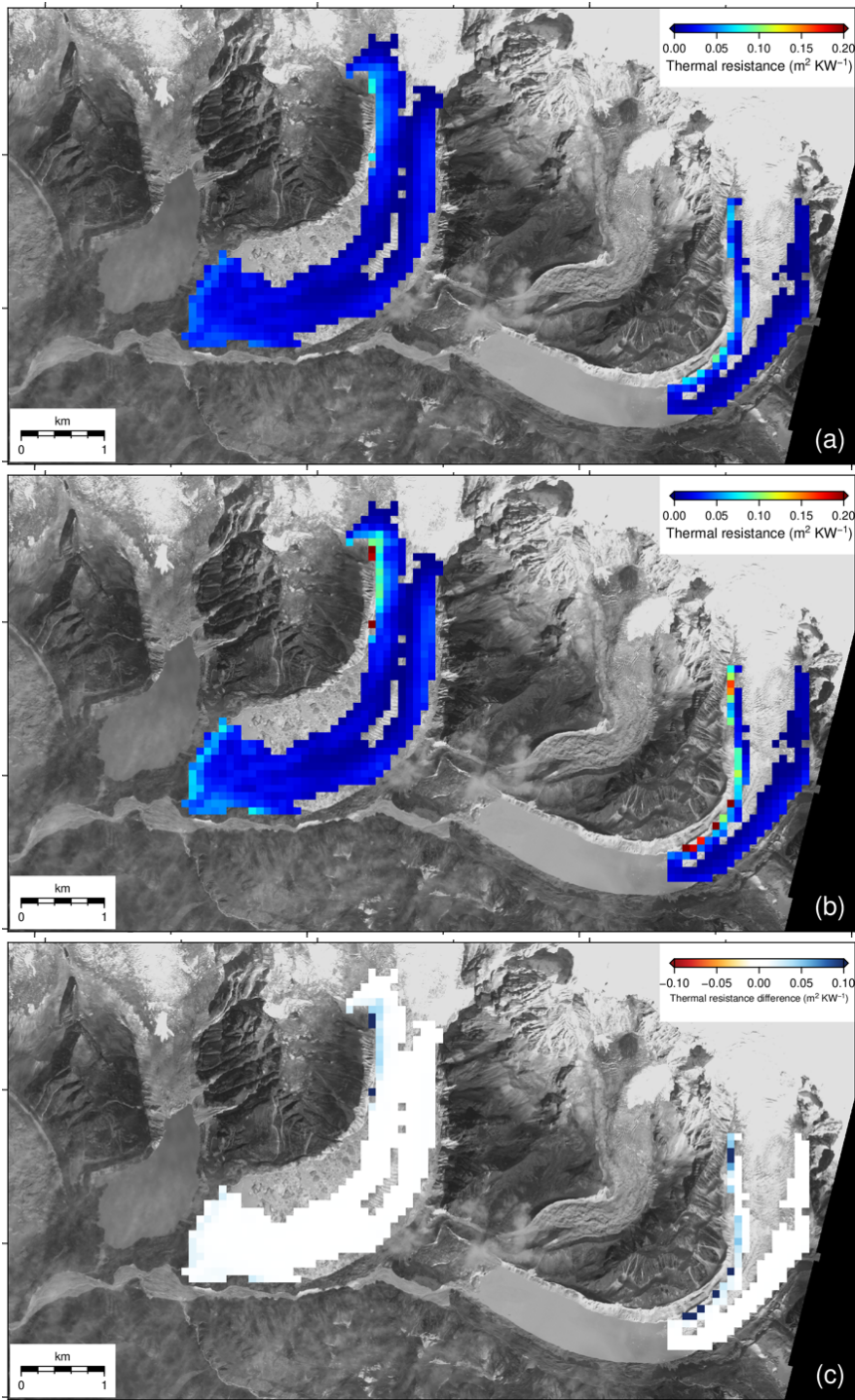


Figure R5: Spatial distribution of thermal resistance calculated (a) from only net radiation, (b) from net radiation + sensible heat and (c) difference of thermal resistance calculated by the two methods.

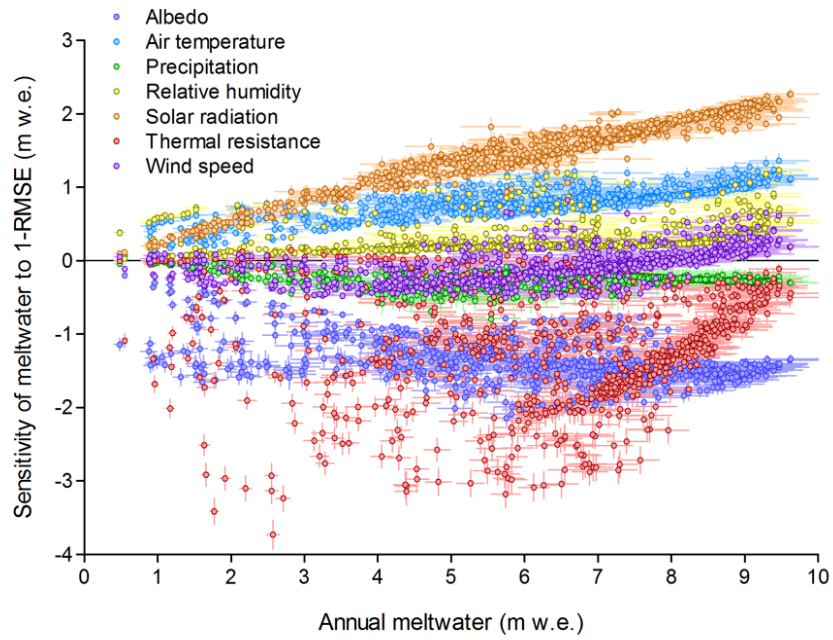


Figure R6: Sensitivity analysis of annual meltwater at debris-covered area as a function of variation of each parameter. RMSEs of ERA-Interim against the observed data were used for the meteorological variables. Uncertainty derived from 8 satellite images are used for thermal resistance and albedo.

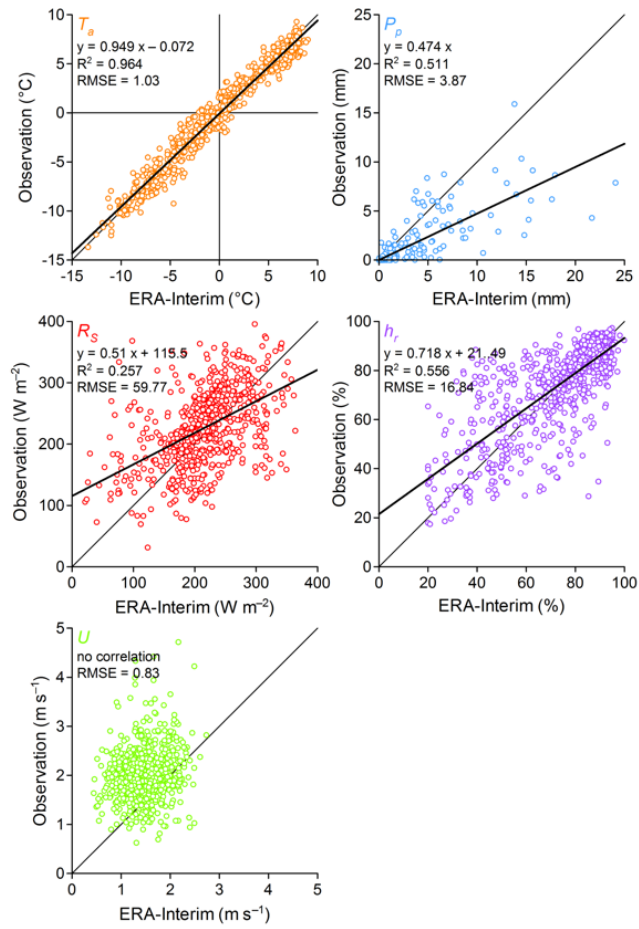


Figure R7: Scatter plot of air temperature, precipitation, solar radiation, relative humidity and wind speed between ERA-Interim reanalysis and observational data for 2002–2004.

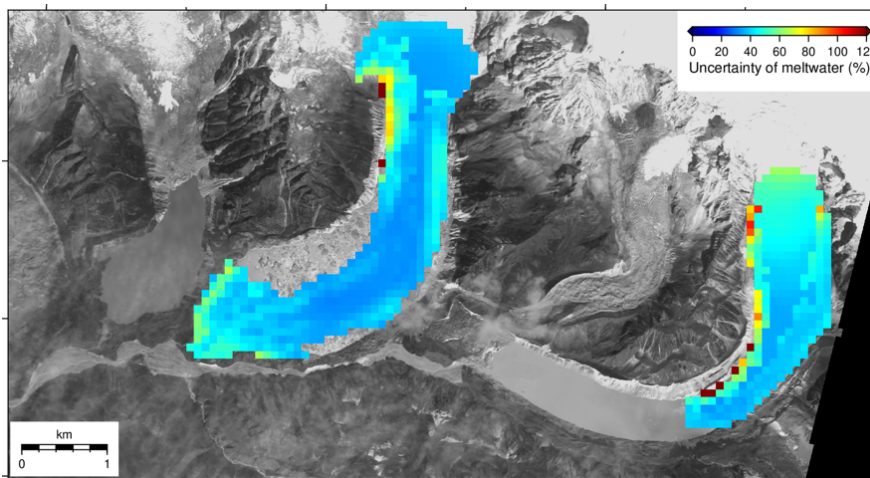


Figure R8: Spatial distribution of uncertainty of meltwater.

The accuracy of the '1 m resolution' DEM obtained by IDW interpolation of a seemingly very limited number of moderately well distributed DGPS points (Fig 1a) is also uncertain. Maybe it's spatial variability could be validated/substituted with other DEMs. What about the new High Mountain Asia DEMs available at NSIDC DAAC? I think the manuscript would greatly benefit from a more comprehensive sensitivity analysis (e.g. Monte Carlo) to show the total range of uncertainties affecting the final interpretations.

In order to evaluate spatial representativeness of glacier surface elevation change obtained from our DGPS measurements, we compared elevation changes obtained from DGPS-DEMs and from ASTER-DEMs acquired on 11 October 2004 and 6 April 2011, which cover similar period of our field campaign (2004–2011). ASTER-DEMs with 30 m resolution provided by the ASTER-VA (<https://gbank.gsj.jp/madas/map/index.html>) were used to compute the surface elevation change. Elevation of ASTER-DEMs was calibrated by the DGPS data on ice-free terrain in 2011. The 2004 and 2011 ASTER-DEMs showed positive biases (dZ) of 12.73 and 11.20 m, and standard deviations (σ) of 20.24 and 14.04 m, respectively (Fig. R9). Vertical coordinates of the ASTER-DEMs were then corrected for the corresponding bias. Elevation change over the glacier surface was computed as difference of the calibrated DEMs in 2004 and 2011 (see Fig. R1). Given the error range of ASTER-DEM, the rate of elevation change derived from DGPS-DEMs is similar to that from ASTER-DEMs (Fig. R10). In order to evaluate spatial representativeness of the DGPS survey, we compared the rate of elevation change of 1-m-grid DGPS-DEMs with that of 30-m-grid ASTER-DEMs along elevation (Fig. R11). Mean rates of elevation change with its standard deviation from DGPS-DEMs are -1.40 ± 0.77 and -4.67 ± 1.36 m a⁻¹ for Thorthormi and Lugge Glaciers, respectively, while those from ASTER-DEMs over the elevation range where the DGPS measurements exist are -0.70 ± 1.25 and -4.87 ± 1.29 m a⁻¹ for Thorthormi and Lugge Glaciers, respectively. Figure R4 shows that the rates from DGPS-DEMs fall within those of ASTER-DEMs, and thus it supports applicability of our survey results to the entire ablation zone.

In the revised manuscript, we will take into account spatial variability in the rate of elevation change from ASTER-DEMs to uncertainty of the mean rate over the entire ablation zone.

We evaluate uncertainties from each analysis (DGPS-DEM, thermal resistance, SMB model and flow model) and a total uncertainty in the revised manuscript. We believe that these new evaluations for uncertainties increase reliability of our results.

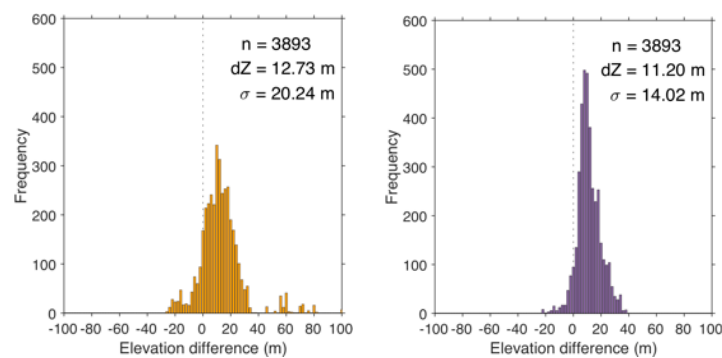


Figure R9: Elevation differences in the ice-free area (left) between 2004 ASTER-DEM and DGPS-DEM and (right) between 2011 ASTER-DEM and DGPS-DEM.

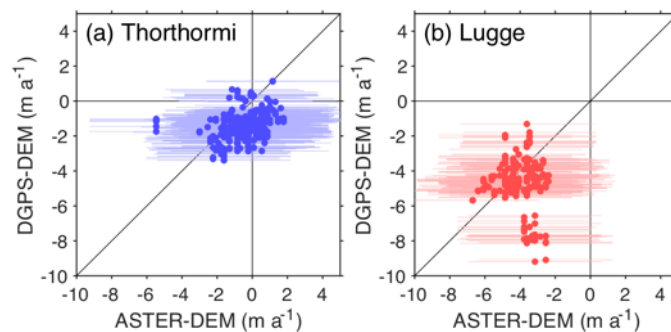


Figure R10: Scatter plot of the rate of surface elevation change between from ASTER-DEMs and DGPS-DEMs at (a) Thorthormi and (b) Lugge Glaciers. Error bars denote standard deviations of DEM differences over the ice-free terrain.

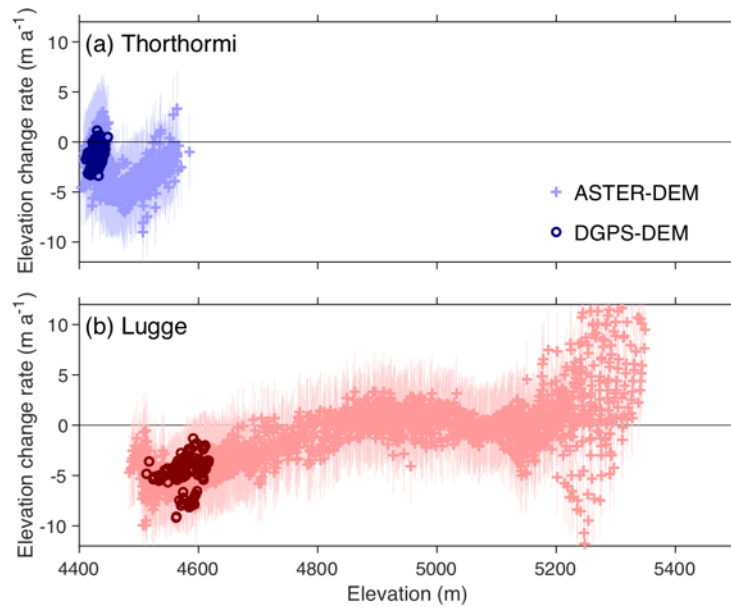


Figure R11: Rate of elevation change along elevation at (a) Thorthormi and (b) Lugge Glaciers. Dark-colored circles are from DGPS-DEM and light-colored crosses are from ASTER-DEM. Error bars denote standard deviations of DEM differences over the ice-free terrain.

Line by line comments:

12: Why 'more' than offsets? Rephrase

We will change “more than offsets” to “compensates” in the revised manuscript.

18: Maybe add Scherler 2011 (10.1038/ngeo1068)

We will add Scherler et al. (2011) in the revised manuscript.

30: There are some more recent papers on this, also by Huss and Hock themselves: 10.1038/s41558-017-0049-x, 10.1038/nature23878, 10.1038/s41558-018-0093-1.

We will change a citation to their latest study in the revised manuscript.

54: 'of most spaceborne DEMs'. DEMs of high resolution stereo satellite imagery (e.g. Pleiades), LIDAR and UAVs are remote sensing methods perfectly capable of deriving several metres (even sub-metre) elevation change

Reviewer #1 and #2 also pointed out accuracy of DEMs derived from UAV and laser/radar altimetry, and we agree. We will remove the statement “However, the accuracy of the remotely sensed DEMs is still insufficient to measure several metres of glacier elevation change.” in the revised manuscript.

59-66: The aim of the paper is not entirely clear to me from the introduction. This paragraph now is more of a methods summary. Consider changing it to clearly convey the research aim and question.

We will add the aim of this study as “The aim of this study is to quantify contribution of dynamic ice thickness change and SMB to thinning of adjacent land- and lake-terminating glaciers.” in the revised manuscript.

69: Is the glacier area measurement really accurate to 0.01 km²?. Same for other glaciers.

In a recently published glacier inventory of glaciers in Bhutan (Nagai et al., 2016), accuracy of glacier areas delineated using ALOS PRISM imagery (2.5 m resolution) was reported as 0.01 km².

75: Use separate paragraphs per glacier to improve readability.

We will separate the text into several paragraphs.

77: moraine-dammed

We will change to “A moraine-dammed” in the revised manuscript.

75: No space between '~' and the number. Throughout.

We will remove space in the revised manuscript.

86: 'were carried out on/around' -> 'were performed for'

We will change as suggested in the revised manuscript.

*92: These are surface flow velocities, right, not integrated over the vertical?
Rephrase into something like 'surface flow velocity of Thorthormi'.*

We will change from "The ice flow velocity across" to "Surface flow velocity of" in the revised manuscript.

101: I've never seen full web URLs in a body of a paper. Use a reference entry for the website in the bibliography instead.

As replied to a comment from Referee #2, this format was used in a paper recently published in The Cryosphere (e.g., Friedl et al., 2018). Therefore, our manuscript also follows this format.

104: Are the elevation variations caused by a person carrying the pack on a debris-covered glacier really only 10 cm? How were these estimated?

Change in the height between GPS antenna and surface was measured at the beginning and the end of the observation. We neglected the influence of debris-cover on change in the height of GPS antenna is thought to be negligible because debris-cover over the observed glaciers is sparse and thin, and we therefore could walk on ice surface in the most of the surveyed area.

106: Mentioning UTM is not quite relevant.

DGPS-DEM was generated in the UTM coordinate system. Mentioning UTM is important to ensure DEM reproducibility with our method.

107: Why this 1 m resolution?

If the grid size sets larger (e.g., >5 m), it is difficult to capture detailed change in surface elevation in Himalayan glaciers where surface slope significantly varies. However, if the grid size set smaller (e.g., <1 m), the number of points of elevation change significantly decrease. As a compromise between the two, we have adopted the 1-m grid as used in previous studies in the Himalayas (Fujita et al., 2011; Tshering and Fujita, 2016).

122: remove 'the' after calculated.

We will remove it in the revised manuscript.

125-126: There is no info whatsoever on the accuracy of the orthorectification of the ASTER images? Could these maybe be retrieved? This can be quite an issue in steep mountainous regions.

Accuracy of 3D orthorectified ASTER image is reported to be <16.9 m in a flat area and <28.4 m in a mountain region (ASTER Science Project, Japan Space Systems, 2012). An error caused by orthorectification is small in the studied region because glacier surface is flat.

131: Why did you select the statistical correlation mode. I was under the impression that the mode that works on the frequency domain is better and is better suited detect subpixel displacements. Please elaborate on the choice.

We agree that the frequency domain is suitable for detecting subpixel displacements (e.g., Abe et al., 2016; Sakakibara and Sugiyama, 2018). COSI-Corr performed well with a statistical correlation mode to detect displacements of

glaciers in the Nepal Himalayas (e.g., Lamsal et al., 2017; Nuimura et al., 2017). Our study also used the statistical correlation following the previous studies.

134: So no filtering was applied using the signal to noise ratio statistics that are provided by COSI-Corr?

We removed data with the signal to noise ratio < 0.9 .

137: The SLC-off gaps in the ETM+ imagery did not provide an issue in the analysis? This should at least be mentioned.

We used multiple ETM+ images acquired from October to December for each year to avoid the SLC-off gaps. We will add this explanation in the revised manuscript.

139: 'that possessed the' -> 'with'

We will change as suggested in the revised manuscript.

141: Use of QGIS in particular is not relevant and, again, the weblink is unnecessary. Just state that delineations were performed in a geographical information system.

We will change as suggested in the revised manuscript.

143: So there is no user-induced accuracy error?

According to analysis using Landsat images with 30 m resolution (Paul et al., 2013), a user-induced accuracy error was estimated to be 5% of delineated area of glaciers with more than 1 km². Following the previous study, we estimated user-induced accuracy error by 5% in the revised manuscript.

162-163: These are quite bold assumptions and this should be acknowledged.

We explicitly mention the assumption was taken in the analysis. We evaluated uncertainty from the thermal resistance based on these assumption (see Fig. R2).

260: Preferably also show the off-glacier displacements in figure 3a.

Figure R12 shows surface displacement off the glacier derived from an image pair on 3 February 2006 and 30 January 2007. Displacements were excluded where surface slopes exceeded 25 degrees. The mean displacement is 12.1 m a^{-1} , which will be given as a measure of uncertainty in the revised manuscript. Figure R12 will be added in the revised supplement.

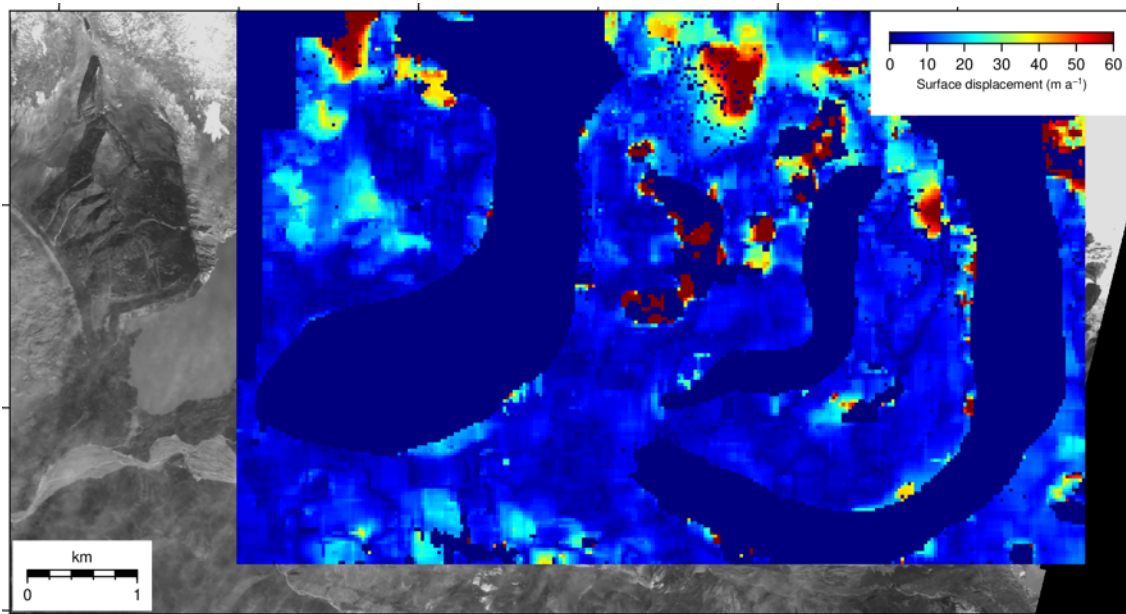


Figure R12: Surface displacements on ice-free terrain derived from image pair on 3 February 2006 and 30 January 2007.

273: Is does not appear that heterogeneous to me. Especially since the actual heterogeneity is likely much higher given the hummocky surface of most debris-covered glaciers. I understand that this is not captured by the ASTER data, and that this is the variability that is obtained, but it should be reworded.

See a reply to the major comment #3.

330-333: The authors speak of accelerating mass losses, but the numbers and accompanying year ranges do not show this per se.

The mass loss has increased since 2000 according to the studies by Gardelle, Brun, Kaab and this study with Maurer's result. But detailed and quantitative discussion is difficult. So, we will change to "Regional mass balances in northern Bhutan have accelerated from the period for 1974–2006 to after 1999. For example, the region-wide mass balance is -0.17 ± 0.05 m w.e. a^{-1} for 1974–2006 (Maurer et al., 2016), -0.22 ± 0.12 m w.e. a^{-1} for 1999–2011 (Gardelle et al., 2013), -0.42 ± 0.20 m w.e. a^{-1} for 2000–2016 (Brun et al., 2017) and -0.52 ± 0.16 m w.e. a^{-1} for 2003–2008 (Kääb et al., 2012)." in the revised manuscript.

341-342: Please elaborate.

We will add "A likely interpretation is that the expansion of Lugge Glacial Lake after the 1960s and glacier thinning decreases the effective pressure (ice overburden minus basal water pressure). A decrease in the effective pressure causes glacier acceleration by enhancing basal ice motion as seen previously near the front of a lake-terminating glacier (Sugiyama et al., 2011). It is likely that acceleration and enhanced longitudinal stretching near the terminus resulted in further ice thinning." in the revised manuscript.

344-365: I found this section rather confusing. There are methods and results presented in the discussion section. I strongly suggest relocating this to the appropriate sections.

We will relocate method to "3.6" and results to "4.6" in the revised manuscript.

360: This is not due to differences in debris cover and debris thickness?

Debris cover is thin and sparse in the ablation area of Thorthormi and Lugge Glaciers. Therefore, we consider that 37% more negative SMB of Thorthormi Glacier is not totally due to debris, but also other factors including difference of surface elevation. Details are addressed in a reply to the major comment #3.

375: A difference of 5 ma-1 is a lot. As suggested in the main comments, I think a comprehensive sensitive analysis would be a great addition to the paper and could help to support the conclusions.

Thanks to the suggestion. We evaluate uncertainties in each analysis (DGPS-DEM, thermal resistance, SMB model and flow model) in the revised manuscript.

Contrasting thinning patterns between lake- and land-terminating glaciers in the Bhutan Himalaya

Shun Tsutaki^{1,a}, Koji Fujita¹, Takayuki Nuimura^{1,b}, Akiko Sakai¹, Shin Sugiyama², Jiro Komori^{1,3,c}, and Phuntsho Tshering^{1,3,d}

5 ¹Graduate School of Environmental Studies, Nagoya University, Nagoya, Japan

²Institute of Low Temperature Science, Hokkaido University, Sapporo, Japan

³Department of Geology and Mines, Ministry of Economic Affairs, Thimphu, Bhutan

^anow at: Atmosphere and Ocean Research Institute, The University of Tokyo, Kashiwa, Japan

^bnow at: Chiba Institute of Science, Choshi, Japan

10 ^cnow at: Department of Modern Life, Teikyo Heisei University, Tokyo, Japan

^dnow at: Cryosphere Services Division, National Center for Hydrology and Meteorology, Thimphu, Bhutan

Correspondence to: Shun Tsutaki (tsutshun@frontier.hokudai.ac.jp)

Abstract. Despite the importance of glacial lake development in ice dynamics and glacier thinning, in situ and satellite-based measurements from lake-terminating glaciers are sparse in the Bhutan Himalaya, where a number of supraglacial lakes exist.

15 ~~To better understand the influences of glacial lake formation and expansion on ice dynamics and glacier thinning, we~~ We acquired in situ and satellite-based observations across lake- and land-terminating debris-covered glaciers in the Lunana region, Bhutan Himalaya. A repeat differential ~~GPS~~ global positioning system survey reveals that thinning of the debris-covered ablation area of the lake-terminating Lugge Glacier ~~for the 2004–2011 period~~ ($-4.67 \pm 0.02 \text{ m a}^{-1}$) is more than three times greater than that of the land-terminating Thorthormi Glacier ($-1.40 \pm 0.01 \text{ m a}^{-1}$) ~~for the 2004–2011 period~~. The surface ~~ice-~~ flow ~~velocity field decreases in the~~ ~~direction~~ ~~along~~ Thorthormi Glacier, whereas ~~it~~ ~~increases~~ ~~they~~ increase from the ~~accumulation zone~~ upper part of the ablation area to the terminus of Lugge Glacier. Numerical experiments ~~with~~ using a two-dimensional ice- flow model demonstrate that the rapid thinning of Lugge Glacier is driven primarily by a negative surface mass balance and that the dynamically induced change in ice thickness is small. However, the thinning of Thorthormi Glacier is suppressed by a longitudinally compressive flow regime. The magnitude of dynamic ice

25 thickening ~~more than offsets~~ ~~compensates~~ the glacier thinning, suggesting that over half of the negative surface mass balance is counterbalanced by the ice dynamics of Thorthormi Glacier. Multiple ponds on Thorthormi Glacier have been expanding since 2000 and merged into a single proglacial lake, with the glacier terminus detaching from its terminal moraine in 2011. Numerical experiments suggest that the speed up and thinning of Thorthormi Glacier will accelerate with continued proglacial lake development.

30 1 Introduction

The spatially heterogeneous shrinkage of Himalayan glaciers has been revealed by in situ measurements (Yao et al., 2012; Azam et al., ~~in press~~2018), satellite-based observations (Scherler et al., 2011a; Bolch et al., 2012; Kääb et al., 2012; Brun et al., 2017), mass balance and climate models (Fujita and Nuimura, 2011; ~~Mörg~~Mölg et al., 2014), and a compilation of multiple methods (Cogley, 2016). Glaciers in Bhutan in the southeastern Himalayas have experienced significant shrinkage and thinning
35 over the past four decades. For example, the Bhutanese glaciers shrank by 23.3 ± 0.91 % between ~~the 1980s~~1990 and 2010, based on repeated decadal glacier inventories (Bajracharya et al., 2014). Multitemporal digital elevation models (DEMs) revealed that the ~~ice thinning rate in the ablation area~~glacier-wide mass balance of Bhutanese glaciers was -0.17 ± 0.05 m w.e. a^{-1} during 1974–2006 (Maurer et al., 2016) and -0.22 ± 0.12 m w.e. a^{-1} during 1999–2010 (Gardelle et al., 2013). Bhutanese glaciers are inferred to be particularly sensitive to changes in air temperature and precipitation, because they are affected by
40 monsoon-influenced humid climate conditions (Fujita, 2008; Sakai and Fujita, 2017). Tshering and Fujita (2016) reported a mass balance record of Gangju La Glacier in the central Bhutan Himalaya between 2003 and 2014, based on in situ measurements, where the glacier experienced much greater mass loss than neighboringneighbouring glaciers in the eastern Himalaya and southeastern Tibet. It is ~~therefore~~crucial to investigate the mechanisms driving the mass loss of Bhutanese glaciers to ~~advance our understanding of their mechanics and dynamics, to~~provide more accurate analyses of regional water
45 availability (Immerzeel et al., 2010) and ~~to~~improve projections of global sea level rise and glacier evolution (Huss and Hock, 20152018).

In recent decades, glacial lakes have formed and expanded at the termini of retreating glaciers in the Himalayas (~~Ageta et al., 2000; Komori, 2008; Fujita et al., 2009; Hewitt and Liu, 2010; Sakai and Fujita, 2010; Gardelle et al., 2011; Nie et al., 2017~~)-(Ageta et al., 2000; Komori, 2008; Fujita et al., 2009; Hewitt and Liu, 2010; Sakai and Fujita, 2010; Gardelle et al.,
50 2011; Nie et al., 2017). Such proglacial lakes are dammed by terminal and lateral moraines, or stagnant ice masses at the glacial front (~~Sakai, 2012; Carrivick and Tweed, 2013~~)-(Sakai, 2012; Carrivick and Tweed, 2013). The formation and expansion of proglacial lakes accelerates glacier retreat through flotation of the terminus, increased calving, and ice flow (e.g., ~~Funk and Röthlisberger, 1989; Warren and Kirkbride, 2003; Tsutaki et al., 2013~~)-Funk and Röthlisberger, 1989; Warren and Kirkbride,
55 neighboringneighbouring land-terminating glaciers in the Nepal and Bhutan Himalayas (Nuimura et al., 2012; Gardelle et al., 2013; Maurer et al., 2016; King et al., 2017)-2012; Gardelle et al., 2013; Maurer et al., 2016; King et al., 2017). Increases in ice discharge and ~~ice-surface~~ flow velocity at the glacier terminus cause rapid thinning due to longitudinal stretching, known as dynamic thinning. For example, dynamic thinning accounted for 17 % of the total ice thinning at lake-terminating Yakutat Glacier, Alaska, during 2007–2010 (Trüssel et al., 2013). Therefore, it is important to quantify the contributions of dynamic
60 thinning and surface mass balance (SMB) to evaluate ongoing mass loss and predict the future evolution of lake-terminating glaciers in Bhutan.

To investigate the contribution of dynamically induced changes in ice thickness to glacier thinning, it is beneficial to compute the ice- flow velocity field of a lake-terminating glacier using an ice- flow model. Two-dimensional ice- flow models have been ~~utilized~~utilised to investigate the dynamic thinning of marine-terminating outlet glaciers (Benn et al., 2007a; Vieli and Nick, 2011), which require the ice- flow velocity field and glacier thickness. In Bhutan, ice- flow velocity measurements have been carried out via remote sensing techniques with optical satellite images (Kääb, 2005; Bolch et al., 2012; Dehecq et al., 2015) and in situ ~~GPS~~global positioning system (GPS) surveys (Naito et al., 2012), but no ice thickness data are available. Another approach to investigate the relative importance of ice dynamics in glacier thinning is to compare lake- and land-terminating glaciers in the same region. This method has been applied to ~~neighboring~~neighbouring lake- and land-terminating glaciers in Nepal and other regions (Nuimura et al., 2012; Trüssel et al., 2013; ~~Tsutaki et al., 2016;~~King et al., 2017).

Widespread thinning of Himalayan glaciers has been revealed by differencing multitemporal DEMs constructed from satellite image photogrammetry (e.g., Gardelle et al., 2013; Maurer et al., 2016; Brun et al., 2017). ~~However,~~Remote-sensing techniques (e.g., unmanned autonomous vehicle surveys) hold a key advantage over debris-covered glaciers, where the ~~accuracy~~thinning also depends on variations in debris thickness and the spatial distribution of ~~the remotely sensed DEMs is still insufficient to measure several meters of glacier elevation change.~~supraglacial ponds or ice cliffs (Vincent et al., 2016). Repeated differential GPS (DGPS) measurements, which are acquired with ~~sub-meter~~centimetre-scale accuracy, enable us to evaluate elevation changes of several ~~meters~~metres (e.g., Fujita et al., 2008). Although their temporal and spatial coverage is limited, repeated ~~differential-GPS~~DGPS measurements have been successfully ~~performed~~acquired to investigate ~~glacier~~the surface elevation ~~change~~changes of debris-free glaciers in Bhutan (Tshering and Fujita, 2016), ~~Nepal (Vincent et al., 2016;)~~ and the Inner Tien Shan (Fujita et al., 2011).

This study aims to quantify the contributions of ice dynamics and SMB to the thinning of adjacent land- and lake-terminating glaciers. To investigate the importance of glacial lake formation and expansion on ~~rapid~~ glacier thinning, we measured surface elevation changes on lake- and land-terminating glaciers in the Lunana region, Bhutan Himalaya. Following a previous report of surface elevation measurements from a ~~differential-GPS~~DGPS survey (Fujita et al., 2008), we repeated the ~~differential-GPS~~DGPS survey on the lower parts of the land-terminating Thorthormi ~~and Lugge II glaciers,~~Glacier as well as the adjacent lake-terminating Lugge Glacier. Thorthormi and Lugge glaciers were selected for analysis because ~~these glaciers are situated around~~they are located at similar elevations. Lugge Glacier terminates in a proglacial lake, Lugge Glacial Lake, while the terminus of Thorthormi Glacier is grounded but a large supraglacial lake has developed in its ablation area (Bajracharya et al., 2014). ~~same elevation, thus making~~These contrasting conditions make them suitable for evaluating the contribution of ~~dynamic thinning~~ice dynamics to the observed ice thickness changes. The glaciers are also suitable for field measurements because of their relatively safe ice-surface conditions and proximity to trekking routes. We also performed numerical simulations to evaluate the contributions of SMB and ~~dynamic thinning to the surveyed glacier thinning~~ice dynamics to surface elevation changes.

2 Study site

95 This study focuses on ~~three~~two debris-covered glaciers (Thorthormi, ~~Lugge~~, and Lugge ~~H~~ glaciers) in the Lunana region of northern Bhutan (Fig. 1a, ~~28°06' N, 90°18' E~~). Thorthormi Glacier covers an area of 13.16 km², based on a satellite image from 17 January 2010 (Table S1 in the Supplement, Nagai et al., 2016). The ice flows to the south in the upper part and to the southwest in the terminal part of the glacier at rates of 60–100 m a⁻¹ (Bolch et al., 2012). The surface is almost flat (< 1°) within 3000 m of the glacier terminus. The ~~ablation area of the~~ glacier thinned at a rate of -3 m a⁻¹ during the 2000–2010
100 period (Gardelle et al., 2013). A large supraglacial lake, which is inferred to possess a high potential for outburst ~~flooding~~flood (Fujita et al., 2008, 2013), formed on the western ablation area by the merging of multiple supraglacial ponds (Ageta et al., 2000; Komori, 2008). ~~In 2011, the glacier terminus was in contact with the terminal moraine, and thus became~~Thorthormi Glacier is termed a land-terminating glacier ~~– here since the glacier terminus was grounded in 2011.~~

Lugge Glacier is a lake-terminating glacier with an area of 10.93 km² in May 2010 (Table S1, Nagai et al., 2016). The
105 mean surface slope is 12° within 3000 m of the glacier terminus. A moraine-dammed proglacial lake has expanded since the 1960s (Ageta et al., 2000; Komori, 2008), and the glacier terminus retreated by ~~~3000 m~~~1 km during ~~1980~~1990–2010 (Bajracharya et al., 2014). Lugge Glacier thinned near the terminus at a rate of -8 m a⁻¹ during 2000–2010 (Gardelle et al., 2013). On 7 October 1994, an outburst flood, with a volume of 17.2 × 10⁶ m³, occurred from Lugge Glacial Lake (Fujita et al., 2008). The depth of Lugge Glacial Lake was 126 m at its deepest location, with a mean depth of 50 m, based on a bathymetric
110 survey in September 2002 (Yamada et al., 2004). ~~Lugge H Glacier is a land-terminating glacier with an area of 3.18 km² in January 2010 (Table S1; Nagai et al., 2016), whose terminus retreated by < 200 m from 1980 to 2010 (Bajracharya et al., 2014). The mean surface slope is 15° within 3000 m of the glacier terminus. The mean thinning rate over the entire glacier was -1 m a⁻¹ during 2000–2010 (Gardelle et al., 2013).~~

~~Although the debris thickness was not measured during the field campaigns, there were regions of debris-free surface across the ablation areas of Thorthormi and Lugge glaciers (Fig. S1 in the Supplement). Debris cover is therefore considered to be thin and sparse across the study area. Furthermore, few supraglacial ponds and ice cliffs were observed across Thorthormi and Lugge glaciers.~~

Meteorological and glaciological in situ observations were ~~carried out on/around~~acquired across the glaciers and lakes in the Lunana region from 2002 to 2004 (Yamada et al., 2004). Automatic weather station (AWS) observations from the terminal moraine of Lugge Glacial Lake (4524 m a.s.l., Fig. 1a) showed that the annual mean air temperature during 2002–2004 was
120 ~~~-0 °C~~, and ~~900 mm of annual~~precipitation ~~fell~~was 900 mm in 2003 (Suzuki et al., 2007b). Naito et al. (2012) reported changes in surface elevation and ice- flow ~~speed~~velocity along the central flowline in the lower parts of Thorthormi and Lugge glaciers for the ~~period~~2002–2004 ~~period~~. The ice- thinning rate at Lugge Glacier was ~~~-5 m a⁻¹ during 2002–2004~~, which is much higher than that at Thorthormi Glacier (0–3 m a⁻¹). The ~~ice-surface~~ flow ~~velocity field across~~velocities of Thorthormi Glacier
125 ~~decreases~~decrease down-glacier from ~~~-90 to~~ ~30 m a⁻¹ at 2000–3000 m from the terminus, while the ~~ice-surface~~ flow ~~velocity field~~velocities of Lugge Glacier ~~is~~are nearly uniform at 40–55 m a⁻¹ within 1500 m of the terminus (Naito et al., 2012).

3 Data and methods

3.1 Surface elevation change

We surveyed the surface elevations in the lower parts of Thorthormi, ~~Lugge~~, and Lugge-II glaciers from 19 to 22 September 2011, and then compared them with those observed from 29 September to 10 October 2004 (Fujita et al., 2008). We used dual- and single-frequency carrier phase GPS receivers (GNSS Technologies, GEM-1, and MAGELLAN ProMark3). One receiver was installed 2.5 km west of the terminus of Thorthormi Glacier as a reference station; (Fig. 1a), whose location was determined by an online precise point positioning processing service (<https://webapp.geod.nrcan.gc.ca/geod/tools-outils/ppp.php?locale=en>, last accessed: ~~14 December 2017~~ 31 May 2018), which provided standard deviations of < 4 mm for both the horizontal and vertical coordinates after one week of continuous measurements in 2011. Observers walked on/around the glaciers with a GPS receiver and antenna fixed to a frame pack. The height uncertainty of the GPS antenna during the survey was < 0.1 m (Tsutaki et al., 2016). **We neglected the influence of debris cover on changes in the GPS antenna height because the debris cover across the glaciers is sparse and thin, and we therefore could walk on the ice surface across most of the surveyed area.** The GPS data were processed with RTKLIB, an open source software for GNSS positioning (<http://www.rtklib.com/>, last accessed: ~~14 December 2017~~ 31 May 2018). Coordinates were projected onto a common Universal Transverse Mercator projection (UTM zone 46N, WGS84 reference system). We generated DEMs with 1- m resolution by interpolating the surveyed points with an inverse distance weighted method, as used in previous studies (e.g., Fujita ~~et al.~~, and Nuimura, 2011; Tshering and Fujita, 2016). The 2004 survey data were calibrated with four benchmarks around the glaciers (Fig. 1a) to generate a 1- m resolution DEM. Details of the 2004 and 2011 GPS surveys, along with their respective DEMs, are ~~summarized~~ summarised in Table S1. The surface elevation changes between 2004 and 2011 were computed at points where data were available for both dates. Elevation changes were obtained at 431, ~~248~~, and ~~258~~ 248 DEM grid points for Thorthormi, ~~Lugge~~, and Lugge-II glaciers, respectively (Table 1).

The horizontal uncertainty of the GPS survey was evaluated by comparing the positions of four benchmarks installed around Lugge and Thorthormi glaciers (Fig. 1a). We evaluated the vertical uncertainty (σ_e) from the off-glacier elevation difference between the 2004 and 2011 DEMs ($n = 3893$; Table 1), which was calculated as the quadratic sum of the mean elevation difference (dZ) and standard deviation (σ_z) (Bolch et al., 2011). In previous studies, the vertical uncertainty in differentiation of two satellite-based DEMs has been expressed by the standard error (σ_{se}) as follows:

$$\sigma_{se} = \frac{\sigma_e}{\sqrt{n}} \quad (1)$$

The number of DEM grid points over a glacier is generally used as the sample number n (e.g., Berthier et al., 2007; Bolch et al., 2011; Maurer et al., 2016).

3.2 Surface ice-flow velocity

160 ~~We calculated~~To evaluate the spatial representativeness of the change in glacier surface ~~ice-flow velocities by processing~~
elevation change derived from DGPS measurements, we compared the elevation changes derived from the DGPS-DEMs and
Advanced Spaceborne Thermal Emission and Reflection Radiometer (ASTER) DEMs acquired on 11 October 2004 and 6
165 April 2011, respectively, which cover a similar period to our field campaigns (2004–2011). The 30 m ASTER-DEMs were
provided by the ASTER-VA (<https://gbank.gsj.jp/madas/map/index.html>, last accessed: 31 May 2018) and used to compute
the surface elevation change. The ASTER-DEM elevations were calibrated using the DGPS data on the ice-free terrain in 2011.
The 2004 and 2011 ASTER-DEMs had positive biases of 12.73 and 11.20 m, and standard deviations of 20.24 and 14.04 m,
respectively. The vertical coordinates of the ASTER-DEMs were then corrected for the corresponding bias, with the elevation
change over the glacier surface computed as the difference between the calibrated DEMs.

3.2 Surface flow velocities

170 We calculated surface flow velocities by processing ASTER images (15- m resolution, near- infrared-, (NIR), near- nadir 3N
band) with the COSI-Corr feature- tracking software (Leprince et al., 2007), which is commonly adopted in mountainous
terrain to measure surface displacements with an accuracy of one-fourth to one-tenth of the pixel size (e.g., Heid and Kääh,
2012; Scherler and Strecker, 2012; Lamsal et al., 2017). Orthorectification and coregistration of the images were performed
by Japan Space Systems before processing. ~~The orthorectification and coregistration accuracies were reported as 16.9 m and~~
175 ~~0.05 pixel, respectively~~. We selected five image pairs from seven scenes between 22 October 2002 and 12 October 2010, with
temporal separations ranging from 273 to 712 days (Table S2), to obtain annual surface ~~ice-flow~~ velocities of the glaciers. It
should be noted that the aim of our ~~ice-flow~~ velocity measurements is to investigate the mean surface ~~ice-flow~~ regime of the
glaciers rather than its interannual variability. The subpixel displacement of features on the glacier surface was recorded at
every fourth pixel in the orthorectified ASTER images, providing the horizontal ~~ice-flow~~ ~~velocity field~~ velocities at a 60- m
180 resolution (Scherler et al., ~~2011~~2011b). We used a statistical correlation mode, with ~~multiscale~~ correlation window ~~sizesize~~
of 16×16 pixels (Leprince et al., 2007). ~~We applied a filter with a signal to noise ratio threshold of < 0.9~~. The obtained ice-
flow velocity fields were filtered to remove residual attitude effects and miscorrelations (Scherler et al., ~~2011~~2011b; Scherler
and Strecker, 2012). The filters eliminated those ~~ice-flow~~ vectors showing a large deviation in magnitude (greater than $\pm 1 \sigma$)
or direction ($> 20^\circ$) relative to the mean of the ~~neighboring~~neighbouring 21×21 data points.

185 3.3 Glacier area

We ~~analyzed~~analysed the ~~aerial~~areal variations in the ablation area of Thorthormi and Lugge glaciers using 12 satellite images
acquired by the Landsat 7 ~~Enhanced Thematic Mapper Plus (ETM+)~~ETM+ between November 2000 and December 2011
(distributed by the United States Geological Survey, <http://landsat.usgs.gov/>, last accessed: ~~14 December 2017~~31 May 2018).
We selected images taken in either November or December ~~that possessed~~with the least snow and cloud cover. ~~We also~~

190 analysed multiple ETM+ images acquired from the October to December timeframe of each year to avoid the scan line
corrector-off gaps. The lowermost 4000 m of Thorthormi Glacier and the lowermost 2000 m of Lugge Glacier were manually
delineated on false color composite images (bands 3–5, 30- m spatial resolution) using the QGIS in a geographical
information system software (<http://qgis.org/en/site/>, last accessed: 14 December 2017). For Thorthormi Glacier, following
195 to the previously proposed delineation methods (e.g., Bajracharya et al., 2014; Nuimura et al., 2015; Nagai et al., 2016),
supraglacial ponds surrounded by ice were included in the glacier surface, whereas marginal ponds in contact with
bedrock/moraine ridge were excluded. The accuracy of the outline mapping is equivalent to the image resolution (30 m). The
coregistration error in the repeated images was ± 30 m, based on visual inspection of the horizontal shift of a stable bedrock
and lateral moraines on the coregistered imagery. The user-induced error was estimated to be 5 % of the glacier area delineated
from the Landsat images (Paul et al., 2013). The total error of the area analysis was ± 0.00217 and ± 0.05 km² ($\sqrt{30^2 + 30^2} =$
200 42.43 m) for Thorthormi and Lugge glaciers, respectively.

3.4 Mass balance of the debris-covered surface

SMB is an essential component of ice thickness change, but no in situ SMB data are available in the Lunana region. Therefore,
the spatial distributions of the SMB on the debris-covered Thorthormi, Lugge, and Lugge H-glaciers were computed with a
heat- and mass- balance model, which quantifies the spatial distribution of the mean SMB for each glacier.

205 Thin debris accelerates surface ice melt by lowering surface albedo, while thick debris (generally more than a few
centimeters) suppresses surface ice melt and acts as an insulating layer (Østrem, 1959; Mattson et al., 1993). To
obtain the spatial distributions of debris thickness and SMB, we estimated the thermal resistance from remotely
sensed data and reanalysis climate data (Suzuki et al., 2007a; Zhang et al., 2011; Fujita and Sakai, 2014). The thermal resistance
(R_T , m² K W⁻¹) is defined as follows:

$$R = \frac{h}{\lambda}, \quad (2)$$

$$R_T = \frac{h}{\lambda}, \quad (2)$$

215 where h and λ are the debris thickness (m) and thermal conductivity (W m⁻¹ K⁻¹), respectively. This method has been applied
to reproduce debris thickness and SMB in southeastern Tibet (Zhang et al., 2011) and glacier runoff in the Nepal Himalaya
(Fujita and Sakai, 2014). Assuming no heat storage, a linear temperature profile within the debris layer, and the melting point
temperature at the ice–debris interface (T_i , 0 °C), the conductive heat flux through the debris layer (G_d , W m⁻²) and the heat
balance at the debris surface are described as follows:

220

$$G_d = \frac{(T_s - T_i)}{R_T} = (1 - \alpha_d)R_{Sd} + R_{Ld} - R_{Lu} + H_S + H_L, \quad (3)$$

225 where α_d is the debris surface albedo; R_{Sd} , R_{Ld} , and R_{Lu} are the downward short wave radiation, and downward and upward long wave radiation, respectively (positive sign, W m^{-2}); and H_S and H_L are the sensible and latent heat fluxes (W m^{-2}),
 230 respectively, which are positive when the fluxes are directed toward the ground. Both turbulent fluxes were ignored in the original method to obtain the thermal resistance based on a sensitivity analysis and field measurements (Suzuki et al., 2007a). However, we improved the method by taking the sensible heat into account because several studies have indicated that ignoring the sensible heat can result in an underestimation of the thermal resistance (e.g., Reid and Brock, 2010). Using eight ASTER images obtained between October 2002 and October 2010 (Table S3), along with the NCEP/NCAR reanalysis climate data (NCEP-2; Kanamitsu et al., 2002), we calculated the distribution of mean thermal resistance on the ~~three~~two target glaciers. The ~~uncertainty~~air temperature at the AWS elevation (4524 m a.s.l., Fig. 1a) was estimated using the pressure level atmospheric temperature and geopotential height (Sakai et al., 2015), and then modified for each 90×90 m mesh grid points using a single temperature lapse rate ($0.006 \text{ }^\circ\text{C km}^{-1}$). The wind speed was assumed to be 2.0 m d^{-1} , which is the two-years average of the 2002–2004 AWS record (Suzuki et al., 2007b). The uncertainties in the thermal resistance ~~was~~ and albedo were evaluated as
 235 ~~64%~~107 and 40 %, respectively, by taking the standard deviations calculated from multiple images at the same location (Fig. S1 in the supplementS2).

The SMB of the debris-covered ablation area was calculated by a heat- and mass- balance model that included debris-covered effects (Fujita and Sakai, 2014). ~~By assuming no heat storage, a linear temperature profile within a debris layer, and~~First, the melting point temperature at the ice-debris interface ($T_i, 0 \text{ }^\circ\text{C}$), the conductive heat flux through the debris layer
 240 ($G_d, \text{W m}^{-2}$) and the heat balance at the debris surface are described as follows:

~~$$G_d = \frac{(T_s - T_i)}{R} = (1 - \alpha_d)R_{Sd} + R_{Ld} - R_{Lu} + H_S + H_L, \quad (3)$$~~

245 where ~~α_d is the debris surface albedo; R_{Sd} , R_{Ld} , and R_{Lu} are the radiations of the downward shortwave radiation and downward and upward longwave radiation, respectively (positive sign, W m^{-2}); and H_S and H_L are the sensible and latent heat fluxes (W m^{-2}), respectively, which are positive when the fluxes are directed toward the ground.~~ The surface temperature is determined to satisfy Eq. (3) using the **estimated thermal resistance** and an iterative calculation, and then, if the heat flux toward the ice-debris interface is positive, the daily amount of ice melt beneath the debris mantle ($M_d, \text{kg m}^{-2} \text{ d}^{-1}$) is obtained as follows:

~~$$M_d = \frac{t_D G_d}{l_m}, \quad (4)$$~~

$$b = c + \left(\sum_{D=1}^{365} \frac{t_D H_L}{l_m} - D_s - M_d \right) / 1000 \quad (5)$$

255

where t_D is the length of a day in seconds (86,400 s), and l_m is the latent heat of fusion of ice ($3.33 \times 10^5 \text{ J kg}^{-1}$). b and c are annual mass balance and accumulation (m w.e. a⁻¹), respectively, and D_s is the daily discharge ($\text{kg m}^{-2} \text{ d}^{-1}$). Further details on the equations and methodology used in the model are described by Fujita and Sakai (2014). The mass balance was calculated at $90 \text{ m} \times 90 \text{ m}$ mesh grid points on the ablation area of the two glaciers using 38 years of ERA-Interim reanalysis data (1979–2017), with the results given in metres of water equivalent (w.e.). The meteorological variables in the ERA-Interim reanalysis data (2002–2004) were calibrated with in situ meteorological data (2002–2004) from the terminal moraine of Lugge Glacier (Fig. 1a; Suzuki et al., 2007b), with the results given in meters of water equivalent (m w.e.) (S3). The ERA-Interim wind speed was simply multiplied by 1.3 to obtain the same average as in the observational data. The SMBs calculated with the observed and calibrated ERA-Interim data for 2002–2004 were compared with those from the entire 38-year ERA-Interim data set. The SMBs for 2002–2004 (from both the observational and ERA-Interim data sets) show no clear anomaly against the long-term mean SMB (1979–2017) (Fig. S4).

260

265

The sensitivity of the simulated meltwater was evaluated against the meteorological parameters used in the SMB model. We chose meltwater instead of SMB to quantify the uncertainty because the SMB uncertainty cannot be evaluated as absolute value. The tested parameters are surface albedo, air temperature, precipitation, relative humidity, solar radiation, thermal resistance and wind speed. The thermal resistance and albedo uncertainties were based on the standard deviations derived from the eight ASTER images used to estimate these parameters (Fig. S2). Each meteorological variable uncertainty, with the exceptions of the thermal resistance and albedo uncertainties, was assumed to be the root mean square error (RMSE) of the ERA-Interim reanalysis data against the observational data (Fig. S3). The simulated meltwater uncertainty was estimated as the variation in meltwater within a possible parameter range via a quadratic sum of the results from each meteorological parameter.

270

275

3.5 Ice dynamics

3.5.1 Model descriptions

To investigate the dynamically induced ice thickness change, numerical experiments were carried out by applying a two-dimensional ice-flow model to the longitudinal cross-sections of Thorthormi and Lugge glaciers. The aim of the experiments was to investigate whether the ice thickness changes observed at Thorthormi and Lugge glaciers were affected by the presence of proglacial lakes.

280

The model was developed for a land-terminating glacier (Sugiyama et al., 2003, 2014), and is applied to the lake-terminating glaciers in this study. Taking the x and z coordinates in the along-flow and vertical directions, the momentum and mass conservation equations in the $x-z$ plane are:

$$\frac{\partial \sigma_{xx}}{\partial x} + \frac{\partial \sigma_{xz}}{\partial z} = 0, \quad (5)$$

(6)

$$\frac{\partial \sigma_{zx}}{\partial x} + \frac{\partial \sigma_{zz}}{\partial z} = \rho_i g, \quad (6)$$

(7)

$$\frac{\partial u_x}{\partial x} + \frac{\partial u_z}{\partial z} = 0, \quad (7)$$

(8)

where σ_{ij} ($i, j = x, z$; $i, j = x, z$) are the components of the Cauchy stress tensor, ρ_i is the density of ice (910 kg m^{-3}), g is the vertical component of the gravitational acceleration vector (9.81 m s^{-2}), and u_x and u_z are the horizontal and vertical components of the flow velocity vector, respectively. The stress in Eqs. (6) and (7) is linked to the strain rate via the constitutive equation given by Glen's flow law (Glen, 1955):

$$\dot{\epsilon}_{ij} = A \tau_e^{n-1} \tau_{ij}, \quad (8)$$

(9)

where $\dot{\epsilon}_{ij}$ and τ_{ij} are the components of the strain rate and deviatoric stress tensors, respectively, and τ_e is the effective stress, which is defined as

$$\tau_e = \frac{1}{2} (\tau_{xx}^2 + \tau_{zz}^2) + \tau_{xz}^2. \quad (9)$$

(10)

The rate factor (A) and flow-law exponent (n) are material parameters. We used the commonly accepted value of $n = 3$ for the flow-law exponent, and employed a rate factor of $A = 75 \text{ MPa}^{-3} \text{ a}^{-1}$, which was previously used for modeling a temperate valley glacier (Gudmundsson, 1999). We assumed the glaciers were temperate because there was no available information on the thermal states of the studied glaciers.

The model domain was within 5100 m and 3500 m ~~of~~ from the ~~termini~~ terminus of Thorthormi (red and white lines in Fig. 1b) and Lugge glaciers; (red line in Fig. 1b), respectively. The surface elevation of the model domain ranges from 4442 to 4813 m for Thorthormi Glacier, and from 4530 to 5244 m for Lugge Glacier. The surface geometry was obtained from ASTER Global Digital Elevation Model (GDEM) version 2 after filtering the elevations with a smoothing routine at a bandwidth of 1000 m. The ice thickness distribution was estimated from a method proposed for alpine glaciers (Farinotti et al., 2009). We applied the same local regression filter to smooth the estimated bedrock geometry. The bedrock elevation of Thorthormi Glacier was estimated from bathymetry data acquired in September 2011 at 1400 m from the terminus (Fig. 6a). For Lugge Glacier, the bed elevation at the glacier front was estimated from the bathymetric map of Lugge Glacial Lake, surveyed in September 2002 (Fig. 6b; Yamada et al., 2004). To solve Eqs. (67) and (78) for u_x and u_z , the modelled domain was discretized with a finite element mesh. The mesh resolution was 100 m in the horizontal direction, and several meters near the bed and 10–28 m near the surface in the vertical direction. The total numbers of elements were 612 and 420 for Thorthormi and Lugge glaciers, respectively (Fig. 6a and 6b).

The upper surface of the domain was assumed to be stress free. The ice flux through the upper boundary was prescribed according to the measured surface ice-flow velocities. The basal sliding velocity (u_b) was given as a linear function of the basal shear traction ($\tau_{xz,b}$):

$$u_b = C \tau_{xz,b}, \quad (11)$$

where C is the sliding coefficient. We used constant sliding coefficients of $C = 766$ and $125 \text{ m a}^{-1} \text{ MPa}^{-1}$ over the entire domains of Thorthormi and Lugge glaciers, respectively. These parameters were obtained by minimizing the root mean square error (RMSE) between the modelled and measured surface ice-flow velocities over the entire model domains (Fig. S2S5).

3.5.2 Experimental configurations

To quantify the effect of glacier dynamics on ice thickness change, we performed two experiments for Thorthormi and Lugge glaciers. Experiment 1 was performed to compute the ice-flow velocity fields under the present terminus conditions. In this experiment, Thorthormi Glacier was treated as a land-terminating glacier by prescribing zero horizontal velocity at the glacier front, whereas Lugge Glacier was treated as a lake-terminating glacier by applying hydrostatic pressure at the front as a function of water depth. A stress-free boundary condition was given to the calving front above the lake level.

Experiment 2 was designed to investigate the influence of proglacial lakes on glacier dynamics. For Thorthormi Glacier, we assumed a calving front with an initial calving front thickness of 106 m (red line in Fig. 7a1b). The surface level of the proglacial lake was assumed to be 4432 m a.s.l., which is the mean surface level of the supraglacial ponds measured in

September 2004 (Fujita et al., 2008). Hydrostatic pressure and stress-free conditions were applied to the lower boundary below and above the lake level, respectively. For Luge Glacier, ~~the present 2200-m-long Luge Glacial Lake is filled~~ we simulated a lake-free situation, with ice flowing to the contemporary terminal moraine, so that the glacier terminates on land. Bedrock topography is derived from the bathymetric map (red and white lines in Fig. 7b; 1b, Yamada et al., 2004). The surface topography is linearly extrapolated from the surface elevations at the calving front in 2002, and zero flow velocity was assumed at the terminus. In the experiment, we used 444 and 684 elements for Thorthormi and Luge glaciers, respectively (~~Fig. 7a and 7b~~).

3.6 Simulated ice thickness change

To compare the influence of ice dynamics on glacier thinning in lake- and land-terminating glaciers, we calculated the emergence velocity (v_e) as follows:

$$v_e = (v_z - v_h \tan \alpha) \frac{\rho_i}{\rho_w}, \quad (12)$$

where v_z and v_h are the vertical and horizontal flow velocities, respectively, and α is the surface slope (Cuffey and Paterson, 2010). The surface slope α was obtained every 100 m from the surface topography of the ice flow model. The emergence velocity was converted to water equivalent (m w.e. a⁻¹), using the densities of ice (ρ_i , 910 kg m⁻³) and water (ρ_w , 1000 kg m⁻³), for comparison with the SMB. The surface elevation change over time (dh/dt , m a⁻¹), which is caused by the imbalance of the emergence velocity and SMB (b) along the central flowline, is calculated as

$$\frac{dh}{dt} = (b + v_e) \frac{\rho_w}{\rho_i}. \quad (13)$$

The magnitude of the emergence velocity is approximately proportional to the horizontal flow velocity (Truffer et al., 2009). Assuming this relationship, the emergence velocity uncertainty (σ_{v_e}) was estimated as

$$\sigma_{v_e} = \frac{v_e}{u_{model}} \times \sigma_{u_{model}}, \quad (14)$$

where u_{model} is the simulated horizontal flow velocity and $\sigma_{u_{model}}$ is the mean uncertainty of the simulated surface flow velocity.

4 Results

375 4.1 Surface elevation change

Figure 1a shows the rate of surface elevation change of Thorthormi, ~~Lugge~~, and ~~Lugge-II~~ glaciers from 2004 to 2011. The rates for Thorthormi Glacier range from -3.37 to $+1.14$ m a^{-1} , with a mean rate of -1.40 m a^{-1} (Table 1). ~~These~~ These rates show large variability within the limited elevation band (4410–4450 m a.s.l., Fig. 2b). No clear trend is observed at 1000–3000 m from the terminus (Fig. 2c). The rates for Lugge Glacier range from -9.13 to -1.30 m a^{-1} , with a mean rate of -4.67 m a^{-1} (Table 1). The most negative values (-9 m a^{-1}) are found in the lower elevation band (4560 m a.s.l., Fig. 2b), which corresponds to 1300 m from the 2002 terminus position (Fig. 2c). ~~The rates of surface elevation change for Lugge-II Glacier range from -3.99 to $+0.10$ m a^{-1} , with a mean rate of -0.63 m a^{-1} (Table 1).~~

The RMSE between the surveyed positions (five measurements in total, with one or two measurements for each benchmark) is 0.21 m in the horizontal direction. The mean elevation difference between the 2004 and 2011 DEMs (dZ/dZ) is 0.48 m, with a standard deviation (σ_z) of 1.91 m (Fig. 2a) and a vertical uncertainty (σ_e) of 1.97 m (0.28 m a^{-1}). According to Eq. (1), the standard error for this study ranges from 0.09 to 0.12 m (~ 0.02 m a^{-1}), while those for the remotely sensed studies of Himalayan glaciers have been evaluated at 1.1–6.4 m (e.g., Berthier et al., 2007; Bolch et al., 2011; Maurer et al., 2016), suggesting that our data are considerably more accurate than those reported in the aforementioned studies.

Given the ASTER-DEM uncertainties, the DGPS-DEMs and ASTER-DEMs yield a similar rate of elevation change that falls within the uncertainty range (Fig. S6). The mean rates of elevation change, with their respective standard deviations, from the DGPS-DEMs are -1.40 ± 0.77 and -4.67 ± 1.36 m a^{-1} for Thorthormi and Lugge glaciers, respectively, while those from the ASTER-DEMs over the same elevation range as the DGPS measurements are -0.70 ± 1.25 and -4.87 ± 1.29 m a^{-1} , respectively. The DGPS-DEM rates are in good agreement with the ASTER-DEM rates (Fig. S7), thus supporting the applicability of the DGPS measurements to the entire ablation area.

395 4.2 Surface ice-flow velocity velocities

Figure 1b shows the surface ice-flow velocity field from 30 January 2007 to 1 January 2008 (337 days). On Thorthormi Glacier, the ice-flow velocity field decreases velocities decrease down-glacier, ranging from ~ 110 m a^{-1} at the foot of the icefall to < 10 m a^{-1} at the terminus (Fig. 3a). The ice-flow velocity field velocities of Lugge Glacier increases increase down-glacier, ranging from 20–60 to 50–80 m a^{-1} within 2 km 2000 m of the calving front (Fig. 3b). In this region, the ice flow converges as the glacier width narrows down-glacier. ~~Lugge-II Glacier flows more slowly than the other two glaciers, typically at < 40 m a^{-1} across the entire glacier (Fig. 3c).~~

The surface ice-flow velocity field of Thorthormi Glacier shows little variability from 2002–2003 to 2009–2010. The only exception is at 900–1200 m from the terminus, where the velocity increased by ~ 20 m a^{-1} (Fig. 3a). The ice-flow velocity field

of Lugge Glacier showed no significant change between 2002–2003 and 2008–2009. The glacier then decelerated in 2009–2010 at 500–2000 m from the terminus (Fig. 3b). No clear temporal variation was observed at Luge II Glacier (Fig. 3e). Uncertainties in the ice flow velocities were 5 The flow velocity uncertainty was estimated to be 12.1 m a^{-1} , as given by the mean off-glacier displacement from 3 February 2006 to 30 January 2007 (0.99 years). Scherler and Strecker (2012) applied the same procedures to Biafo Glacier in Karakoram with ASTER images and obtained an uncertainty of $1–5 \text{ m a}^{-1}$ for timespans of 1–3 years. Thus, our velocity calculations are of the same quality as those reported by Scherler and Strecker (2012) (Fig. 410 S8).

4.3 Changes in glacier terminus

Thorthormi Glacier progressively shrank in size from 2000 to 2010, at thea mean rate of $-0.09 \text{ km}^2 \text{ a}^{-1}$ and accelerated loss between 2010 and 2011 ($-0.49 \text{ km}^2 \text{ a}^{-1}$) (Figs. 4a and 5). This change was due to the rapid retreat of the northern half of the glacier front by 200–1400 m (~~400 m~~). Luge Glacier also shrank in size from 2000 to 2011, at a mean rate of $-0.03 \text{ km}^2 \text{ a}^{-1}$ (Figs. 4b and 5). Since 2009, the calving front has retreated more rapidly along the northern half of the glacier front (by 300–400 m) than along the southern half (by $< 200 \text{ m}$) (Fig. 4b). The total area changes from 2000 to 2011 are -1.40 km^2 for Thorthormi Glacier and -0.33 km^2 for Thorthormi and Luge Glacier glaciers, respectively.

4.4 Mass balance of the debris-covered surface

The simulated SMB calculations show shows a spatially heterogeneous distribution amongbetween the threetwo glaciers (Fig. 420 1c). For example, the debris free surface alongSMB ranges from -9.5 to $-2.0 \text{ m w.e. a}^{-1}$, with a mean rate of $-7.4 \pm 0.1 \text{ m w.e. a}^{-1}$, over the center simulated region of Thorthormi Glacier shows. For Luge Glacier, the SMB ranges from -8.7 to $-0.9 \text{ m w.e. a}^{-1}$, with a mean rate of $-5.3 \pm 0.1 \text{ m w.e. a}^{-1}$. The mean SMB is -9.0 ± 0.1 and $-6.7 \pm 0.2 \text{ m w.e. a}^{-1}$ across the DGPS survey area of Thorthormi and Luge glaciers, respectively (Table 1). The debris-free surface has a more negative SMB (~~7.5 to 8.5 m w.e. a⁻¹~~) than the debris-covered regions (~~5.0 to 7.0 m w.e. a⁻¹~~; Fig. 1c). The SMB is more uniformly distributed within 2000 m of the calving front glaciers. The mean SMB over the simulated region of LugeThorthormi Glacier; is -9.3 ± 0.7 and $-7.3 \pm 0.1 \text{ m w.e. a}^{-1}$ on both the debris-free (~~6.0~~ and debris-covered surfaces, respectively. The mean SMB of Luge Glacier is $-7.3 \pm 0.4 \text{ m w.e. a}^{-1}$ and $-5.4 \pm 0.2 \text{ m w.e. a}^{-1}$ on the debris-free and debris-covered surfaces, respectively.

The sensitivity of simulated meltwater in the SMB model was evaluated as a function of the RMSE of each meteorological variable across the debris-covered area (Fig. S9). Ice melting is more sensitive to ~~7.5 m w.e. a⁻¹~~ and debris covered (~~5.5 solar radiation and thermal resistance. The influence of thermal resistance on meltwater formation is considered to 7.0 m w.e. a⁻¹~~) surfaces. The SMB of Luge II Glacier is significantly less negative than those of other two glaciers, ranging from ~~5.5 to +0.0 m w.e. a⁻¹~~ (Fig. 2b). Over the studied area, the mean SMB is ~~7.9, 6.0, and 4.4 m w.e. a⁻¹~~ for Thorthormi, Luge, be

small since the debris cover is thin and sparse over the glaciers. The estimated meltwater uncertainty is < 50 % across most of Thorthormi and Luggé glaciers, respectively (Table 1 (Fig. S10)).

435 4.5 Numerical experiments of ice dynamics

The ice thinning of Luggé Glacier was three times faster than that of Thorthormi Glacier. However, the mean SMB was 1.34 times more negative at Thorthormi Glacier, suggesting a substantial influence of glacier dynamics on ice thickness change. To quantify the contribution of ice dynamics to the ice thickness change, we performed numerical experiments with the present (Experiment 1) and prescribed (Experiment 2) glacier geometries.

440 4.5.1 Experiment 1 – present geometry

Modeled/Modelled results for the present geometry show significantly different ice-flow velocity fields for Thorthormi and Luggé glaciers (Fig. 6c and 6d). Thorthormi Glacier flows faster ($> 150 \text{ m a}^{-1}$) in the upper reaches, where the surface is steeper than the other regions (Fig. 6c). Down-glacier of the icefall, where the glacier surface is flatter, the ice motion slows in the down-glacier direction, with the flow velocities decreasing to $< 10 \text{ m a}^{-1}$ near the terminus (Fig. 6e). Ice flows upward relative to the surface across most of the modeled region (Fig. 6c). In contrast to the observed decrease in the ice-flow velocity field at Thorthormi, the computed ice-flow velocities of Luggé Glacier gradually increase down-glacier, up to $\sim 40 \text{ m a}^{-1}$, and then sharply increase to $\sim 80 \text{ m a}^{-1}$ at the calving front (Fig. 6f). Ice flow is nearly parallel to the glacier surface, except for the more downward motion near the calving front (Fig. 6d). Within 3000 m of the terminus of Thorthormi Glacier, the modeled surface ice-flow velocities are in good agreement with the satellite-derived ice-flow velocity field (Fig. 6e). The calculated surface flow velocities of Luggé Glacier are within 7 % of the satellite-derived flow velocities (Fig. 6f).

445 4.5.2 Experiment 2 – contrasting geometry

Figure 7c shows the ice-flow velocities simulated for the lake-terminating boundary condition of Thorthormi Glacier, in which the ice-flow velocities within 200 m of the calving front are three to four times faster than those of Experiment 1 (Figs. 6c and 7c). The mean vertical surface ice-flow velocity within 2000 m of the front is still positive (0.9 m a^{-1}), but is smaller than that for the land-terminating condition (1.6 m a^{-1}). The modeled result demonstrates significant acceleration as the glacier dynamics change from a compressive to stretching flow regime after proglacial lake formation. For Luggé Glacier, the ice-flow velocity decreases over the entire glacier in comparison with Experiment 1 (Figs. 6d and 7d). The upward ice motion appears within 3000 m of the terminus. The numerical experiments demonstrate that the formation of a proglacial lake causes significant changes in ice dynamics.

4.5.3 Simulated surface flow velocity uncertainty

Although we assumed Thorthormi and Lugge glaciers were temperate in the model, the simulated ice flow is mostly due to basal sliding in the ablation area of both glaciers (Figs. 6e and 6f). The influence of this assumption on the flow velocity computations is therefore small because our model indicated moderate ice deformation in the glaciers. The RMSEs between the modelled and measured flow velocities were computed as a measure of the model performance (Fig. S5). For Thorthormi Glacier, the model exhibits similar sensitivities to the sliding coefficient and ice thickness. For Lugge Glacier, the model is more sensitive to the ice thickness than the sliding coefficient. Sensitivity tests demonstrate that the simulated surface flow velocities of Thorthormi Glacier vary by $\pm 30\%$ when the constant sliding coefficient (C) and ice thickness are varied by $\pm 30\%$ (Fig. S11). For Lugge Glacier, the simulated flow velocities vary by 22 and 65 % when the sliding coefficient and ice thickness are varied by $\pm 30\%$, respectively. The simulated surface flow velocity uncertainty is estimated as the quadratic sum of the accuracy of the surface flow velocity measurements, interannual variability in the measured surface flow velocities and the RMSE between the modelled and measured surface flow velocities. The mean uncertainty of the simulated surface flow velocity ($\sigma_{u_{model}}$) is 20.7 and 26.9 m a^{-1} for Thorthormi and Lugge glaciers, respectively.

4.6 Simulated ice thickness change

Figure 8a shows the computed emergence velocity and SMB along the central flowlines of the glaciers. Given the computed surface flow velocities from Experiment 1, the emergence velocity of Lugge Glacier ranges from -1.3 to $0.3 \text{ m w.e. a}^{-1}$, with a mean value of $-0.2 \pm 0.1 \text{ m w.e. a}^{-1}$ within 700–1500 m of the terminus (Fig. 8a) and more negative values near the calving front, reaching approximately $-10 \text{ m w.e. a}^{-1}$ due to the increase in surface flow velocities toward the glacier front (Fig. 6f). In contrast to Lugge Glacier, the emergence velocity of Thorthormi Glacier is positive over the entire model domain, ranging from 1.9 to 5.4 m w.e. a^{-1} , with a mean value of $3.1 \pm 0.4 \text{ m w.e. a}^{-1}$ within 1300–2800 m of the terminus that increases to $> 10 \text{ m a}^{-1}$ in the upper reaches of the glacier (Fig. 8a).

The emergence velocity computed under contrasting geometries (Experiment 2) varies from that with the present geometries (Experiment 1) for both Thorthormi and Lugge glaciers. For the land-terminating condition of Lugge Glacier, the mean emergence velocity is positive ($1.4 \pm 0.1 \text{ m w.e. a}^{-1}$) within 700–1500 m of the terminus. The mean emergence velocity of Thorthormi Glacier computed with the lake-terminating condition is $1.8 \pm 0.4 \text{ m w.e. a}^{-1}$ within 1300–2800 m of the terminus, which decreases by 42 % from the land-terminating condition.

Under the modelled conditions of Experiment 1, the computed rate of elevation change of Lugge Glacier is -9.0 to -5.2 m a^{-1} , with a mean rate of $-7.7 \pm 0.7 \text{ m a}^{-1}$ within 700–1500 m from the calving front, which is 61 % more negative than the observations (Fig. 8). For Thorthormi Glacier, the rate of elevation change ranges from -7.1 to -4.1 m a^{-1} , with a mean rate of $-6.1 \pm 0.9 \text{ m a}^{-1}$ over the in situ surveyed domain (Fig. 8). These values agree with the observations that were made 2400–

3200 m from the terminus, falling within the uncertainty range, whereas they are much more negative than the observations along the lower reaches of the glacier.

Given the same SMB distribution of Experiment 1, the mean rate of elevation change was computed as $-7.4 \pm 1.0 \text{ m a}^{-1}$ (1300–2800 m) for Thorthormi Glacier with the lake-terminating condition and $-6.0 \pm 0.8 \text{ m a}^{-1}$ (1300–2800 m) for the land-terminating Lugge Glacier.

The mean uncertainty of the emergence velocity is 2.0 and 1.7 m w.e. a^{-1} for Thorthormi and Lugge glaciers, respectively. The uncertainty of the computed rate of elevation change is estimated to be 2.4 to 8.3 m a^{-1} for Thorthormi Glacier and 1.6 to 8.3 m a^{-1} for Lugge Glacier.

5 Discussion

5.1 Glacier thinning

The repeated GPS surveys revealed rapid thinning of Lugge Glacier between 2004 and 2011. The mean rate of surface elevation change ($-4.67 \pm 0.02 \text{ m a}^{-1}$) is comparable to that for the 2002–2004 period (-5 m a^{-1} ; Naito et al., 2012). Gardelle et al. (2013) reported the rates of surface elevation change ranging from -8 to -3 m a^{-1} during 2000–2010, as determined from the differencing of satellite-derived DEMs. Lugge Glacier is thinning more rapidly than neighboring glaciers in the Nepal and Bhutan Himalayas. The mean rate of surface elevation change was $-0.50 \pm 0.14 \text{ m a}^{-1}$ in the ablation area of Bhutanese glaciers for the period 2000–2010 (Gardelle et al., 2013), and $-2.30 \pm 0.53 \text{ m a}^{-1}$ for debris-free glaciers in eastern Nepal and Bhutan during 2003–2009 (Kääb et al., 2012). Maurer et al. (2016) reported that the mean thinning rate for Lugge Glacier during 1974–2006 ($-0.6 \pm 0.2 \text{ m a}^{-1}$) was greater than those for other Bhutanese lake-terminating glaciers (-0.2 to -0.4 m a^{-1}). The rate of surface elevation change of Thorthormi Glacier (from -3.37 to $+1.14 \text{ m a}^{-1}$ from 2004 to 2011) is comparable with previous measurements, which range from -3 to 0 m a^{-1} for the period 2002–2004 (Naito et al., 2012) and from -3 to 0 m a^{-1} during 2000–2010 (Gardelle et al., 2013). The mean rate across Thorthormi Glacier was $-0.3 \pm 0.2 \text{ m a}^{-1}$ during 1974–2006 (Maurer et al., 2016), which is a typical rate in the Bhutan Himalaya.

Lugge Glacier thinned more rapidly than Thorthormi and Lugge II glaciers, which is consistent with previous satellite-based studies. For example, the thinning rates of the lake-terminating Imja and Lumding glaciers (-1.14 and -3.41 m a^{-1} , respectively) were ~ 4 times greater than those of the land-terminating glaciers (approximately -0.87 m a^{-1}) in the Khumbu region of the Nepal Himalaya (Nuimura et al., 2012). King et al. (2017) measured the thinning of the lower parts of nine lake-terminating glaciers in the Everest area (approximately -2.5 m a^{-1}), which was 67 % faster than that of 18 land-terminating glaciers (approximately -1.5 m a^{-1}). The lake-terminating glaciers in the Yakutat ice field, Alaska, thinned at a rate of -4.76 m a^{-1} , which was ~ 30 % greater than the neighboring land-terminating glaciers (Trüssel et al., 2013). It should

520 be noted that the difference in thinning rate between Lugge and Thorthormi glaciers (3.3 times) is much greater than the numbers previously reported in the Nepal Himalaya, suggesting that ice dynamics play a more significant role here.

Glacier thinning has accelerated ~~in recent decades~~ from 1970s to 2000s, particularly in the lower parts of Lugge and Thorthormi glaciers. For example, the mean rates of elevation change over Lugge ($-4.67 \pm 0.02 \text{ m a}^{-1}$) and Thorthormi ($-1.40 \pm 0.01 \text{ m a}^{-1}$) are more negative than those reported for the 1974–2006 period ($-1.7 \pm 0.2 \text{ m a}^{-1}$ for Lugge and $-0.9 \pm 0.2 \text{ m a}^{-1}$ for Thorthormi; Maurer et al., 2016). These changes are consistent with the accelerating mass loss of glaciers in northern Bhutan. ~~Regional~~ The regional mass balances in northern Bhutan have accelerated from the 1974–2006 period to the post 2000 period. For example, the region-wide mass balance is $-0.17 \pm 0.05 \text{ m w.e. a}^{-1}$ for 1974–2006 (Maurer et al., 2016) ~~to~~, $-0.22 \pm 0.12 \text{ m w.e. a}^{-1}$ for 1999–2011 (Gardelle et al., 2013), ~~to~~ $-0.42 \pm 0.20 \text{ m w.e. a}^{-1}$ for 2000–2016 (Brun et al., 2017) ~~;~~ and $-0.52 \pm 0.16 \text{ m w.e. a}^{-1}$ for 2003–2008 (Kääb et al., 2012). The mass change of Bhutanese glaciers is expected to be sensitive to precipitation, which varies under the influence of the summer monsoon (Fujita and Ageta, 2000; Fujita, 2008). The summer monsoon has been weakening since the 1950s (Bollasina et al., 2011), which might have reduced the amount of snowfall across the present study area. This trend is likely one of the reasons for the accelerated glacier thinning in recent years. However, care should be taken in making such inferences because previous studies covered different spatial extents, used different methods to fill data gaps in the accumulation ~~zones~~ areas, and suffered from uncertainties in ~~Shuttle Radar Topography Mission~~ SRTM data due to radar penetration (Zemp et al., 2015; Maurer et al., 2016). Regardless, the thinning rate increased by a greater amount at Lugge Glacier than at Thorthormi Glacier from 1974–2006 to 2004–2011, indicating that the rapid thinning of Lugge Glacier is affected by a change in ice dynamics. A likely interpretation is that ~~dynamic thinning was enhanced by glacier acceleration after the expansion of Lugge Glacial Lake in the 1960s~~ the expansion of Lugge Glacial Lake after the 1960s and glacier thinning decreased the effective pressure (ice overburden minus basal water pressure), resulting in glacier acceleration by enhancing basal ice motion, as previously seen near the front of a lake-terminating glacier (Sugiyama et al., 2011). It is likely that the acceleration and enhanced longitudinal stretching near the terminus resulted in further ice thinning.

5.2 Influence of ice dynamics on glacier thinning

The simulated SMB of Lugge Glacier for the ~~2002–2004~~ 1979–2017 period (-5.98 ± 1.11 $6.77 \pm 0.17 \text{ m w.e. a}^{-1}$) is 1.36 times more negative than its thinning rate for the 2004–2011 period ($-4.25 \pm 0.02 \text{ m w.e. a}^{-1}$), which is converted to water equivalent using an ice density of 910 kg m^{-3} , while the negative SMB of Thorthormi Glacier (-7.87 ± 1.46 $9.03 \pm 0.14 \text{ m w.e. a}^{-1}$) is 6.27.1 times more negative than its thinning rate ($-1.27 \pm 0.01 \text{ m w.e. a}^{-1}$). This result suggests that the rapid thinning is due mainly to surface melting along Lugge Glacier, whereas the negative SMB is counterbalanced by the vertical straining of Thorthormi Glacier (Fig. 6c and 6d). The horizontal ~~ice-flow~~ velocity field velocities of Lugge Glacier ~~is~~ are nearly uniform along the central flowline, with ice flow parallel to the glacier surface (Fig. 6d), suggesting that the dynamically induced change in ice thickness is small. However, the ~~ice-flow~~ velocity field velocities of Thorthormi Glacier ~~decreases~~ decrease

toward the terminus (Fig. 6c), resulting in thickening under a longitudinally compressive flow regime. ~~To compare the influence of ice dynamics on glacier thinning in lake and land terminating glaciers, we calculated the emergence velocity (v_e) as follows:~~

$$v_e = (v_z - v_h \tan \alpha) \frac{\rho_i}{\rho_w}, \quad (11)$$

where v_z and v_h are vertical and horizontal velocities, respectively, and α is the surface slope (Cuffey and Paterson, 2010). The emergence velocity is converted into water equivalent (m w.e. a^{-1}) using the densities of ice (ρ_i , 910 kg m^{-3}) and water (ρ_w , 1000 kg m^{-3}), for comparison with SMB. Figure 8a shows the computed emergence velocity and SMB along the central flowlines of the glaciers. The emergence velocity of Luggé Glacier ranges from -1.1 to $-0.1 \text{ m w.e. a}^{-1}$ within 780–1510 m of the terminus (Fig. 8a), with more negative values near the calving front, at around $-10 \text{ m w.e. a}^{-1}$; of Luggé Glacier is slightly negative ($-0.2 \pm 0.1 \text{ m w.e. a}^{-1}$), suggesting that the contribution of dynamic ice thickness change to ice thinning is small, with the significant thinning of Luggé Glacier caused mainly by its negative SMB. However, the emergence velocity of Thorthormi Glacier is positive ($3.1 \pm 0.4 \text{ m w.e. a}^{-1}$), suggesting that the glacier is thickening due to the increase in a vertically straining flow speed toward the glacier front (Fig. 6f) regime. The mean SMB of Thorthormi Glacier is 3733 % more negative than that of Luggé Glacier, which is due to the glacier being. Since a sparse distribution of thin debris cover is present across the ablation area of both glaciers, the more negative SMB of Thorthormi Glacier cannot be fully explained by differences in the thickness and spatial distribution of debris cover, with a more likely explanation being that the glacier is situated at lower elevations (Fig. 6a and 6b). The surface elevation change over time (dh/dt , m a^{-1}), caused by the imbalance of the emergence velocity and SMB along the central flowline, is calculated as

$$\frac{dh}{dt} = (\text{SMB} + v_e) \frac{\rho_w}{\rho_i} \quad (12)$$

Under the modeled conditions, the rate of elevation change of Luggé Glacier is -6.3 to -7.4 m a^{-1} within 700–1500 m of the calving front, which is -60% more negative than the observations (Fig. 8). In contrast to Luggé Glacier, the emergence velocity of Thorthormi Glacier is positive over the entire model domain. The emergence velocity ranges from 2.9 to $4.0 \text{ m w.e. a}^{-1}$ within 1300–2800 m of the terminus and increases to $> 10 \text{ m a}^{-1}$ near the accumulation zone (Fig. 8a). The rate of elevation change estimated by Eq. (12) ranges from -4.7 to $+5.0 \text{ m a}^{-1}$ over the in situ surveyed domain (Fig. 8). These values agree with the observation at 2400–3200 m from the terminus, falling within the uncertainty range, while they are much more negative than the observation near the terminus (Fig. 8b). The calculated rate of elevation change over the surveyed domain is of Thorthormi Glacier is equivalent to one-third fourth of the SMB, implying

that approximately ~~two-thirds~~ ~~three-fourths~~ of the surface ablation is counterbalanced by ice dynamics. In other words, dynamically induced thickening compensates for the negative SMB.

585 Experiment 1 demonstrates that the difference in emergence velocity between land- and lake-terminating glaciers leads to contrasting thinning patterns. Based on this result, we hypothesise that the emergence velocity of Luge Glacier would be positive in the absence of a glacial lake. Furthermore, the emergence velocity of Thorthormi Glacier will decrease in association with lake development. The results from Experiments 1 and 2 support this hypothesis, with a positive emergence velocity (1.4 ± 0.1 m w.e. a^{-1}) modelled for Luge Glacier under the land-terminating condition, resulting in a decrease in the thinning rate of 28 % compared with the lake-terminating condition. This result suggests that the decrease in emergence velocity caused by the development of Luge Glacial Lake should have accelerated the thinning in addition to the more negative SMB since the 1960s. For Thorthormi Glacier, the emergence velocity under the lake-terminating condition is still positive (1.8 ± 0.4 m w.e. a^{-1}) but it decreases by 72 % from the land-terminating condition, resulting in an increase in the thinning rate from 6.1 to 7.4 m a^{-1} . Our ice flow modelling demonstrates that thinning will accelerate in association with the development of a supraglacial lake in the terminal part of Thorthormi Glacier.

590 Contrasting patterns of glacier thinning and horizontal flow velocities between land- and lake-terminating glaciers are consistent with satellite-based observations over lake or ocean-terminating glaciers and neighbouring land-terminating glaciers in the Nepal Himalaya (King et al., 2017) and Greenland (Tsutaki et al., 2016). A decrease in the down-glacier flow velocities over the lower reaches of land-terminating glaciers suggests a longitudinally compressive flow regime, which would result in a positive emergence velocity and therefore less thinning to compensate for the negative SMB, as demonstrated in the ice flow model. Conversely, for lake-terminating glaciers, an increase in the down-glacier flow velocities suggests a longitudinally stretching flow regime, which would yield a negative emergence velocity, resulting in accelerated ice thinning. Such mechanisms should not only be active for Thorthormi and Luge glaciers, but any lake- and land-terminating glaciers worldwide where contrasting thinning patterns between glaciers are observed.

600 The thinning rate calculated from the model is ~ 5 m a^{-1} more negative than the ~~observations~~ ~~observation~~ over the entire domain of Luge Glacier and also the lower part of Thorthormi Glacier (Fig. 8b), which is probably due to the uncertainties in the estimated ice thickness and basal sliding conditions. ~~Sensitivity tests demonstrate that the surface ice flow velocities vary by $\pm 10\%$ and $\pm 19\%$ when changing the constant sliding coefficient (C) by $\pm 10\%$ and the ice thickness by ± 10 m (Fig. S3), respectively. Changes as discussed in the emergence velocity for the same sensitivity tests are $\pm 7\%$ and $\pm 11\%$, respectively~~section 4.5.3. The two-dimensional feature is another reason for the insufficient ~~modeled~~ ~~modelled~~ results, because the model neglects drag from the ~~sidewalls~~ ~~side walls~~ and changes in glacier width. The SMB (meltwater) uncertainty is ~~estimated to be 11% from thermal resistance (Fig. S1b)~~ $< 50\%$ over a large portion of Thorthormi and Luge glaciers (Fig. S10). Nevertheless, our numerical experiments demonstrate that dynamically induced ice thickening compensates the negative SMB in the lower part of a land-terminating glacier, resulting in less ice thinning in comparison with a lake-terminating glacier.

615 Further measurements of the spatial distributions of ice thickness and SMB will help in deriving more accurate estimates of the effect of ice dynamics on glacier thinning.

5.3 Glacier retreat

Lugge Glacier has retreated continuously and at a nearly constant rate from 2000 to 2011 (Fig. 5). The mean rate of area change over the 2000–2010 period ($-0.03 \text{ km}^2 \text{ a}^{-1}$) is comparable to a previously reported value for 2000–2010 ($-0.04 \text{ km}^2 \text{ a}^{-1}$, Bajracharya et al., 2014). Bathymetric data suggest that glacier ice below the lake level accounted for 89 % of the full ice thickness at the calving front in 2002 (Fig. 6b). The lake level is close to the ice flotation level, where the basal water pressure equals the ice overburden pressure, suggesting that calving caused by ice flotation regulates the glacier front position (Van der Veen, 1996). Glaciers rapidly retreat by calving when the lake level reaches the flotation level (e.g., Motyka et al., 2002; Tsutaki et al., 2011). Moreover, retreat is accelerated when the glacier terminus is situated on a reversed bed slope (e.g., Nick et al., 2009). A recent numerical study estimated overdeepening of Lugge Glacier within 1500 m of the 2009 terminus (Linsbauer et al., 2016), suggesting further rapid retreat in the future. Recent glacier inventories indicate that Lugge Glacier has a smaller accumulation area than Thorthormi Glacier (Nuimura et al., 2015; Nagai et al., 2016), suggesting that a sufficient ice flux cannot be supplied to the lower part of the glacier to compensate for the ongoing ice thinning.

The mean rate of area change for Thorthormi Glacier over the 2000–2010 period ($-0.09 \text{ km}^2 \text{ a}^{-1}$) is comparable to a previously reported value for 2000–2010 ($-0.04 \text{ km}^2 \text{ a}^{-1}$, Bajracharya et al., 2014). After progressive mass loss since 2000, the front of Thorthormi Glacier detached from the terminal moraine and retreated further from November 2010 to December 2011 (Fig. 4a). The glacier ice was still in contact with the moraine during the field campaign in September 2011, but the glacier was completely detached from the moraine on the 2 December 2011 Landsat 7 image. Satellite images taken after 2 December 2011 show a large number of icebergs floating in the lake, suggesting rapid calving due to ice flotation. A numerical study suggested that a proglacial lake longer than a certain longitudinal length is also preferable for autonomous expansion through valley wind over the lake surface (Sakai et al., 2009). A previous study estimated that the overdeepening of Thorthormi Glacier extends for $> 3000 \text{ m}$ from the terminal moraine (Linsbauer et al., 2016), which suggests that continued glacier thinning will lead to rapid retreat of the entire section of the terminus as the ice thickness reaches flotation.

Experiment 2 simulates a significant increase in surface ice-flow velocity at the lower part of Thorthormi Glacier when a proglacial lake forms (Fig. 7e). Previous studies reported the speed up and rapid retreat of glaciers after detachment from a terminal ridge or bedrock bump (e.g., Boyce et al., 2007; Sakakibara and Sugiyama, 2014; Trüssel et al., 2015). In addition to the reduction in back stress, thinning itself decreases the effective pressure ($\text{ice overburden minus basal water pressure}$), which enhances basal ice motion and increases ice-flow velocity (Sugiyama et al., 2011). A decrease in the effective pressure also enhances shear stress in the water-saturated till layer beneath the glacier (Cuffey and Paterson, 2010), though little information is available on subglacial sedimentation in the Himalayas. Acceleration near the terminus results in ice thinning and a decrease in effective pressure, which in turn leads to further acceleration of glacier flow (e.g., Benn et al., 2007b). Although no clear

acceleration was observed during 2002–2011 (Fig. 3a), it is likely that the thinning and retreat of Thorthormi Glacier will be accelerated in the near future due to the formation and expansion of the proglacial lake.

6 Conclusions

650 To better understand the importance of glacial lake formation on rapid glacier thinning, we carried out field and satellite-based ~~campaigns~~ ~~measurements~~ across the lake-terminating Lugge Glacier and the land-terminating Thorthormi ~~and Lugge-H~~ ~~glaciers~~ Glacier in the Lunana region, Bhutan Himalaya. Surface elevations were surveyed in 2011 by differential GPS across the lower parts of the glaciers and compared with a 2004 GPS survey. The ~~ice~~-flow velocity ~~fields~~ and terminus positions of the glaciers were determined from ~~Landsat~~ ~~optical~~ satellite images. We also performed numerical experiments to quantify the

655 contributions of surface mass balance (SMB) and ice dynamics in relation to the observed ice thinning.

Lugge Glacier has experienced rapid ice thinning at an average rate of $-4.67 \pm 0.02 \text{ m a}^{-1}$, which is 3.3 times greater than that of Thorthormi Glacier, even though the SMB was less negative. The numerical ~~modeling~~ ~~modelling~~ results, using the present glacier geometries, demonstrate that Thorthormi Glacier is subjected to a longitudinally compressive flow regime, suggesting that dynamically induced thickening compensates for the negative SMB, and thus results in less ice thinning than

660 at Lugge Glacier. Conversely, the flow of Lugge Glacier is nearly uniform along its central flowline, suggesting that the dynamically induced change in ice thickness is small, with the rapid thinning of Lugge Glacier driven by surface melt. This study reveals that contrasting ice flow regimes cause different ice thinning observations between lake- and land-terminating glaciers in the Bhutan Himalaya.

Lugge Glacier retreated continuously from 2000 to 2011, shrinking at a rate of $0.03 \text{ km}^2 \text{ a}^{-1}$. The ice approaching the calving

665 front is near flotation, suggesting that the terminus retreat will be accelerated by active calving in the future. Thorthormi Glacier has been retreating since 2000, resulting in the detachment of the glacier front from the terminal moraine and the formation of a proglacial lake in 2011. Ice flow ~~modeling~~ ~~modelling~~ with the lake-terminating boundary condition indicates a significant increase in surface ~~ice~~-flow velocities near the calving front, which leads to continued glacier retreat. This positive feedback will be activated in Thorthormi Glacier with the expansion of the proglacial lake, causing further thinning and retreat

670 in the near future.

Data availability. The data for Figs. 1–8 are provided in Microsoft Excel format in the ~~Supplementary Materials. The Advanced Land Observing Satellite (ALOS)~~ ~~Supplement. The ALOS satellite~~ data are available for purchase from the Remote Sensing Technology Center of Japan (<https://www.restec.or.jp/en/>). The Landsat 7 ETM+ satellite data are distributed by the United

675 States Geological Survey (<http://landsat.usgs.gov/>).

Author contributions. KF and AS designed the study. KF, JK, TN, PT, and ST conducted the field survey in 2011. KF analyzed the survey data in 2004 and 2011, and simulated the surface mass balance. TN calculated the satellite-based surface ice-flow velocity field. SS provided ice flow models. ST analyzed the data. ST and KF wrote the paper, with contributions from AS and SS.

680

Competing interests. The authors declare that they have no conflict of interest.

685 **Acknowledgement.** We thank the Department of Geology and Mines, Bhutan, for providing the opportunity and permission to
conduct the field observations. We thank S. Takenaka, M. Sano, A. Sasaki, K. Ghallay and logistic members for their support
during the field campaign. We appreciate F. Pellicciotti and three anonymous referees for their thoughtful and constructive
comments. This research was supported by the Science and Technology Research Partnership for Sustainable Development
690 (SATREPS), supported by the Japan Science and Technology Agency (JST) and the Japan International Cooperation Agency
(JICA). Support was also provided by the Funding Program for Next Generation World Leading Researchers (NEXT Program,
GR052), and JSPS-KAKENHI (grant numbers 26257202 and 17H06104).

References

- Ageta, Y., Iwata, S., Yabuki, H., Naito, N., Sakai, A., Narama, C., and Karma.: Expansion of glacier lakes in recent decades
in the Bhutan Himalayas, *IAHS Publ.*, 264, 165–175, 2000.
- 695 Azam, M. F., Wagnon, P., Berthier, E., Vincent, C., Fujita, K., and Kargel, J. S.: Review of the status and mass changes of
Himalayan-Karakoram glaciers, *J. Glaciol.*, 1–14, <https://doi.org/10.1017/jog.2017.86>, 2018.
- Bajracharya, S. R., Maharjan, S. B., and Shrestha, F.: The status and decadal change of glaciers in Bhutan from the 1980s to
2010 based on satellite data, *Ann. Glaciol.*, 55 (66), 159–166, <https://doi.org/10.3189/2014AoG66A125>, 2014.
- Benn D., Hulton, N. R. J., and Mottram, R. H.: ‘Calving lows’, ‘sliding laws’, and the stability of tidewater glaciers, *Ann.*
700 *Glaciol.*, 46 (1), 123–130, <https://doi.org/10.3189/172756407782871161>, 2007a.
- Benn, D., Warren, C., and Mottram, R.: Calving processes and the dynamics of calving glaciers, *Earth-Sci. Rev.*, 82, 143–179,
<https://doi.org/10.1016/j.earscirev.2007.02.002>, 2007b.
- Berthier, E., Arnaud, Y., Kumar, R., Ahmad, S., Wagnon, P., and Chevallier, P.: Remote sensing estimates of glacier mass
balances in the Himachal Pradesh (Western Himalaya, India), *Remote Sens. Environ.*, 108 (3), 327–338,
705 <https://doi.org/10.1016/j.rse.2006.11.017>, 2007.
- Bolch, T., Pieczonka, T., and Benn, D. I.: Multi-decadal mass loss of glaciers in the Everest area (Nepal Himalaya) derived
from stereo imagery, *The Cryosphere*, 5 (2), 349–358, <https://doi.org/10.5194/tc-5-349-2011>, 2011.
- Bolch, T., Kulkarni, A., Käab, A., Huggel, C., Paul, F., Cogley, J. G., Frey, H., Kargel, J. S., Fujita, K., Scheel, M., Bajracharya,
S., Stoffel, M.: The state and fate of Himalayan Glaciers, *Science*, 336 (6079), 310–314,
710 <https://doi.org/10.1126/science.1215828>, 2012.
- Bollasina, M., Ming, Y., and Ramaswamy, V.: Anthropogenic aerosols and the weakening of the South Asian summer
monsoon, *Science*, 334, 502–505, <https://doi.org/10.1126/science.1204994>, 2011.

- Boyce, E. S., Motyka, R. J., and Truffer, M.: Flotation and retreat of a lake-calving terminus, Mendenhall Glacier, southeast Alaska, USA, *J. Glaciol.*, 53 (181), 211–224, <https://doi.org/10.3189/172756507782202928>, 2007.
- 715 Brun, F., Berthier, E., Wagnon, P., Käab, A., and Treichler, D.: A spatially resolved estimate of High Mountain Asia glacier mass balances from 2000 to 2016, *Nat. Geosci.*, 10, 668–673, <https://doi.org/10.1038/ngeo2999>, 2017.
- Carrivick, J. L., and Tweed, F. S.: Proglacial lakes: character, behaviour and geological importance, *Quaternary Sci. Rev.*, 78, 34–52, <https://doi.org/10.1016/j.quascirev.2013.07.028>, 2013.
- Cogley, J. G.: Glacier shrinkage across High Mountain Asia, *Ann. Glaciol.*, 57 (71), 41–49, <https://doi.org/10.3189/2016AoG71A040>, 2016.
- 720 Cuffey, K. M. and Paterson, W. S. B.: *The physics of glaciers*, Oxford, Butterworth-Heinemann, 2010.
- Dehecq, A., Gourmelen, N., and Trouve, E.: Deriving large-scale glacier velocities from a complete satellite archive: Application to the Pamir–Karakoram–Himalaya, *Remote Sens. Environ.*, 162, 55–66, <https://doi.org/10.1016/j.rse.2015.01.031>, 2015.
- 725 Farinotti, D., Huss, M., Bauder, A., Funk, M., and Truffer, M.: A method to estimate the ice volume and ice-thickness distribution of alpine glaciers, *J. Glaciol.*, 55 (191), 422–430, <https://doi.org/10.3189/002214309788816759>, 2009.
- Fujita, K.: Effect of precipitation seasonality on climatic sensitivity of glacier mass balance, *Earth Planet. Sci. Lett.*, 276 (1–2), 14–19, <https://doi.org/10.1016/j.epsl.2008.08.028>, 2008.
- Fujita, K., and Ageta, Y.: Effect of summer accumulation on glacier mass balance on the Tibetan Plateau revealed by mass-balance model, *J. Glaciol.*, 46 (153), 244–252, <https://doi.org/10.3189/172756500781832945>, 2000.
- 730 Fujita, K., and Nuimura, T.: Spatially heterogeneous wastage of Himalayan glaciers, *P. Natl. Acad. Sci. USA*, 108 (34), 14011–14014, <https://doi.org/10.1073/pnas.1106242108>, 2011.
- Fujita, K., and Sakai, A.: Modelling runoff from a Himalayan debris-covered glacier, *Hydrol. Earth Syst. Sci.*, 18 (7), 2679–2694, <https://doi.org/10.5194/hess-18-2679-2014>, 2014.
- 735 Fujita, K., Suzuki, R., Nuimura, T., and Sakai, A.: Performance of ASTER and SRTM DEMs, and their potential for assessing glacial lakes in the Lunana region, Bhutan Himalaya, *J. Glaciol.*, 54 (185), 220–228, <https://doi.org/10.3189/002214308784886162>, 2008.
- Fujita, K., Sakai, A., Nuimura, T., Yamaguchi, S., and Sharma, R. R.: Recent changes in Imja Glacial Lake and its damming moraine in the Nepal Himalaya revealed by in situ surveys and multi-temporal ASTER imagery, *Environ. Res. Lett.*, 4 (4), 045205, <https://doi.org/10.1088/1748-9326/4/4/045205>, 2009.
- 740 Fujita, K., Takeuchi, N., Nikitin, S. A., Surazakov, A. B., Okamoto, S., Aizen, V. B., and Kubota, J.: Favorable climatic regime for maintaining the present-day geometry of the Gregoriev Glacier, Inner Tien Shan, *The Cryosphere*, 5 (3), 539–549, <https://doi.org/10.5194/tc-5-539-2011>, 2011.

- 745 Fujita, K., Sakai, A., Takenaka, S., Nuimura, T., Surazakov, A. B., Sawagaki, T., and Yamanokuchi, T.: Potential flood volume of Himalayan glacial lakes, *Nat. Hazards Earth Syst. Sci.*, 13 (7), 1827–1839, <https://doi.org/10.5194/nhess-13-1827-2013>, 2013.
- Funk, M., and Röthlisberger, H.: Forecasting the effects of a planned reservoir which will partially flood the tongue of Unteraargletscher in Switzerland, *Ann. Glaciol.*, 13, 76–81, <https://doi.org/10.1017/S0260305500007679>, 1989.
- 750 Gardelle, J., Arnaud, Y., and Berthier, E.: Contrasted evolution of glacial lakes along the Hindu Kush Himalaya mountain range between 1990 and 2009, *Global Planet. Change*, 75 (1–2), 47–55, <https://doi.org/10.1016/j.gloplacha.2010.10.003>, 2011.
- Gardelle, J., Berthier, E., Arnaud, Y., and Kääb, A.: Region-wide glacier mass balances over the Pamir-Karakoram-Himalaya during 1999–2011, *The Cryosphere*, 7 (4), 1263–1286, <https://doi.org/10.5194/tc-7-1263-2013>, 2013.
- 755 Glen, J. W.: The creep of polycrystalline ice, *Proc. R. Soc. London, Sea. A*, 228 (1175), 519–538, <https://doi.org/10.1098/rspa.1955.0066>, 1955.
- Gudmundsson, G. H.: A three-dimensional numerical model of the confluence area of Unteraargletscher, Bernese Alps, Switzerland, *J. Glaciol.*, 45 (150), 219–230, <https://doi.org/10.3198/1999JoG45-150-219-230>, 1999.
- Heid, T., and Kääb, A.: Evaluation of existing image matching methods for deriving glacier surface displacements globally from optical satellite imagery, *Remote Sens. Environ.*, 118, 339–355, <https://doi.org/10.1016/j.rse.2011.11.024>, 2012.
- 760 Hewitt, H. and Liu, J.: Ice-dammed lakes and outburst floods, Karakoram Himalaya: historical perspectives on emerging threats, *Physical Geography*, 31 (6), 528–551, <https://doi.org/10.2747/0272-3646.31.6.528>, 2010.
- Huss, M., and Hock, R.: Global-scale hydrological response to future glacier mass loss, *Nature Climate Change*, 8, 135–140, <https://doi.org/10.1038/s41558-017-0049-x>, 2018.
- 765 Immerzeel, W. W., Van Beek, L. P., and Bierkens, M. F.: Climate change will affect the Asian water towers, *Science*, 328 (5984), 1382–1385, <https://doi.org/10.1126/science.1183188>, 2010.
- Kääb, A.: Combination of SRTM3 and repeat ASTER data for deriving alpine glacier flow velocities in the Bhutan Himalaya, *Remote Sens. Environ.*, 94, 463–474, <https://doi.org/10.1016/j.rse.2004.11.003>, 2005.
- Kääb, A., Berthier, E., Nuth, C., Gardelle, J., and Arnaud, Y.: Contrasting patterns of early twenty-first-century glacier mass change in the Himalayas, *Nature*, 488 (7412), 495–498, <https://doi.org/10.1038/nature11324>, 2012.
- 770 Kanamitsu, M., Ebisuzaki, W., Woollen, J., Yang, S-K., Hnilo, J. J., Fiorino, M., and Potter, G. L.: NCEP-DOE AMIP-II Reanalysis (R-2), *B. Am. Meteorol. Soc.*, 1631–1643, <https://doi.org/10.1175/BAMS-83-11-1631>, 2002.
- King, O., Quincey, D. J., Carrivick, J. L., and Rowan, A. V.: Spatial variability in mass loss of glaciers in the Everest region, central Himalayas, between 2000 and 2015, *The Cryosphere*, 11 (1), 407–426, <https://doi.org/10.5194/tc-11-407-2017>, 2017.
- 775 Komori, J.: Recent expansions of glacial lakes in the Bhutan Himalayas, *Quatern. Int.*, 184 (1), 177–186, <https://doi.org/10.1016/j.quaint.2007.09.012>, 2008.

- Lamsal, D., Fujita, K., and Sakai, A.: Surface lowering of the debris-covered area of Kanchenjunga Glacier in the eastern Nepal Himalaya since 1975, as revealed by Hexagon KH-9 and ALOS satellite observations, *The Cryosphere*, 11, 2815–2827, <https://doi.org/10.5194/tc-11-2815-2017>, 2017.
- 780 Leprince, S., Barbot, S., Ayoub, F., and Avouac, J-P.: Automatic and precise orthorectification, coregistration, and subpixel correlation of satellite images, application to ground deformation measurements, *IEEE Trans. Geosci. Remote Sens.*, 45, 1529–1558, <https://doi.org/10.1109/TGRS.2006.888937>, 2007.
- Linsbauer, A., Frey, H., Haerberli, W., Machguth, H., Azam, M., and Allen, S.: Modelling glacier-bed overdeepenings and possible future lakes for the glaciers in the Himalaya–Karakoram region, *Ann. Glaciol.*, 57 (71), 119–130, <https://doi.org/10.3189/2016AoG71A627>, 2016.
- 785 Mattson, L. E., Gardner, J. S., and Young, G. J.: Ablation on debris covered glaciers: an example from the Rakhiot Glacier, Punjab, Himalaya, *IAHS Publication*, 218, 289–296, 1993.
- Maurer, J. M., Rupper, S. B., and Schaefer, J. M.: Quantifying ice loss in the eastern Himalayas since 1974 using declassified spy satellite imagery, *The Cryosphere*, 10 (5), 2203–2215, doi:10.5194/tc-10-2203-2016, 2016.
- Mölg, T., Maussion, F., and Scherer, D.: Mid-latitude westerlies as a driver of glacier variability in monsoonal High Asia, 790 *Nature Climate Change*, 4, 68–73, <https://doi.org/10.1038/nclimate2055>, 2014.
- Motyka, R. J., O’Neel, S., Connor, C. L., and Echelmeyer, K. A.: Twentieth century thinning of Mendenhall Glacier, Alaska, and its relationship to climate, lake calving, and glacier runoff, *Global Planet. Change*, 35 (1–2), 93–112, [https://doi.org/10.1016/S0921-8181\(02\)00138-8](https://doi.org/10.1016/S0921-8181(02)00138-8), 2002.
- Nagai, H., Fujita, K., Sakai, A., Nuimura, T., and Tadono, T.: Comparison of multiple glacier inventories with a new inventory derived from high-resolution ALOS imagery in the Bhutan Himalaya, *The Cryosphere*, 10 (1), 65–85, 795 <https://doi.org/10.5194/tc-10-65-2016>, 2016.
- Naito, N., Suzuki, R., Komori, J., Matsuda, Y., Yamaguchi, S., Sawagaki, T., and Tshering, P.: Recent glacier shrinkages in the Lunana region, Bhutan Himalayas, *Global Environ. Res.*, 16 (1), 13–22, 2012.
- Nick, F. M., Vieli, A., Howat, I. M., and Joughin, I.: Large-scale changes in Greenland outlet glacier dynamics triggered at the 800 terminus, *Nature Geosci.*, 2 (2), 110–114, <https://doi.org/10.1038/ngeo394>, 2009.
- Nie, Y., Sheng, Y., Liu, Q., Liu, L., Liu, S., Zhang, Y., and Song, C.: A regional-scale assessment of Himalayan glacial lake changes using satellite observations from 1990 to 2015, *Remote Sens. Environ.*, 189, 1–13, <https://doi.org/10.1016/j.rse.2016.11.008>, 2017.
- Nuimura, T., Fujita, K., Yamaguchi, S., and Sharma, R. R.: Elevation changes of glaciers revealed by multitemporal digital 805 elevation models calibrated by GPS survey in the Khumbu region, Nepal Himalaya, 1992–2008, *J. Glaciol.*, 58 (210), 648–656, <https://doi.org/10.3189/2012JoG11J061>, 2012.

- Nuimura, T., Sakai, A., Taniguchi, K., Nagai, H., Lamsal, D., Tsutaki, S., Kozawa, A., Hoshina, Y., Takenaka, S., Omiya, S., Tsunematsu, K., Tshering, P., and Fujita, K.: The GAMDAM glacier inventory: a quality-controlled inventory of Asian glaciers, *The Cryosphere*, 9 (3), 849–864, <https://doi.org/10.5194/tc-9-849-2015>, 2015.
- 810 Østrem, G.: Ice melting under a thin layer of moraine and the existence of ice cores in moraine ridges, *Geogr. Ann.*, 41, 228–230, 1959.
- Paul, F., Barrant, N. E., Berthier, E., Bolch, T., Casey, K., Frey, H., Joshi, S. P., Konovalov, V., Le Bris, R., Mölg, N., Nuth, C., Pope, A., Racoviteanu, A., Rastner, P., Raup, B., Scharrer, K., Steffen, S., and Winswold, S.: On the accuracy of glacier outlines derived from remote sensing data, *Ann. Glaciol.*, 54 (63), 171–182, <https://doi.org/10.3189/2013AoG63A296>, 2013.
- 815 Reid, T. D. and Brock, B. W.: An energy-balance model for debris-covered glaciers including heat conduction through the debris layer, *J. Glaciol.*, 56 (199), 903–916, <https://doi.org/10.3189/002214310794457218>, 2010.
- Sakai, A.: Glacial Lakes in the Himalayas: A Review on Formation and Expansion Processes, *Global Environ. Res.*, 16 (1), 23–30, 2012.
- Sakai, A. and Fujita, K.: Formation conditions of supraglacial lakes on debris-covered glaciers in the Himalayas, *J. Glaciol.*, 820 56 (195), 177–181, <https://doi.org/10.3189/002214310791190785>, 2010.
- Sakai, A. and Fujita, K.: Contrasting glacier responses to recent climate change in high-mountain Asia, *Sci. Rep.*, 7 (1), 13717, <https://doi.org/10.1038/s41598-017-14256-5>, 2017.
- Sakai, A., Nishimura, K., Kadota, T., and Takeuchi, N.: Onset of calving at supraglacial lakes on debris covered glaciers of the Nepal Himalayas, *J. Glaciol.*, 55 (193), 909–917, <https://doi.org/10.3189/002214309790152555>, 2009.
- 825 Sakai, A., Nuimura, T., Fujita, K., Takenaka, S., Nagai, H., and Lamsal, D.: Climate regime of Asian glaciers revealed by GAMDAM glacier inventory, *The Cryosphere*, 9, 865–880, <https://doi.org/10.5194/tc-9-865-2015>, 2015.
- Sakakibara, D. and Sugiyama, S.: Ice-front variations and speed changes of calving glaciers in the Southern Patagonia Icefield from 1984 to 2011, *J. Geophys. Res.-Earth*, 119, 2541–2554, <https://doi.org/10.1002/2014JF003148>, 2014.
- Scherler, D., and Strecker, M. R.: Large surface velocity fluctuations of Biafo Glacier, central Karakoram, at high spatial and 830 temporal resolution from optical satellite images, *J. Glaciol.*, 58 (209), 569–580, <https://doi.org/10.3189/2012JoG11J096>, 2012.
- Scherler, D., Bookhagen, B., and Strecker, M. R.: Spatially variable response of Himalayan glaciers to climate change affected by debris cover, *Nat. Geosci.*, 4 (3), 156–159, <https://doi.org/10.1038/ngeo1068>, 2011a.
- Scherler, D., Bookhagen, B., and Strecker, M. R.: Hillslope glacier coupling: The interplay of topography and glacial dynamics 835 in High Asia, *J. Geophys. Res.*, 116, F02019, <https://doi.org/10.1029/2010JF001751>, 2011b.
- Sugiyama, S., Gudmundsson, G. H., and Helbing, J.: Numerical investigation of the effects of temporal variations in basal lubrication on englacial strain-rate distribution, *Ann. Glaciol.*, 37, 49–54, <https://doi.org/10.3189/172765403781815618>, 2003.

- 840 Sugiyama, S., Skvarca, P., Naito, N., Enomoto, H., Tsutaki, S., Tone, K., Marinsek, S., and Aniya, M.: Ice speed of a calving glacier modulated by small fluctuations in basal water pressure, *Nat. Geosci.*, 4 (9), 597–600, <https://doi.org/10.1038/ngeo1218>, 2011.
- Sugiyama, S., Sakakibara, D., Matsuno, S., Yamaguchi, S., Matoba, S., Aoki, T.: Initial field observation on Qaanaaq ice cap, northwestern Greenland, *Ann. Glaciol.*, 55 (66), 25–33, <https://doi.org/10.3189/2014AoG66A102>, 2014.
- 845 Suzuki, R., Fujita, K., and Ageta, Y.: Spatial distribution of thermal properties on debris-covered glaciers in the Himalayas derived from ASTER data, *Bull. Glaciol. Res.*, 24, 13–22, 2007a.
- Suzuki, R., Fujita, K., Ageta, Y., Naito, N., Matsuda, Y., and Karma: Meteorological observations during 2002–2004 in Lunana region, Bhutan Himalayas, *Bull. Glaciol. Res.*, 24, 71–78, 2007b.
- Truffer, M., Motyka, R. J., Hekkers, M., Howat, I. M., and King, M. A.: Terminus dynamics at an advancing glacier: Taku Glacier, Alaska, *J. Glaciol.*, 55 (194), 1052–1060, <https://doi.org/10.3189/002214309790794887>, 2009.
- 850 Trüssel, B. L., Motyka, R. J., Truffer, M., and Larsen, C. F.: Rapid thinning of lake-calving Yakutat Glacier and the collapse of the Yakutat Icefield, southeast Alaska, USA, *J. Glaciol.*, 59 (215), 149–161, <https://doi.org/10.3189/2013JoG12J081>, 2013.
- Trüssel, B. L., Truffer, M., Hock, R., Motyka, R. J., Huss, M., and Zhang, J.: Runaway thinning of the low-elevation Yakutat Glacier, Alaska, and its sensitivity to climate change, *J. Glaciol.*, 61 (225), 65–75, <https://doi.org/10.3189/2015JoG14J125>, 2015.
- 855 Tshering, P., and Fujita, K.: First in situ record of decadal glacier mass balance (2003–2014) from the Bhutan Himalaya, *Ann. Glaciol.*, 57 (71), 289–294, <https://doi.org/10.3189/2016AoG71A036>, 2016.
- Tsutaki, S., Nishimura, D., Yoshizawa, T., and Sugiyama, S.: Changes in glacier dynamics under the influence of proglacial lake formation in Rhonegletscher, Switzerland, *Ann. Glaciol.*, 52 (58), 31–36, <https://doi.org/10.3189/172756411797252194>, 2011.
- 860 Tsutaki, S., Sugiyama, S., Nishimura, D., and Funk, M.: Acceleration and flotation of a glacier terminus during formation of a proglacial lake in Rhonegletscher, Switzerland, *J. Glaciol.*, 59 (215), 559–570, <https://doi.org/10.3189/2013JoG12J107>, 2013.
- Tsutaki, S., Sugiyama, S., Sakakibara, D., and Sawagaki, T.: Surface elevation changes during 2007–13 on Bowdoin and Tugto Glaciers, northwestern Greenland, *J. Glaciol.*, 62 (236), 1083–1092, <https://doi.org/10.1017/jog.2016.106>, 2016.
- 865 van der Veen, C. J.: Tidewater calving, *J. Glaciol.*, 42 (141), 375–385, doi:10.1017/S0022143000004226, 1996.
- Vieli, A., and Nick, F. M.: Understanding and modelling rapid dynamic changes of tidewater outlet glaciers: issues and implications, *Surv. Geophys.*, 32, 437–458, <https://doi.org/10.1007/s10712-011-9132-4>, 2011.
- Vincent, C., Wagnon, P., Shea, J. M., Immerzeel, W. W., Kraaijenbrink, P., Shrestha, D., Soruco, A., Arnaud, Y., Brun, F., 870 Berthier, E., and Sherpa, S. F.: Reduced melt on debris-covered glaciers: investigations from Changri Nup Glacier, Nepal, *The Cryosphere*, 10 (4), 1845–1858, <https://doi.org/10.5194/tc-10-1845-2016>, 2016.

Warren, C. R., and Kirkbride, M. P.: Calving speed and climatic sensitivity of New Zealand lake-calving glaciers, *Ann. Glaciol.*, 36, 173–178, <https://doi.org/10.3189/172756403781816446>, 2003.

875 Yamada, T., Naito, N., Kohshima, S., Fushimi, H., Nakazawa, F., Segawa, T., Uetake, J., Suzuki, R., Sato, N., Karma, Chhetri, I. K., Gyenden, L., Yabuki, H., and Chikita, K.: Outline of 2002 – research activities on glaciers and glacier lakes in Lunana region, Bhutan Himalaya, *Bull. Glaciol. Res.*, 21, 79–90, 2004.

Yao, T., Thompson, L., Yang, W., Yu, W., Gao, Y., Guo, X., Yang, X., Duan, K., Zhao, H., Xu, B., Pu, J., Lu, A., Xiang, Y., Kattel, D. B., and Joswiak, D.: Different glacier status with atmospheric circulations in Tibetan Plateau and surroundings, *Nature Climate Change*, 2, 663–667, <https://doi.org/10.1038/nclimate1580>, 2012.

880 Zhang, Y., Fujita, K., Liu, S. Y., Liu, Q., and Nuimura, T.: Distribution of debris thickness and its effect on ice melt at Hailuoguo glacier, southeastern Tibetan Plateau, using in situ surveys and ASTER imagery, *J. Glaciol.*, 57 (206), 1147–1157, <https://doi.org/10.3189/002214311798843331>, 2011.

885 Zemp, M., Frey, H., Gärtner-Roer, I., Nussbaumer, S. U., Hoelzle, M., Paul, F., Haeberli, W., Denzinger, F., Ahlström, A. P., Anderson, B., Bajracharya, S., Baroni, C., Braun, L. N., Cáceres, B. E., Casassa, G., Cobos, G., Dávila, L. R., Delgado Granados, H., Demuth, M. N., Espizua, L., Fischer, A., Fujita, K., Gadek, B., Ghazanfar, A., Hagen, J. O., Holmlund, P., Karimi, N., Li, Z. Q., Pelto, M., Pitte, P., Popovnin, V. V., Portocarrero, C. A., Prinz, R., Sangewar, C. V., Severskiy, I., Sigurðsson, O., Soruco, A., Usubaliev, R., and Vincent, C.: Historically unprecedented global glacier decline in the early 21st century, *J. Glaciol.*, 61 (228), 745–761, <https://doi.org/10.3189/2015JoG15J017>, 2015.

890

895

900

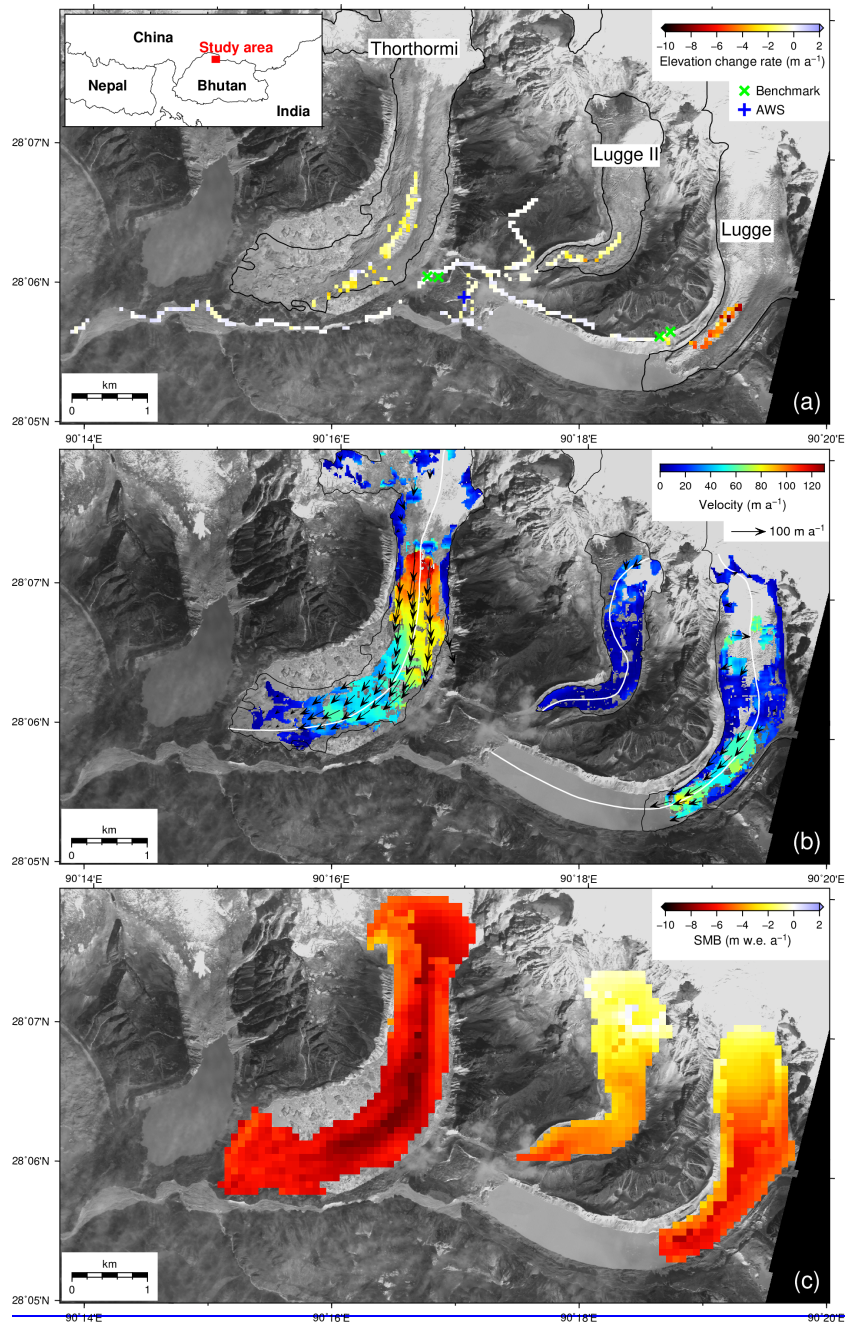
905

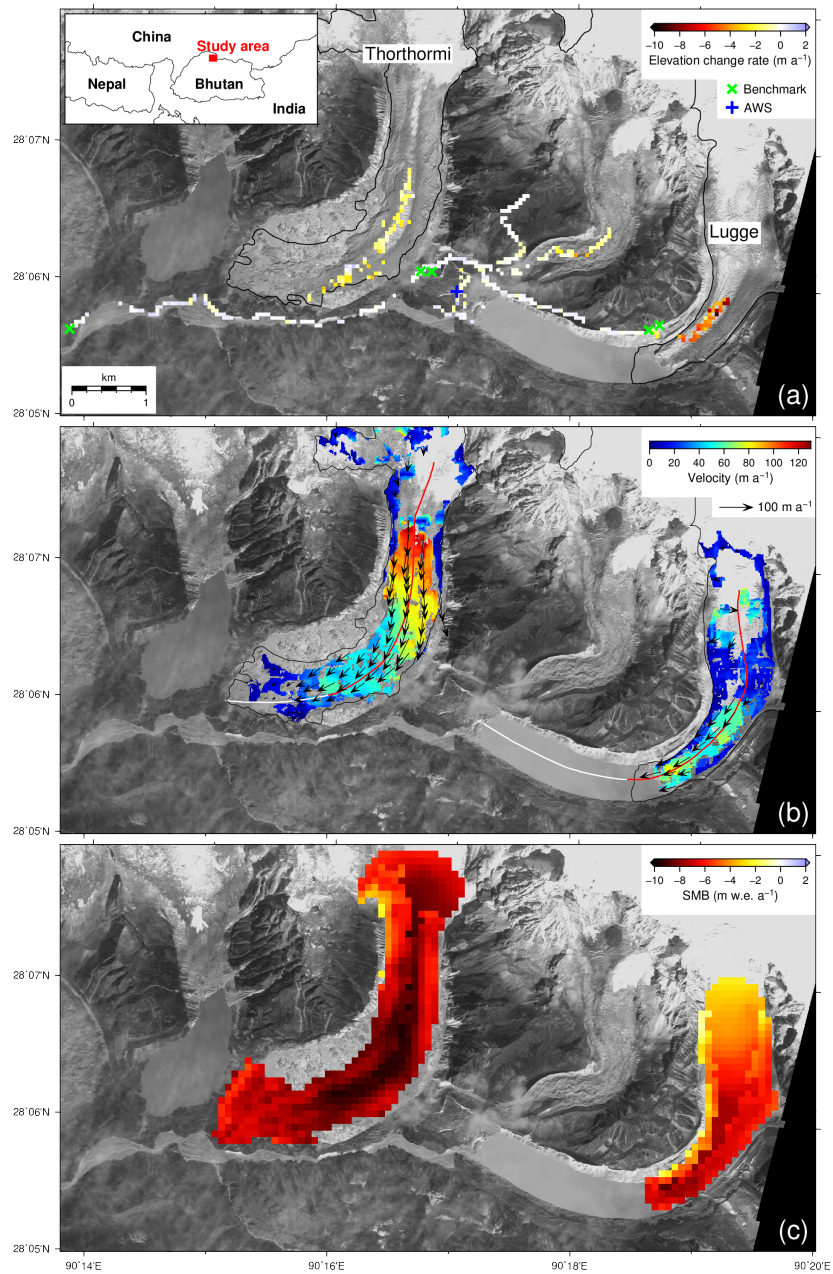
910

915

Table 1: Observed elevation changes (dh) and rate of elevation changes (dh/dt), with standard errors on- and off-glacier glaciers, in the Lunana region, Bhutan Himalaya, during 2004–2011. The simulated surface mass balance (SMB) during 1979–2017, emergence velocity (v_e) during 2002–2010, and rate of elevation change covering only the area of DGPS surveys are also indicated, along with the observed number of 1- × 1 m DEM gridpoints (n cells) (n).

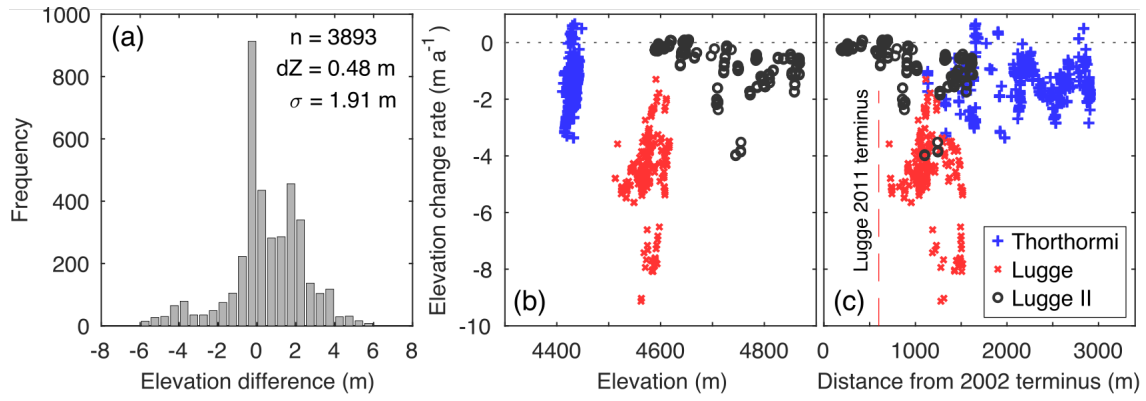
Glacier	n	Observed dh (m)	Observed dh/dt (m a ⁻¹)	SMB (m w.e. a ⁻¹)	v_e (m w.e. a ⁻¹)	Simulated dh/dt (m a ⁻¹)
		-9.79 ± 0.09		$-7.87 \pm$	3.33 ± 0.27	-8.44 ± 4.08
Thorthormi	431		-1.40 ± 0.01	9.03 ± 0.14	2.62	0.87
Lugge	248	-32.70 ± 0.12	-4.67 ± 0.02	-5.98 ± 1.11	-2.18 ± 2.62	-9.07 ± 3.73
		$-4.43 - 32.70 \pm$		-4.38	-0.21 ± 0.05	-7.62 ± 0.72
Lugge-H	258	0.12	-0.63	0.49		
Off-glacier	3893	0.48 ± 0.03				





920 **Figure 14:** Glaciers and glacial lakes in the Lunana region, Bhutan Himalaya, superimposed with (a) the rate of elevation
 change for the 2004–2011 period; (b) surface ice-flow velocities (arrows) with magnitude (color scale), between 30
 925 January 2007 and 1 January 2008; and (c) simulated surface mass balance (SMB) for the 2002–2004/1979–2017 period. The
 inset in (a) shows the location of the study site. The rate of elevation change in (a) is depicted on a 50- m grid, which is
 averaged from the differentiated 1- m DEMs. The light- green crosses are the benchmark locations used for the GPS surveys
 in 2004 and 2011. The blue cross is the location of the automatic weather station installed in 2002 (Yamada et al., 2004). The
 black lines indicate the outline of the glaciers in November 2002. The background image is an ALOS Panchromatic Remote-

sensing Instrument for Stereo Mapping (PRISM) scene from 2 December 2009. The white and red lines in (b) indicate the central flowline of each glacier, which is used for Figs. 3 and 6–8.



930

935

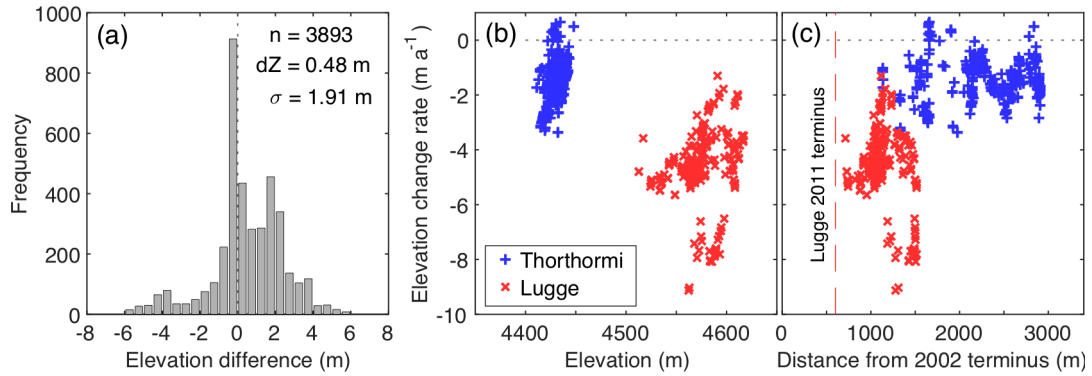
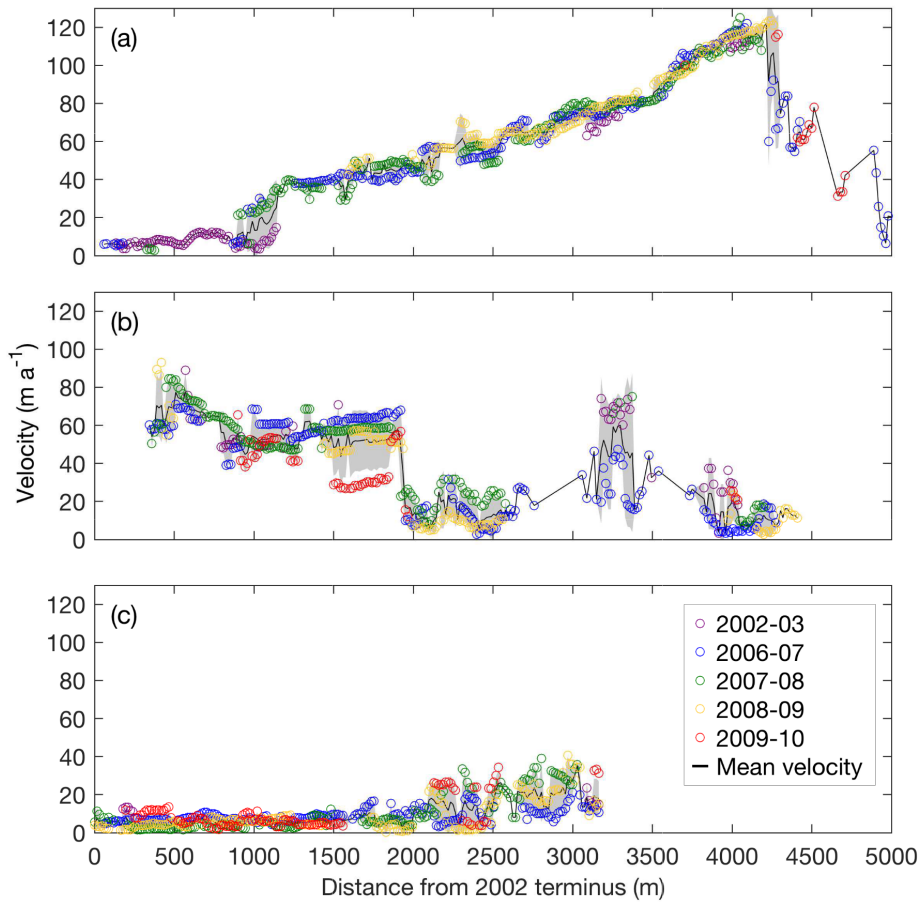


Figure 2: (a) Histogram of the elevation differences across each-off-glacier at 0.5 m elevation bins. The rate of elevation change for Thorthormi (blue), Lugge (red), and Lugge II (black) glaciers is compared with (b) elevation in 2011, and (c) distance from the glacier terminus in 2002 along the central flowlines (Fig. 1b). The red dashed line in (c) denotes the location of the calving front of Lugge Glacier in 2011.

940



945

950

955

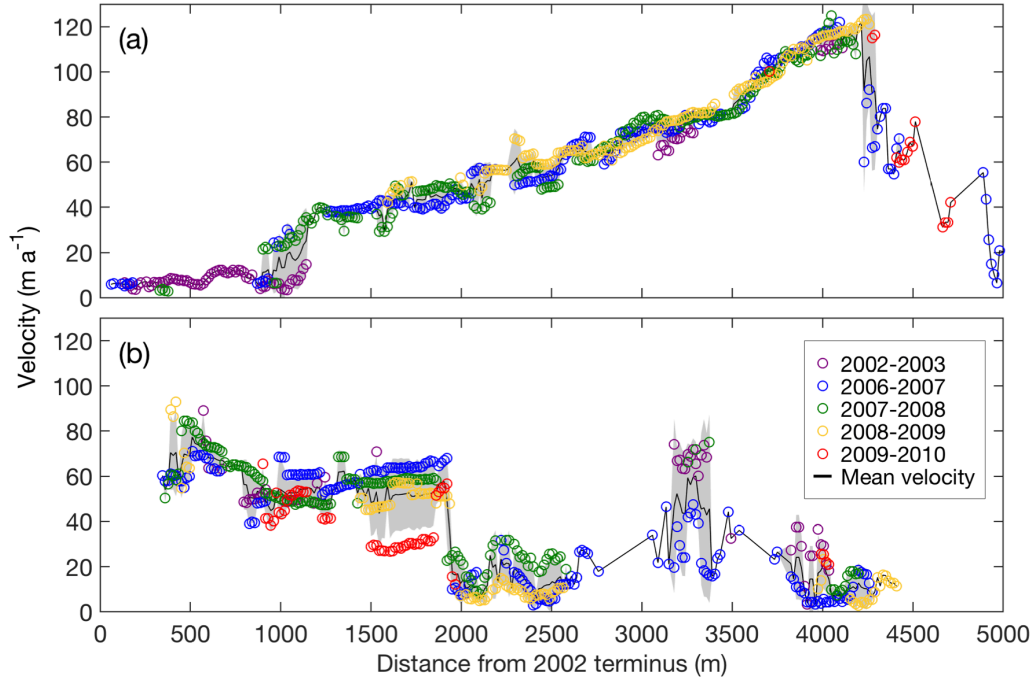
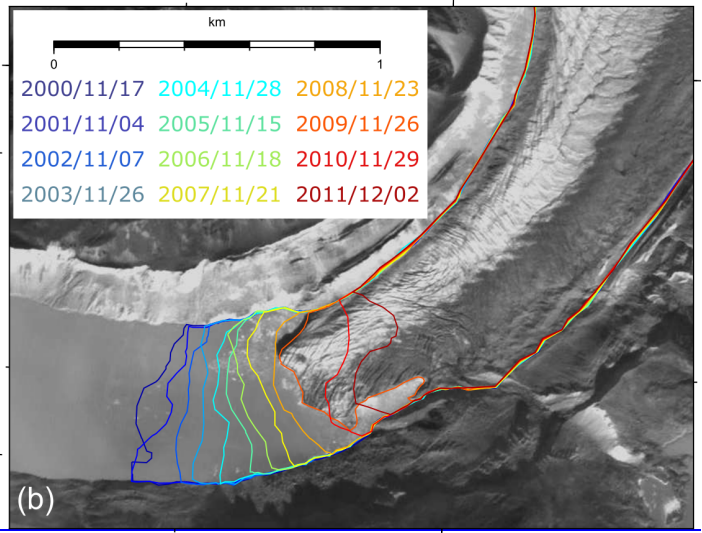
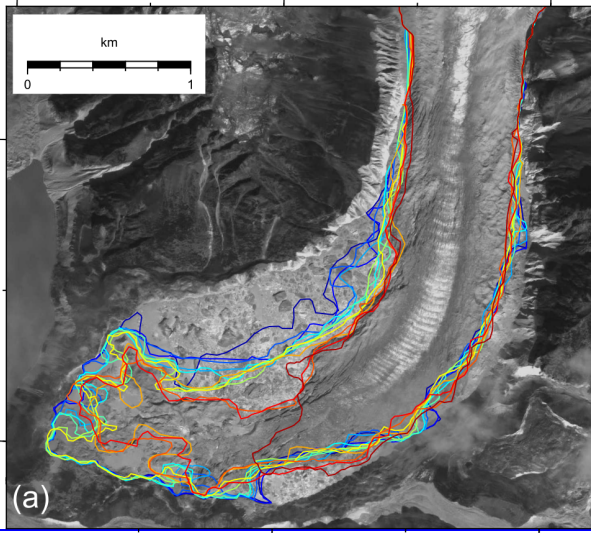


Figure 3: Surface ice-flow velocities along the central flowlines of (a) Thorthormi; and (b) Luge and (c) Luge II glaciers for the 2002–2010 study period. The black lines are the mean flow velocities from 2002 to 2010, with the shaded gray regions denoting the standard deviation. The distance from each respective 2002 glacier terminus is indicated on the horizontal axis.



975

980

985

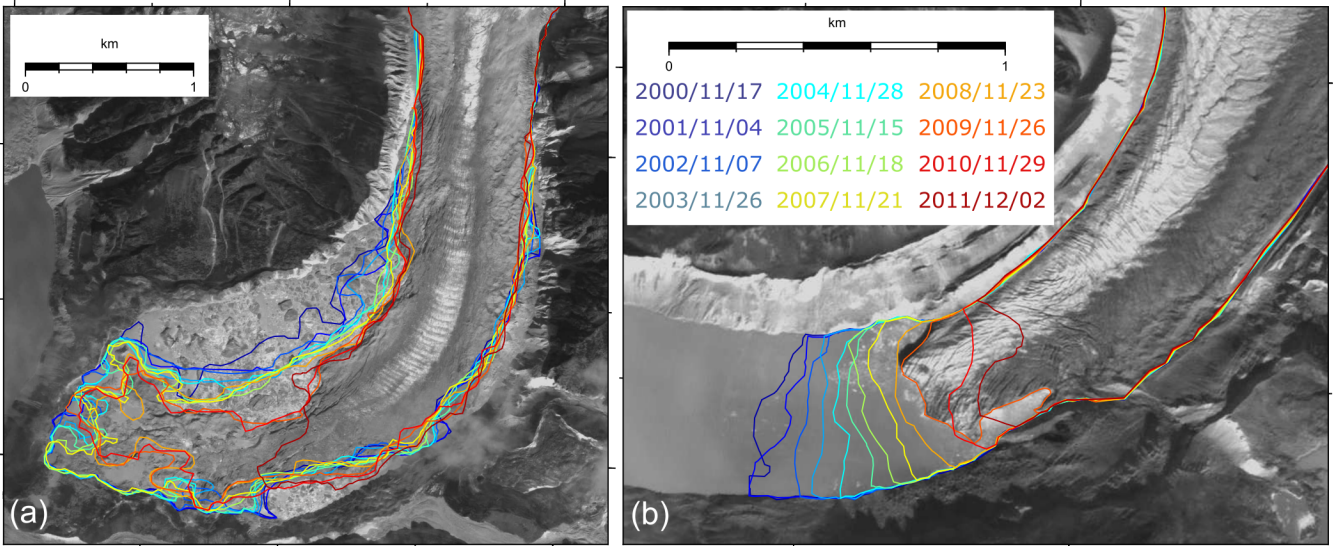
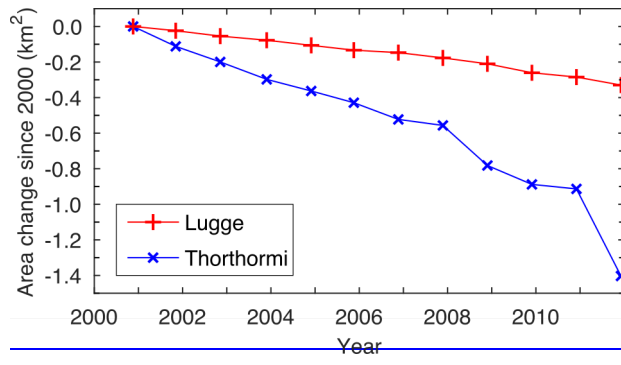


Figure 4: Glacier boundaries in the lower parts of (a) Thorthormi and (b) Lugge glaciers from 2000 to 2011. The background image is an ALOS PRISM image acquired on 2 December 2009.



995

000

005

010

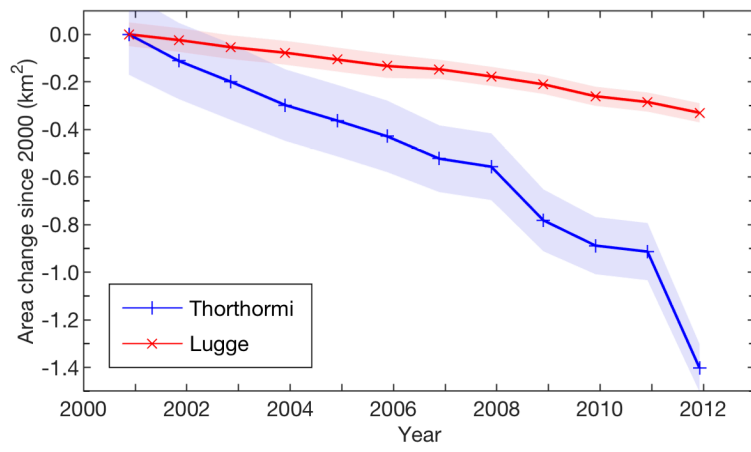
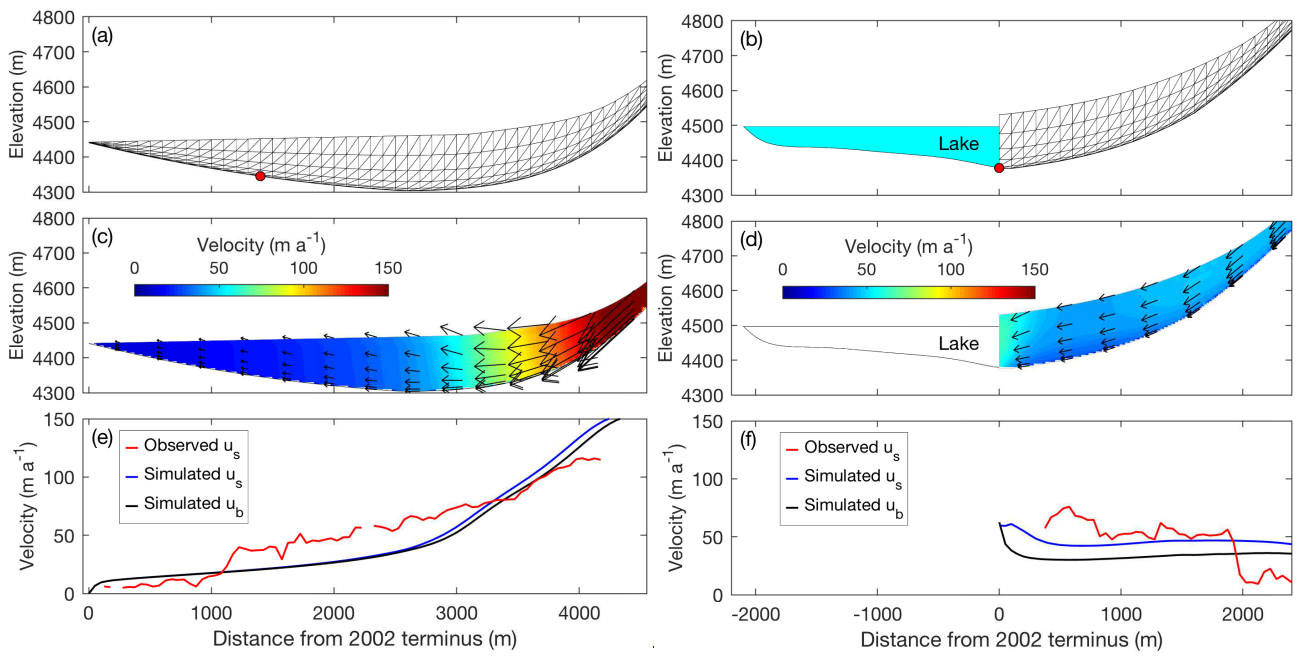


Figure 5: Cumulative area changes of Thorthormi (blue) and Lugge (red) glaciers since 17 November 2000. The shaded regions denote the uncertainties in the glacial area delineation.

015



020

025

030

035

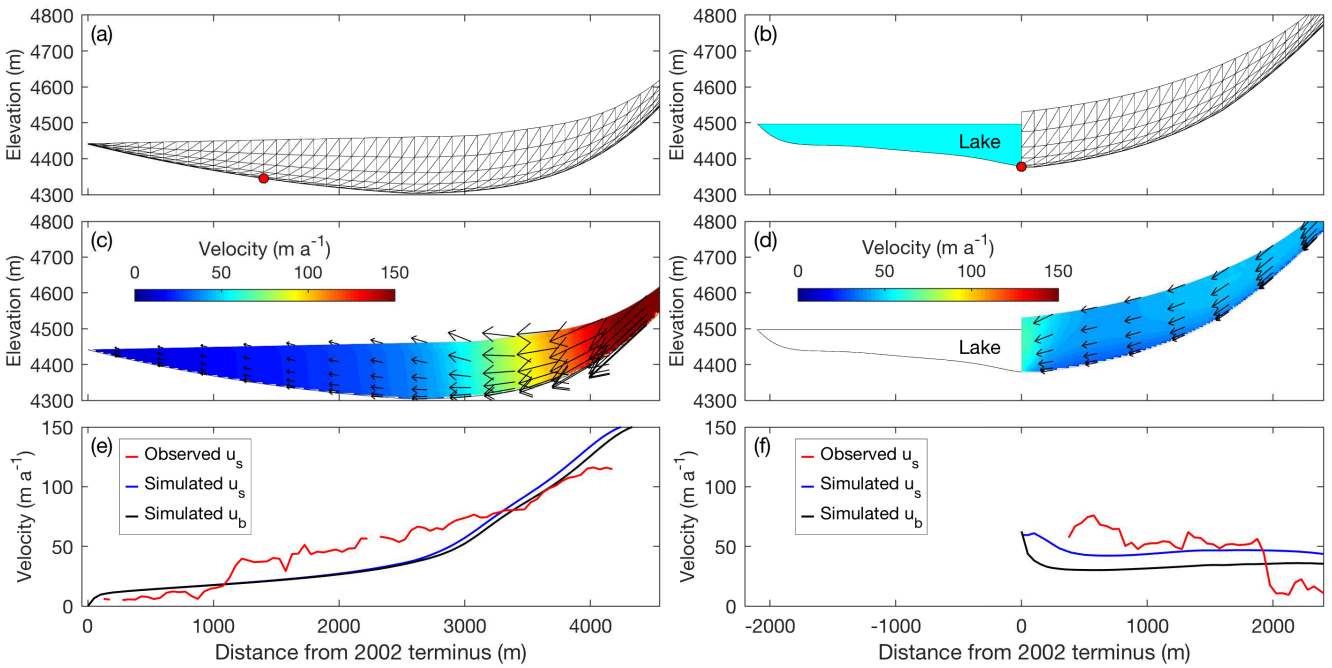
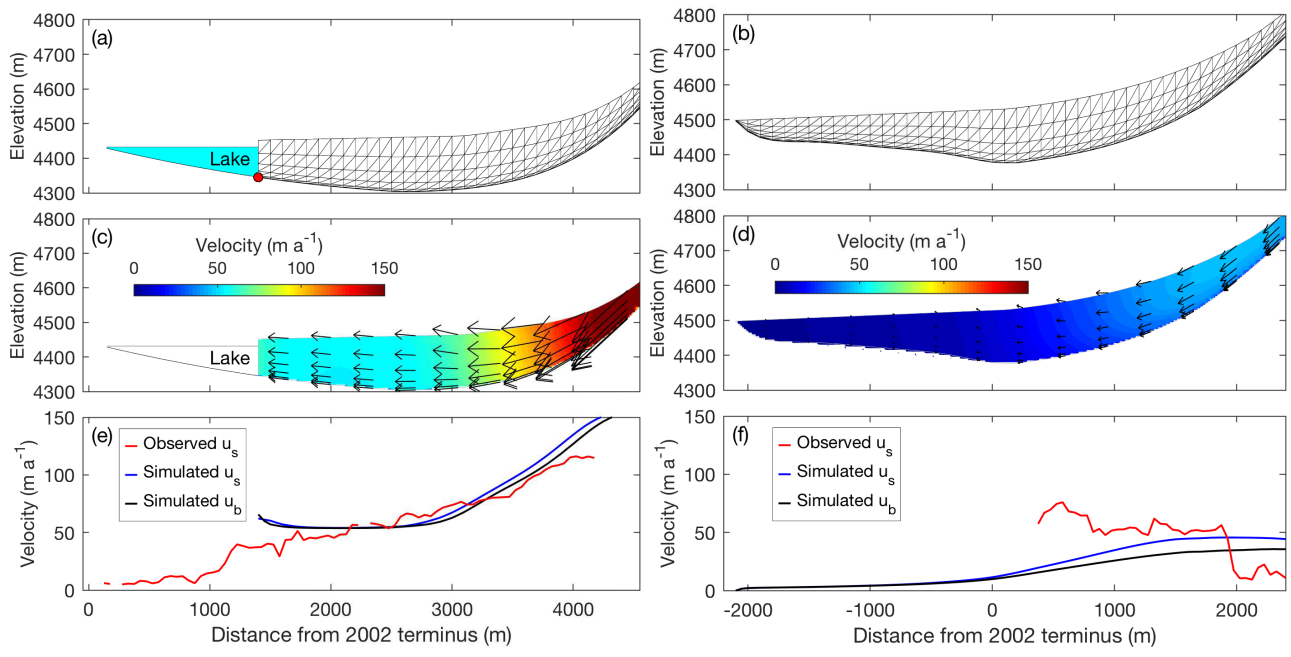


Figure 6: Ice flow simulations in longitudinal cross-sections of Thorthormi (left panels) and Luge (right panels) glaciers, with the present geometries of the glaciers employed in the models. (a and b) Finite element meshes used for the simulations, with red markers indicating the bedrock elevation based on a bathymetric survey. The light-blue shading in (b) indicates Luge Glacial Lake. Simulated (c and d) two-dimensional ice-flow velocity-vectors (magnitude and xz -direction) and (e and f) horizontal components of the ice-flow velocity-field. The blue and black curves are the simulated surface (u_s) and basal velocities (u_b), respectively. The red curves are the observed surface ice-flow velocities for 2002–2010.

040

045



050

055

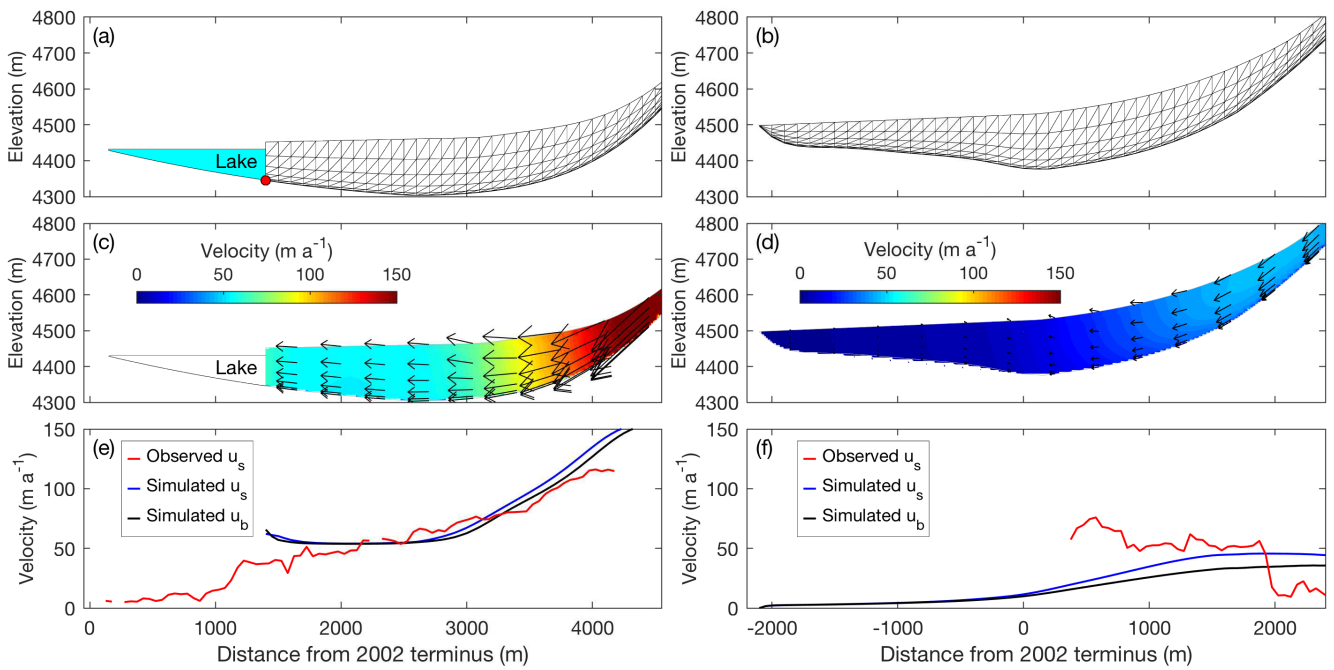


Figure 7: Ice flow simulations in longitudinal cross-sections of Thorthormi Glacier under the lake-terminating condition (left panels), and Lugge Glacier under the land-terminating condition (right panels). (a and b) Finite element meshes used for the simulation. The light-blue shading in (a) indicates the proglacial lake in front of Thorthormi Glacier. Simulated (c and d) two-dimensional ice-flow velocity-vectors (magnitude and xz -direction) and (e and f) horizontal components of the ice-flow velocity-field. The blue and black curves are the simulated surface (u_s) and basal velocities (u_b), respectively. The red curves are the observed surface ice-flow velocities for 2002–2010.

060

065

070

075

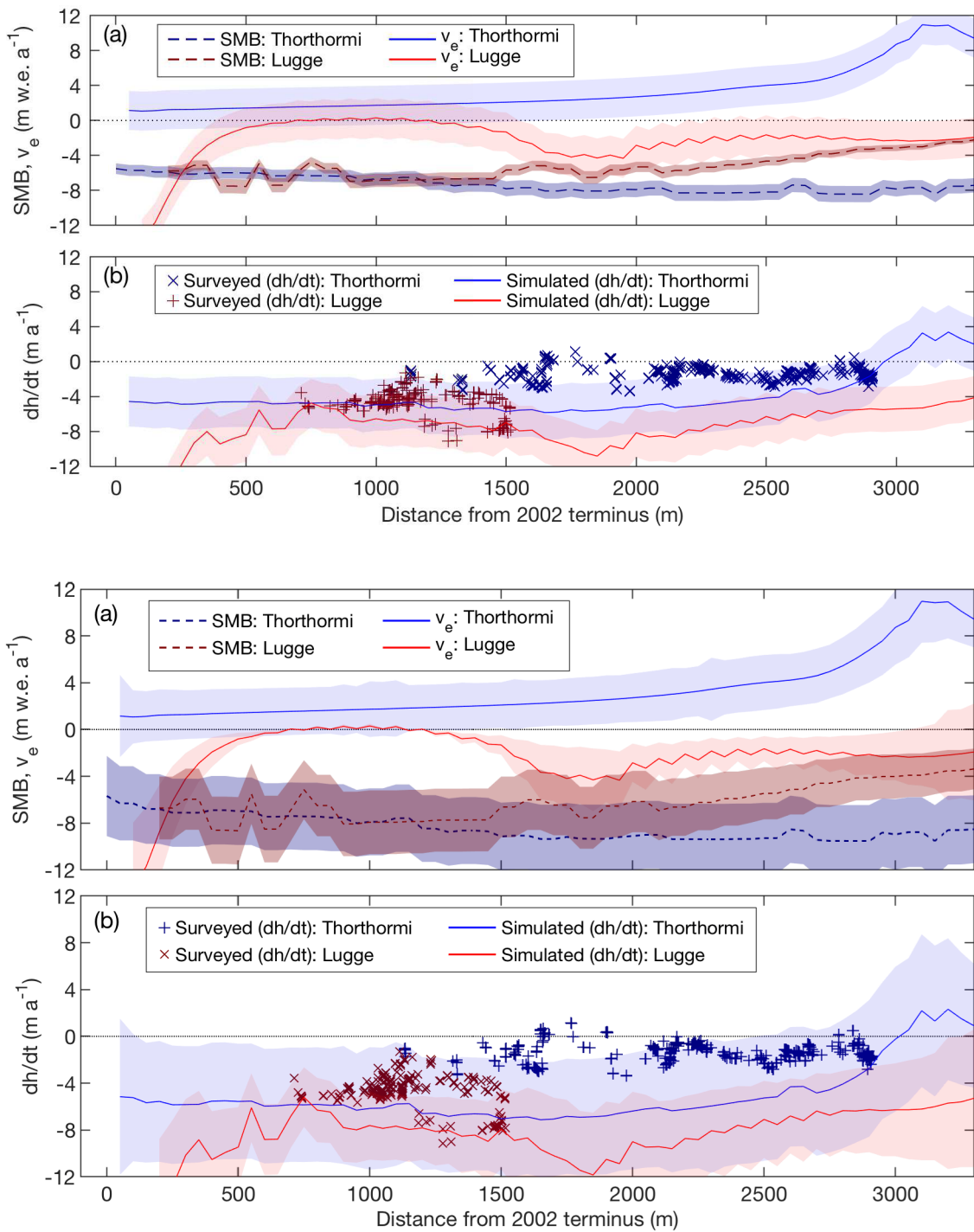


Figure 8: (a) Simulated surface mass balance (SMB) and emergence velocity (v_e) calculations along the central flowlines of Thorthormi and Lugge glaciers. (b) Rate of elevation change (dh/dt), as determined from differential GPS

surveys during 2004–2011 (marks) and model simulations (lines). Shaded regions denote the model uncertainties for each calculation.